The role of the yeast Shu complex in the error-free bypass of abasic sites and 3-Methylcytosines

by

Braulio Bonilla

B.S. Universidad de la Republica, Uruguay, 2008

M.S. Universidad de la Republica, Uruguay, 2013

Submitted to the Graduate Faculty of the

School of Medicine in partial fulfillment

of the requirements for the degree of

Doctor of Philosophy

University of Pittsburgh

2020

UNIVERSITY OF PITTSBURGH

SCHOOL OF MEDICINE

This dissertation was presented

by

Braulio Bonilla

It was defended on

December 3, 2020

and approved by

Ben Van Houten, Ph.D., Richard M. Cyert Professor of Molecular Oncology, Department of Pharmacology and Chemical Biology

Judith L. Yanowitz, Ph.D., Associate Professor, Department of Obstetrics, Gynecology & Reproductive Sciences

Guillermo G. Romero, Ph.D., Associate Professor, Department of Pharmacology and Chemical Biology

Roderick J. O'Sullivan, Ph.D., Associate Professor, Department of Pharmacology and Chemical Biology

Dissertation Director: Kara A. Bernstein, Ph.D., Associate Professor Department of Pharmacology and Chemical Biology

The role of the yeast Shu complex in the error-free bypass of abasic sites and 3-Methylcytosines

Braulio Bonilla, PhD

University of Pittsburgh, 2020

Accurate DNA replication is critical to prevent genomic instability, which is a hallmark of cancer. Homologous recombination (HR) is responsible for error-free DNA damage bypass during replication. The yeast Shu complex is a recombination mediator primarily specialized in preventing replication-associated mutagenesis from endogenous DNA lesions as well as those from the alkylating agent methyl methanesulfonate (MMS). However, it remains unclear which are the specific DNA lesions that are tolerated by a Shu complex-mediated error-free pathway. To approach this problem, we performed a genome-wide sequencing of Shu complex disrupted cells chronically exposed to MMS. The analysis of the mutation pattern suggested abasic sites and 3-Methylcytosines as major contributors of mutagenesis in Shu complex deficient cells exposed to MMS. We, therefore, thought to validate these observations. In this work, we found that the Shu complex is enriched at the chromatin in cells that accumulate abasic sites and that it is important for the error-free bypass of APOBE3B-induced abasic sites. Moreover, we also showed that ectopic expression of the 3-Methylcytosine repair enzyme, ALKBH2, specifically rescues MMS-induced phenotypes seen in Shu complex mutant cells, such as growth defects and increased mutagenesis. Overall, our results demonstrate that yeast cells rely on a Shu complex-mediated error-free pathway to prevent mutagenesis from abasic sites and 3-Methylcytosines.

Table of Contents

List of Figures

List of Tables

Glossary

9-1-1 (complex)- Rad9–Hus1–Rad1

(pG)AD- (GAL1) Activation domain

AP (site) – apurinic/apyrimidinic abasic site

ARS- Autonomously replicating sequence

BCDX2 complex- Complex consisting of RAD51B, RAD51C, RAD51D, and XRCC2

(pG)BD- (GAL1) Binding domain

BIR- Break-Induced Replication

BER- Base Excision Repair

CX3 complex- Complex Consisting of RAD51C and XRCC3

DDT- DNA damage tolerance

D-loop- Displacement-Loop

DRR (assay)- Direct repeat recombination

DSBs- Double-Strand Breaks

dsDNA- Double-Stranded DNA

EdU- 5-ethynyl-2′-deoxyuridine

FA- Fanconi anemia

GC- Gene Conversion

HR- Homologous Recombination

h- Homo sapiens

HU- Hydroxyurea

iPOND- isolation of proteins on nascent DNA

MMS- Methyl Methanesulfonate

MRN- Complex Consisting of MRE11-RAD50-NBS1

NHEJ- Non-Homologous End Joining

PCNA- Proliferating Cell Nuclear Antigen

PLA- proximity ligation assay

PRR-Post-replicative repair

RPA- Replication Protein A

SAM- S-adenosyl methionine

sc- Saccharomyces cerevisiae

SDSA- Synthesis Dependent Strand Annealing

Shu (complex)- Suppressor of sgs1Δ HydroxyUrea sensitivity

sp- Saccharomyces pombe

ssDNA, Single-Stranded DNA

SWIM (domain)- SWI2/SNF2 and MuDR

TLS- Translesion synthesis

Y2H- Yeast two hybrids

Preface

To all who provided help, guidance, and support:

To Kara, my mentor. For her patience, support, and understanding. For all her knowledge she shared and her guidance that made me a better scientist, I take these learnings for the rest of the journey. It was an honor to be her trainee.

To all the members of my dissertation committee, for their invaluable advice for this project. For independently and spontaneously supporting my career on several occasions. In particular, Ben, who went the extra mile not just once to help and guide me.

To all our collaborators, in particular to Joel Rosenbaum and Steve Roberts, their work was critical for our publications.

To the Fulbright Program, for their support.

To all current and past members of the Bernstein lab, for so much fun, true friendship, and science. In particular to Thong Luong, Meghan Sullivan, Greg Brunette, Juli Martino, Robbie Baldock, McKenzie Grundy, Anton Khodakov, Ben Herken, and Mike Mihalevic. Special thanks to Cat Pressimone, and Kyle Rapchak for their great contribution to this project.

To my great friends: *Los Idolos de la Gloria & Tio*, Leti, Gerard, and the Pitt.uy group, *el pelado* Segantini, the IBGP group, *Les Foques*, and *Los Altos Timberos*.

To my family, Mom, Dad, Mauro, Rosalia, Lia, Paco, and Tiki. Now and always.

To my beloved wife, Victoria. This work is dedicated to her.

And to the little ray of sunshine, our son, Oti.

Thank you.

1.0 Introduction

1.1 Double-strand break repair by homologous recombination: an overview

Double-strand breaks (DSBs) are one of the most cytotoxic DNA lesions, and their misrepair leads to mutations and translocations. DSBs can arise from exogenous sources, such as radiation and chemotherapy, as well as from endogenous sources, such as metabolic byproducts, reactive oxygen species, replication stress, and even scheduled endonucleolytic activity [V(D)J recombination and meiosis]. Homologous recombination (HR) and non-homologous end joining (NHEJ) are two major DSB repair pathways. NHEJ is a fast, although potentially error-prone, mechanism that re-ligates the DNA ends. NHEJ is active during all phases of the cell cycle and is the preferred DSB repair pathway in higher eukaryotes [1]. On the other hand, HR uses a homologous DNA template for repair, and in mammalian cells is most active during the S and G_2 phases of the cell cycle [2]. HR is favored over NHEJ at DSBs with dirty ends or when only one DNA end is available, such as in replication-associated DSBs [3]. Thus, HR offers a high-fidelity and versatile alternative for DSB repair.

HR, and the recombinase activity of RAD51, is central to three main DSB repair pathways: gene conversion (GC), synthesis-dependent strand annealing (SDSA), and RAD51-dependent break-induced replication (BIR) (**Figure 1a**). The defining feature of these pathways is the strand exchange of homologous sequences that serve as a template to restore broken DNA. The initial steps of these pathways are shared. Briefly, the MRE11-RAD50-NBS1 (MRN) complex with CtIP recognizes and binds to DSBs [4]. This enables short-range resection (~300 nt) to expose 3' single-stranded DNA (ssDNA) overhangs. Subsequent long-range resection (up to 2–4 kb) is achieved

by the 5' to 3' exonuclease activity of EXO1 or with the combined activities of DNA2 and BLM [5]. This ssDNA is rapidly coated by replication protein A (RPA), preventing the formation of ssDNA secondary structures and degradation [6]. RAD51 then displaces RPA to assemble nucleoprotein filaments with the 3' ssDNA ends. This central HR step is highly regulated to prevent unscheduled recombination. RAD51 filament assembly is stimulated by RAD51 mediators such as the RAD51 loader, BRCA2, and the RAD51 paralogs (RAD51B, RAD51C, RAD51D, XRCC2, XRCC3, and SWSAP1) (**Figure 1b**). The RAD51 nucleoprotein filaments invade a homologous region, forming a displacement loop (D-loop). The way that this heteroduplex DNA intermediate is resolved following DNA synthesis determines whether pathways, GC, SDSA, or BIR occur [7] (**Figure 1a**). Most recombination events are likely resolved through SDSA, where after DNA synthesis the D-loop is disrupted, allowing the newly synthesized DNA end to anneal to the other end of the broken DNA molecule [8-10]. During GC, the second end of the DSB is captured, forming a Holliday junction. This structure is then processed by endonucleases, helicases, and topoisomerases to allow separation of the DNA molecules. Alternatively, when the second end of the DSB is not captured, then DNA synthesis at the D-loop proceeds, resulting in BIR.

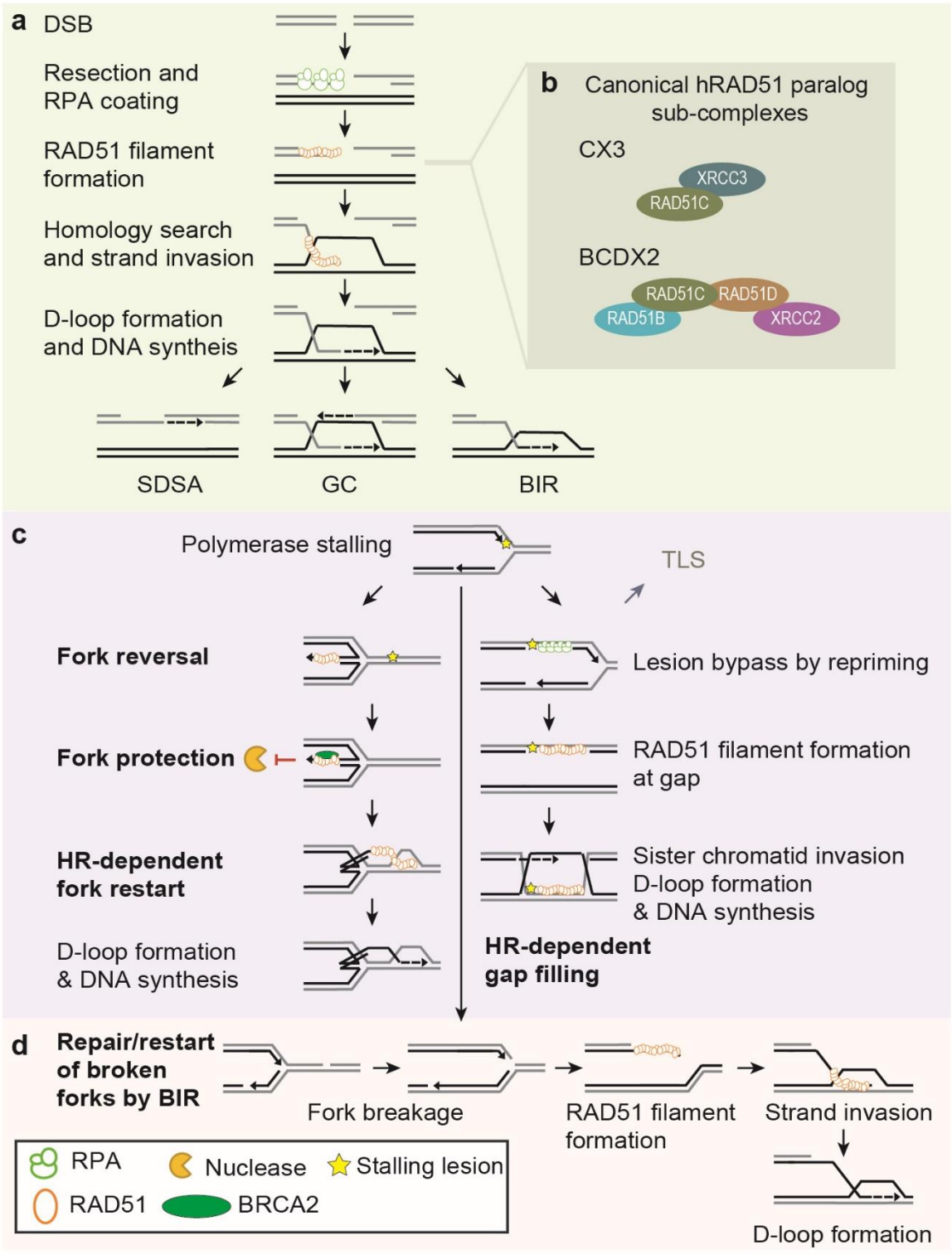

Figure 1. Potential models for the RAD51 gene family roles in mitotic cells

(**a**) Schematic of the initial steps of DSB repair through HR. Upon DSB formation, the 5' strands of the DNA ends are resected by the MRN complex. Further resection is performed by the exonuclease EXO1 and/or DNA2 together with

the BLM helicase (not shown). These exposed 3' ssDNA regions are immediately coated by the RPA complex (*green circles*), thus preventing the formation of secondary structures. RAD51 (*orange circles*) displaces RPA, aided by the RAD51 mediators (i.e., BRCA2 and the RAD51 paralogs) to form a RAD51 nucleoprotein filament on the ssDNA (for simplicity, only one side of the DSB is coated with and or RAD51). The RAD51 filaments perform homology search and strand invasion, leading to D-loop formation. After the D-loop is extended by DNA synthesis, the repair process can be completed by SDSA, GC, or BIR, depending on whether the D-loop is disrupted, the second end is captured, or it is not captured, respectively. (**b**) Schematic of the canonical hRAD51 paralog subcomplexes BCDX2 (consisting of RAD51B, RAD51C, RAD51D, and XRCC2) and CX3 (consisting of RAD51C and XRCC3). The lines indicate where BCDX2 and CX3 function during HR. (**c**) Schematic of the roles of RAD51 during the replication stress response. Replicative polymerases can be stalled by DNA lesions such as methylation adducts or abasic sites (*yellow star*). Fork reversal (*left*) occurs by the annealing of the newly synthesized strands and is dependent on RAD51 and other enzymes such as translocases or helicases (i.e., SMARCL1 and RAD54). This chicken-foot structure protects stalled forks and allows the rescue of the fork by an incoming replication fork or by bypassing the lesion. Protection of the reversed forks from nuclease digestion (*orange Pacman*) prevents ssDNA accumulation and depends on the formation of stable RAD51 filaments at the ssDNA of the reversed arm, which requires BRCA2 (*green oval*). Finally, reversed forks can be restarted by direct reversal (not shown) or HR. Alternatively (*right*) polymerase can resume replication by repriming. This leads to the formation of ssDNA gaps behind the fork, which are RPA coated. These gaps can be filled by TLS or HR-dependent gap filling. During HR-dependent gap filling, RAD51 displaces RPA in the gap and mediates sister chromatid invasion and D-loop formation. DNA synthesis enables the gap to be filled, enabling error-free lesion bypass. (**d**) Broken forks generated by persistent stalling or encountering of a ssDNA break by the replisome, leading to one-ended DSBs. These breaks can be repaired by RAD51-dependent HR where RAD51 filaments form on the broken DSB ends, which then invade the newly synthesized sister chromatid, leading to D-loop formation, which can be extended by BIR. Abbreviations: BIR, break-induced replication; BLM, bloom syndrome protein; D-loop, displacement loop; DSB, double-strand break; GC, gene conversion; HR, homologous recombination; MRN, MRE11-RAD50-NBS1; RPA, replication protein A; SDSA, synthesis-dependent strand annealing; ssDNA, single-stranded DNA; TLS, translesion synthesis. This figure was made by BB and was published in [11].

1.2 RecA/RAD51 family, origin and evolution

The *E. coli* RecA and eukaryotic RAD51 superfamily of recombinases is present across all domains of life, with the only exceptions being some intracellular bacteria with extremely small genomes [12, 13]. In fact, the universal distribution of this gene group has led to its use as an alternative to the 16S ribosomal RNA in phylogenetic analyses [14]. The recA/RAD51 superfamily originates from an ancient common ancestor before the appearance of Archaea and Eukarya. Early seminal work by Lin et al. [15] divided this family into three groups: recA, RADα, and RADβ [16]. The recA group includes all bacterial recA genes as well as eukaryotic recA genes present in plants, protists, and some fungi [15]. The RADα group includes the primary recombinases in eukaryotes (RAD51 and DMC1) and Archaea (radA). Vertebrate RAD51 shares ~74% amino acid sequence identity with yeast and plants, while RAD51 from humans and mice are 99% identical [17]. The RADβ group includes the canonical eukaryotic RAD51 paralogs (RAD51B, RAD51C, RAD51D, XRCC2, and XRCC3) and the archaeal radB. Members of the RADβ group have typically evolved distinctive functions that have yet to be fully characterized [18, 19]. The RADβ group exhibits a great deal of diversity, with highly divergent and rapidly evolving genes that share little sequence homology. In light of this, several proteins from different organisms have been proposed as RAD51 paralogs based on small conserved motifs, structural and/or functional conservation. These are often referred to as noncanonical RAD51 paralogs and include *S. pombe rlp1* and *rdl1* [20]; *S. cerevisiae CSM2*, *PSY3*, and *SHU1* [21-23]; human *SWSAP1* [24]; and *C. elegans rip-1* and *rfs-1* [25]. Sequence alignment of the RADα, RADβ, and noncanonical paralog SWSAP1 highlights that while their sequences are highly variant, key regions like the Walker A and B motifs are conserved.

The current diversity observed in the recA/RAD51 superfamily in Archaea and eukaryotes is a result of ancestral gene duplications followed by diversification in function as well as horizontal gene transfer after endosymbiotic events [15]. Most bacteriophages have proteins that perform DNA recombination, with several of them being recA homologs (UvsX, SAR1) [14, 26]. More recent studies propose that the bacterial sms (also known as radA) are recA paralogs [27], as well as a group of archaeal radA paralogs named radC [28]**.** This analysis suggests that there are likely additional undiscovered members of the *RADβ* gene group. Given the limits of phylogenetic analyses, functional and structural criteria will be critical to further define additional *RAD51* gene family members.

Throughout this article, we use RAD51 when referring to general properties common across species, whereas species-specific properties use a species-designated name (i.e., *Homo sapiens* RAD51 as hRAD51, murine RAD51 as mRAD51, and *S. cerevisiae* Rad51 as scRad51). Similarly, species-specific observations for complexes that are shared between species use a species designation (i.e., hShu complex versus scShu complex).

1.3 RAD51 mediators

RAD51 displaces RPA-coated ssDNA with the aid of the RAD51 mediators. The main RAD51 mediator in vertebrates is BRCA2 [29], whose function is performed by Rad52 in yeast [30]. scRad52 and BRCA2 are responsible for accelerating the rate-limiting step of recruiting and nucleating RAD51 on RPA-coated ssDNA [31]. Among vertebrates, other mediators include the RAD51 paralogs (RAD51B, RAD51C, RAD51D, XRCC2, and XRCC3) and the Shu complex,

which contains the RAD51 paralog SWSAP1[19]. The function of the RAD51 paralogs is discussed separately.

BRCA2 is recruited to DSBs through its interaction with PALB2, which itself interacts with BRCA1, binds DNA, and associates with chromatin [29]. BRCA2 then binds to ssDNA through its oligonucleotide/oligosaccharide-binding (OB)-fold-domain -containing C-terminal DNA-binding domain [32]. BRCA2 interacts through eight conserved BRC domains and a C-terminal motif with RAD51, which facilitates its recruitment to ssDNA [33]. Binding of the BRCA2 BRC motif to RAD51 inhibits RAD51 ATPase activity, which in turn enhances RAD51's affinity for ssDNA [34]. Additionally, the fifth to eighth BRC motifs preferentially bind the RAD51 filament, promoting its stability [35]. Also contributing to RAD51 filament stabilization are additional interactions between RAD51 and PALB2, BRCA1, and BARD1 [36-38]. RAD51 is also post-translationally modified by the phosphorylation of tyrosine 54 [39]. hRAD51 phosphorylation enhances the recombinase activity of hRAD51 by increasing its ability to compete with RPA for ssDNA and stimulating its strand exchange activity. This modification likely enables a conformation of the hRAD51 filament that is optimal for recombination.

1.4 RAD51 paralogs

The RAD51 paralogs are conserved mediators of RAD51, supporting their function in DSB repair, meiosis, and replication [18, 40]. Despite their importance, mechanistic details on how they promote HR are still unclear. In this section, we describe RAD51 paralog complexes, their properties, and their general role in promoting HR.

In budding yeast, the scRad51 paralogs form two distinct complexes: the Rad55-Rad57 complex and the Shu complex. The canonical scRad51 paralogs Rad55-Rad57 are required for DSB repair and interact with scRad51 and scRad52 [41-44]. Rad55 also interacts with the other scRad51 paralog complex, the Shu complex [41, 45]. The yeast Shu complex is the focus of this dissertation and is discussed in detail in section 1.5. Both scRad51 paralog complexes promote HR by at least two mechanisms: (*a*) helping scRad51 overcome the inhibitory effect of RPA during filament formation [41, 43] and (*b*) stabilizing scRad51 filaments by counteracting the anti-recombinase activity of Srs2 helicase [42, 46]. Notably, the Rad55-Rad57 complex also promotes scRad51-mediated strand exchange [43]. In nematodes, *C. elegans* RAD51 (ceRAD-51) paralogs RSF-1 and RIP-1 alter the ceRAD-51 filament by increasing its flexibility, thus enhancing strand exchange and D-loop formation [47]. This RAD51 paralog-mediated filament remodeling is likely conserved in other eukaryotes.

Progress in understanding hRAD51 paralog function has been particularly challenging due to their propensity to form insoluble aggregates *in vitro*, their low cellular abundance, and the fact that knockout mutants show lethality in mice and noncancerous cells [19]. Mutant mice lacking canonical *mRAD51* paralogs die at different developmental stages, ranging from embryonic day 7.5 to 10.5 (reviewed in [19]). Consistent with promoting RAD51 activities, Garcin et al. [48] individually disrupted the canonical *hRAD51* paralogs in U2OS and HEK293 cells and observed reduced RAD51 foci, growth defects, DNA damage sensitivity, and impaired HR. These observations are analogous to CHO and DT40 knockout hamster and chicken cell lines [19]. Unlike the rest of the *hRAD51* paralogs, *RAD51B* disruption generally results in milder phenotypes and is tolerated in non-transformed MCF-10A cells [48]. *SWSAP1* disruption is tolerated in human cell lines and mice [49, 50]. *SWSAP1* disruption leads to decreased RAD51 focus formation upon

treatment with methyl methanesulfonate (MMS), increased sensitivity to mitomycin C and MMS, but no increase in sensitivity to ionizing radiation, mirroring the phenotypes of *scShu*-complex knockout strains [50].

The hRAD51 paralogs function as distinct subcomplexes, including the CX3 complex (RAD51C and XRCC3), the BCDX2 complex (RAD51B, RAD51C, RAD51D, and XRCC2) (**Figure 1b**), the RAD51C-RAD51-BRCA2-PALB2 complex, and the Shu complex (SWSAP1, SWS1 likely with SPIDR and PDS5B) [19, 24, 50, 51]. Like RAD51, the RAD51 paralogs are ATPases with conserved Walker A and B motifs. The BCDX2 complex hydrolyzes ATP in the presence of ssDNA (observed k_{cat} of 0.88 min^{-1}) [52]. The BCDX2 and CX3 paralog complexes bind to a diverse range of DNA substrates such as ssDNA, 3' and 5' flaps, gapped circular DNA, and nicked duplex substrates [52]. Although the BCDX2 complex ssDNA binding activity is ATP-independent, ATP hydrolysis is stimulated by ssDNA. The human Shu (hShu) complex is composed of SWSAP1 and SWS1 (**Figure 2a**). The hShu complex also likely includes SPIDR and PDS5B, although the interaction with PDS5B may not be direct [50]. Consistent with a RAD51 mediator function, SWS1-SWSAP1 promotes RAD51 recruitment into DNA repair foci, enables sister-chromatid exchange and replication restart, and counteracts FIGNL1 anti-recombinase activity [21, 50, 53, 54]. The CX3 complex, like hRAD51, has additional functions in mitochondrial replication and maintenance as well as in the Fanconi anemia (FA) pathway during interstrand crosslink repair [55-57]. The role of the RAD51 paralogs during replicative DNA damage is discussed below.

1.5 The yeast Shu complex

The Shu complex from *S. cerevisiae* is a heterotetramer composed of Csm2, Psy3, Shu1, and Shu2 (**Figure 2**). The Shu complex was first discovered by the Rothstein group in 2005 in a genetic screen for suppressors of *top3Δ* slow growth defects [58]. Shor et al. demonstrated that disruption of the Shu complex genes also suppressed the sensitivity of *sgs1Δ* mutants to hydroxyurea, which inspired the name Shu for Suppressor of *sgs1Δ* HydroxyUrea sensitivity, for its members *SHU1*, *SHU2*, and the complex itself. By that time, *CSM2* (Chromosome Segregation in Meiosis) had been identified in a screen for mutations that lead to defects in meiotic chromosome segregation [59]. Similarly, *PSY3* (Platinum SensitivitY) was named after being obtained as a hit in a screen for mutations conferring sensitivity to cisplatin and oxaliplatin [60]. Previous work had shown that deletion of each of the Shu complex genes leads to a similar mutator phenotype [61] and confers sensitivity to both MMS and 4-Nitroquinoline-1-oxide (4-NQO) [62, 63]. Moreover, a yeast-2-hybrid screen by Ito et al. [64] had reported physical interactions between the Shu complex proteins. Shor et al. [58] further explored these lines of evidence showing that the Shu complex genes are epistatic to each other and belong to the *RAD52* epistasis group and that their gene products localize to the nucleus and prevent mutations from TLS. Importantly, these results suggested that Csm2, Psy3, Shu1, and Shu2 form a complex that promotes error-free repair of DNA lesions through HR. The formation of a stable complex *in vivo* with a 1:1:1:1 ratio was later confirmed by affinity purification and gel filtration of tagged Shu complex proteins from yeast cell extracts [22].

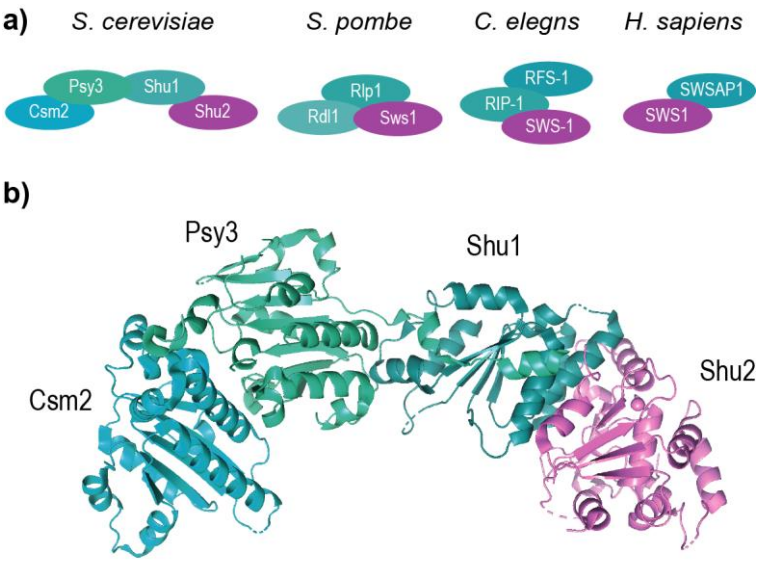

Figure 2. The Shu complex is an evolutionary conserved Rad51 paralog complex.

(**a**) Schematic representation of the Shu complex from different model organisms. The Rad51 paralogs are colored in variations of aquamarine, while the SWIM domain-containing proteins are colored in purple. (**b**) Crystal structure of the budding yeast Shu complex. PDBID: 5XYN. [23].

Shortly after the *S. cerevisiae* Shu complex was described, the Russell group [21] identified *SWS1* as the *S. pombe* and human homologs of *SHU2* (**Figure 2a**). Importantly, Martín et al. showed that deletion of *spSWS1* leads to moderate sensitivity to MMS and suppressed the growth defect and MMS sensitivity associated with the deletion of *RQH1*, the fission yeast homolog of *scSGS1*. These phenotypes resemble the ones observed in budding yeast, and together, these results suggested that the Shu complex is conserved among eukaryotes. Moreover, this work identified the other members of the fission yeast Shu complex to include Rlp1 and Rdl1 (**Figure 2a**). Importantly, *RLP1* and *RDL1* are divergent RAD51 paralogs, which further supports the role of the Shu complex in HR. Martín et al. also identified a hallmark domain of Shu2/SWS1, the SWIM (SWI2/SNF2 and MuDR) domain. The SWIM domain is a zinc finger-like motif of unknown function, a CXC…X_N…CXH, where X is any amino acid, that is found in proteins across all

domains of life [65]. This finding proved of great significance since the phylogenetic analysis based on this domain enabled the identification of Shu complex homologous in other eukaryotic organisms such as flies, fish, and worms [66, 67] (**Figure 2a**). Overall, these findings suggest that the Shu complex is an ancient and conserved HR complex.

Besides being the first identified, the Shu complex from budding yeast is the only one for which crystal structures have been obtained. Three high-resolution crystal structures of the Csm2-Psy3 heterodimer and a more recent crystal structure of the entire Shu complex have been independently solved [22, 23, 68, 69] (**Figure 2b**). Previously, *PSY3* and *SHU1* were proposed as divergent *RAD51* paralogs based on particular similarities in the protein sequences to other *RAD51* paralogs, including the presence of a Walker B motif in Psy3 [21]. This idea was strongly supported by the analyses of the Shu complex structures, which show that Psy3, Csm2, and Shu1 each individually have overall protein folds that resemble Rad51. These results were somewhat surprising because none of these proteins have a Walker A motif, which is typically observed in Rad51 paralogs and Rad51. It worth noting that, so far, no other crystal structure of a Rad51 paralog from any species has been solved, which highlights the relevance of the budding yeast Shu complex as a model to better understand the role of the Rad51 paralogs.

An important finding arising from the structural analysis of the Shu complex is that Csm2 and Psy3 have a disordered loop that is analogous to the L2 loop of Rad51, which is important for DNA binding [68, 70]. The individual contribution of the L2 loops of Csm2 and Psy3 to DNA binding was confirmed by electromobility shift assay (EMSA) using WT purified proteins and purified proteins bearing mutations in their L2 loops [68]. Consistently, recombinant Csm2 and Psy3 form a stable heterodimer that binds DNA in an ATP-independent manner, whereas the Shu1-Shu2 heterodimer does not exhibit DNA binding properties [22]. Later it was shown that Csm2-

Psy3 preferentially bind to double-flap DNA substrates and 3' overhangs, both DNA structures utilized in early HR events [45]. This suggests that Csm2-Psy3 represent the DNA binding subunits of the Shu complex.

The initial clues to understanding the role of the budding yeast Shu complex during HR come from the findings that disruption of the Shu complex partially suppresses the increased Rad52 foci observed in *sgs1Δ* cells [58]. Analogous results were obtained in fission yeast, suggesting a conserved role during early HR [21]. Consistently, siRNA knockdown of SWS1 in human cells leads to a decrease in spontaneous Rad51 foci [21]. Further evidence for an early role for the Shu complex during HR came from Mankouri et al. [71], who demonstrated that the Shu complex promotes the formation of MMS-induced recombination intermediates during S-phase. These recombination intermediates, or X-molecules, can be identified and quantified using 2D gel electrophoresis and are characteristic of *sgs1Δ* mutants treated with MMS [72, 73]. In particular, this work showed that mutation of the Shu complex genes leads to a decrease in the formation of the X-molecules when *sgs1Δ* cells are MMS treated.

An early role during HR is also observed for the canonical *RAD51* paralog complexes in most species. For instance, the budding yeast Rad55-Rad57 paralog complex promotes Rad51 filament formation [43, 74, 75]. Importantly, our group, in collaboration with Dr. Sung's group, demonstrated that *in vitro*, the budding yeast Shu complex enables more efficient loading of Rad51 onto ssDNA that is pre-coated with RPA [41]. These results uncovered the role of the Shu complex as a Rad51 mediator. Interestingly, no direct physical interaction between the yeast Shu complex and Rad51 has been found to date. Instead, the Shu complex role as Rad51 mediator is dependent on its physical interaction with Rad55-Rad57 which directly interacts with Rad51 [41, 45].

Consistently, *RAD55* knockout cells are epistatic to the Shu complex genes for MMS sensitivity [45].

Rad51 filament formation is also controlled by the anti-recombinase activity of the Srs2 helicase [76, 77]. Interestingly, a conserved interaction between Srs2 and Shu2 was first identified in a high-throughput Y2H screen and was later observed in fission yeast [78-80]. In their early work, Shor et al. [58] reported that the disruption of the Shu complex rescued the lethality of an *srs2Δ sgs1Δ* double mutant. Again, this genetic interaction was found to be conserved in fission yeast, as it was also shown that deletion of SWS1 rescues *srs2Δ* phenotypes that are associated with the formation of toxic HR intermediates [21]. These physical and genetic interactions between the Shu complex and Srs2 led Bernstein et al. [46] to explore the hypothesis of a direct functional relationship between them. In their work, Bernstein et al. found that Shu1 modulates Srs2 focus formation, demonstrating that the Shu complex counteracts Srs2 activity. Interestingly, a similar role for the Rad55-Rad57 complex was also reported [42].

Despite these similarities, the Rad55-Rad57 complex is required for DSB repair whereas the Shu complex is dispensable [18]. This difference is reflected by the sensitivity of their mutants: while deletion of *RAD55* or *RAD57* leads to extreme sensitivity to ionizing radiation, Shu complex knock-out cells show no increased sensitivity when challenged with DSB inducing agents including ionizing radiation [58, 81]. Disruption of the Shu complex leads to sensitivity to replication-associated DNA damage, in particular to MMS. MMS damage is repaired by the base excision repair (BER) pathway during the G1 phase in an error-free manner. However, during S-phase, and particularly at replication intermediates, MMS-induced damaged is bypassed by a high-fidelity HR mechanism or by low-fidelity TLS. This DNA damage tolerance response is initiated by the monoubiquitination of PCNA by Rad6-Rad18 at K164 [82], while the high-fidelity branch

of this pathway, called error-free post-replicative repair, depends on further polyubiquitination PCNA by the Mms2-Rad5-Ubc13 complex [82]. Genetic analysis by the Xiao group [83], demonstrated that *MMS2* is epistatic to the Shu complex genes in regards to MMS sensitivity and mutagenesis and that the Shu complex acts downstream to PCNA polyubiquitination [84]. Consistently, our group demonstrated that the Shu complex promotes the error-free tolerance of MMS-induced lesions when the BER pathway is disrupted [18, 81]. While disruption of the Shu complex results in reduced cellular survival when many BER steps are inhibited, the most sensitivity was observed when the abasic sites accumulate. Overall, these findings place the Shu complex as a critical player of the error-free branch of the post replicative repair pathway.

1.6 Roles of RAD51 in replication-associated DNA damage

Accurate and timely DNA replication is critical to prevent genome instability. RAD51 is a central player in overcoming replication stress, which slows or stalls replication forks, threatening replication integrity [85]. In this section, I summarize the roles of the *RAD51* gene family during replication stress, including promoting fork reversal, protecting reversed forks, repairing and restarting broken replication forks, and post-replicative gap filling (**Figure 1c, d**).

1.6.1 RAD51 function in fork reversal

Upon replication fork stalling, fork reversal can promote genome stability by (*a*) limiting ssDNA accumulation, (*b*) relocating replication-blocking lesions in the context of dsDNA to allow the subsequent repair of the lesion by other repair pathways such as base excision repair, (*c*)

providing a template for lesion bypass through template switching, and (*d*) enabling HR-dependent replication restart [86, 87]. Stalled replication fork reversal or regression involves reannealing of the parental strands and annealing of the newly synthesized daughter strands, which converts a three-way DNA junction into a four-way DNA junction (**Figure 1c**). Migration of this Holliday-like junction extends the reversed arm, forming a so-called chicken-foot structure [86]. Many proteins can catalyze fork reversal *in vitro*, such as fork remodelers (SMARCAL1, ZRANB3, HLTF, and RAD54) or helicases (BLM, FBH1, WRN, and FANCM) [86, 88]. hRAD51 is similarly required for fork reversal [89]. How hRAD51 promotes fork reversal is still unclear, but several models are proposed. RAD51 may assist other factors to promote fork reversal where hRAD51 binding to the ssDNA at the chicken-foot arm might drive the reaction toward the reversed products [88, 90]. Alternatively, RAD51 bound to ssDNA at one of the stalled fork strands may invade the newly replicated strand, reannealing the parental DNA and thus displacing the newly synthesized strand [86, 91]. Surprisingly, hRAD51's fork-reversal role does not require its strand exchange activities and is BRCA2-independent [92-94]. The length of the ssDNA at the reversed arm during fork reversal initiation is not sufficient for RPA binding, and thus RAD51 filament mediators may not be needed [88]. Alternatively, the MMS22L-TONSL complex might perform mediator functions in this context [88].

1.6.2 RAD51 function in fork protection of reversed forks

RAD51 also protects reversed forks from uncontrolled enzymatic degradation (**Figure 1c**). When unprotected, the reversed arm is an entry point for CtIP-MRE11 with EXO1 or DNA2-mediated degradation [92, 94-97]. When BRCA2 stabilizes the hRAD51 filament on the ssDNA region of the reversed arm, fork degradation is inhibited [97, 98]. Consistently, hRAD51 filament

stabilization by overexpression of a catalytic dead RAD51 mutant can overcome *BRCA2* loss [99]. Furthermore, a *hRAD51* Fanconi anemia (FA) allele, *RAD51-T131P*, forms unstable filaments that impair fork protection without compromising HR when heterozygous with a wild-type *hRAD51* allele [100, 101]. RAD51 function in fork protection is likely structural, whereas its enzymatic activity is required for HR.

1.6.3 RAD51 function in the restart of reversed forks

When a replication fork is stalled and cannot be rescued by an incoming fork, cells rely on fork restart mechanisms to complete replication (**Figure 1c**). Reversed forks can be directly restarted or restored by the helicase RECQL1 or the translocase SMARCAL1 [102, 103]. An alternative restart mechanism involves DNA2-WRN-mediated limited resection at the regressed arms to produce a 3' overhang [104]. RAD51 filaments formed at a ssDNA 3' overhang regressed arm may drive an HR-directed restart by invading the homologous DNA ahead of the reversed fork [105, 106]. However, a detailed mechanism for HR-directed restart remains obscure. Similarly, in fission yeast, recent work shows that forks stalled at a replication fork barrier (RTS1-RFB) can be restarted by a DSB-independent HR-mediated process [107].

1.6.4 RAD51 function in the restart of broken forks by BIR

Replication fork breakage results in what is usually referred to as one-ended or single end DSB (**Figure 1d**). As mentioned above, the absence of a second DNA end makes cells rely on HR for their repair. Several scenarios can lead to fork breakage, such as the replisome encountering a ssDNA gap or transcription-replication collisions [108]. Broken replication forks can be repaired

by BIR. In yeast, this process begins with DNA end resection, followed by scRad51 filament assembly on the 3' ssDNA [105]. The scRad51 filament performs homology-directed strand invasion of the sister chromatid to form a D-loop that is extended by DNA synthesis [109]. Although error-prone, the range of this synthesis is limited by scMus81 cleavage of the Holliday junction at the D-loop or by merging with an incoming replication fork in the opposite direction [110]. Although most of our knowledge of BIR comes from yeast, there is evidence suggesting that this process is conserved in vertebrates [111, 112]. It is worth noting that an alternative scRad51-independent BIR pathway is also known, and it accounts for several processes described in human cells [109]. Finally, BIR drives the alternative lengthening of telomeres; however, the contribution of the hRAD51-dependent sub-pathway is still debated [109].

1.6.5 RAD51 function in post-replicative repair

In addition to its roles at replication forks, RAD51 is also central in an HR-driven post-replicative gap-filling pathway (**Figure 1c**). This process relies on a template switch between sister chromatids to complete replication at ssDNA gaps and serves as an error-free alternative to translesion synthesis (TLS) [113]. These ssDNA gaps are generated when the replisome bypasses polymerase-stalled DNA lesions, such as those that can arise from ultraviolet or MMS treatment [113]. As demonstrated in yeast, lesions on the lagging strand are bypassed due to the intrinsic discontinuous nature of lagging-strand DNA synthesis [114]. Meanwhile, lesions at the leading strand can be skipped by downstream repriming by PrimPol, a specialized polymerase conserved in many eukaryotes, including mammals [115, 116]. Although there is no PrimPol homolog in yeast, downstream leading strand repriming can be performed by Polα and primase [117]. Details of the gap-filling pathway have been best described in yeast, where it plays a major role in

tolerating replicative damage [91, 113]. In short, the ssDNA gaps are extended by the nucleases scExo1 and scMre11 and the helicase Pif1, followed by scRad51 filament assembly. This scRad51-coated gap invades the sister chromatid and displaces the daughter strand, which becomes paired with the free 3' end [73]. After DNA synthesis occurs, the sister chromatid junctions are dissolved by the Sgs1-Top3-Rmi1 complex. Importantly, this DNA damage-tolerance pathway is dependent on proliferating cell nuclear antigen (PCNA) polyubiquitination by the sequential activities of the Rad6-Rad18 and Mms2-Ubc13-Rad5 complexes. Most of these yeast factors have homologs in higher eukaryotes, suggesting that this process is evolutionarily conserved [118]. In response to replication stress, humans may rely on fork reversal and TLS, whereas yeast is thought to primarily use HR-mediated gap filling.

1.6.6 Role of the RAD51 paralogs in replication-associated DNA damage

Support for a role during the replication stress response comes from findings that, in many eukaryotes, *RAD51* paralog mutations lead to sensitivity to replicative DNA damage and defects in RAD51 recruitment [18, 19]. In yeast, the scRad55-Rad57 complex and scShu complex contribute to the repair and tolerance of replication-associated damage by promoting HR-dependent gap-filling [18]. As with scRad51, mutants lacking either of these complexes show increased mutagenesis that is TLS-dependent and delayed S-phase progression upon MMS treatment [58, 71, 81, 83, 84, 119]. The scShu complex is not required for DSB repair from IR, and Rad55 phosphorylation promotes MMS resistance but is dispensable for DSB repair, further supporting specific roles for these Rad51 paralog complexes during replication stress [58, 119]. Recently, we showed that the scShu complex preferentially binds abasic site-containing substrates and promotes error-free tolerance of these lesions, primarily on the lagging strand [120].

Similarly, recent evidence suggests a role for hRAD51 paralogs in replication-associated damage. For example, like hRAD51, both the BCDX2 and CX3 subcomplexes are required to protect forks from hMRE11 degradation [121]. The CX3 complex also promotes fork restart after hydroxyurea (HU) treatment [106, 121]. Additionally, XRCC2 and XRCC3 are phosphorylated by the ATR DNA damage response kinase to promote fork slowdown upon nucleotide depletion and DSB repair, respectively [122, 123]. Unlike the canonical RAD51 paralogs, our group showed that the hShu complex contributes to fork restart following HU treatment but is dispensable for fork protection [50].

1.7 DMC1 and the role of the RAD51 gene family during meiosis

Meiosis enables the generation of haploid cells or gametes. During meiosis, homologous chromosomes are first paired with each other. Homologous pairing requires an HR-mediated homology search to bring the two chromosomes together. HR during meiosis shares many essential features with mitotic HR-mediated DSB repair, including that both processes begin with a DSB.

Meiotic DSBs are physiologically generated by the meiosis-specific and universally conserved, SPO11 [124]. These DSBs are then processed in the same fashion as during mitotic DSB repair to generate nucleoprotein filaments that are responsible for the homology search. During meiosis, there is a strong preference to use the homologous chromosome as a repair template, as opposed to a preference for the sister chromatid observed in mitotic DSB repair. This process is known as homolog bias [125]. Proper homolog segregation also requires that crossovers are formed, as opposed to during mitotic DSB repair, where crossovers are less desirable [126].

Another key difference between meiotic and mitotic HR is that, in most species, meiosis requires the recombinase function of DMC1 at the core of the nucleoprotein filament [127].

DMC1 is a conserved meiosis-specific RAD51 paralog that arose from an early gene duplication event in the eukaryotic lineage [15]. Unlike the other RAD51 paralogs, DMC1 still resembles RAD51, sharing 54% sequence identity in humans and 45% in yeast. Consistent with this, the biochemical properties, nucleoprotein filament structure, and recombinase activity of DMC1 are remarkably similar to those of RAD51 [128].

scRad51 and scDmc1 have distinct functions during meiosis. scDmc1 acts as the main recombinase, while scRad51 plays an accessory role to mediate the assembly and regulate the activity of scDmc1 [127]. scRad51's recombinase activity is dispensable during meiosis and is actively inhibited, primarily by the Hed1 protein [127, 129]. However, scRad51 is required for scDmc1 focus formation and the establishment of homolog bias [130]. It is still not known if these distinct roles are conserved in vertebrates. scRad51 and scDmc1 are distinctively distributed within the meiotic nucleoprotein filament and tend to self-aggregate forming side-by-side homotypic filaments [128, 131, 132]. Although its role is still unclear, one possibility is that this would prevent Hed1-inactivated RAD51 monomers to intercalate in DMC1 filaments [131].

DMC1 and RAD51 in yeast and humans also demonstrate differences that may explain the nearly universal need for two meiotic recombinases. Unlike RAD51, DMC1 can tolerate mismatches during heteroduplex formation [133]. More recently, Steinfeld et. al. [134] elegantly identified conserved residues in the L1 DNA-binding loop of DMC1 that are responsible for this mismatch tolerance. This DMC1-specific feature likely enables recombination between homologous chromosomes that contain mismatches, contributing to homolog bias.

Recent work shows that meiotic scRad51-scDmc1 filaments are more stable than mitotic scRad51 filaments. Unlike scRad51 filaments, which are readily disassembled by the anti-recombinase Srs2 to promote SDSA during mitotic DSB repair, scDmc1 is a strong inhibitor of Srs2, which renders the meiotic scRad51-Dmc1 filaments resistant to Srs2 disassembly [135]. An exciting possibility is that this enhanced stability of the meiotic filament contributes to the key step of crossover production.

Given the critical role of scRad51 during meiosis, it is not surprising that the scRad51 paralogs are also important for meiosis [136, 137]. Deletion of *RAD55* and *RAD57* leads to meiotic defects that greatly resemble those observed in *rad51* mutants, including impaired homolog bias and decreased spore viability [136, 138]. Like the canonical *scRAD51* paralogs, the *scShu* complex mutants also show meiotic defects, but these are not as severe as those observed upon *RAD51*, *RAD55*, or *RAD57* deletion [22, 137]. Interestingly, unlike during mitotic HR where deletion of any of the four *scShu* complex members leads to a complete loss of function, *C2M2* and *PSY3* are more important during meiosis than *SHU1* and *SHU2* [22]. Consistent with their role as Rad51 mediators, deletion of *RAD55-RAD57* or the *scShu* complex impairs recruitment of scRad51 to meiotic DSBs [22]. Similarly, Rad51 paralogs in fission yeast, worms, and plants are also important for meiosis [67, 139, 140]. Not much is known about the meiotic role of the RAD51 paralogs in vertebrates. However, a recent publication by Abreu et al. [49] shed light on the importance of the murine Shu complex during meiosis. Both female and male mice with either *Sws1*$^{-/-}$ or *Swsap1*$^{-/-}$ knockout mutations are sterile, cannot complete meiosis, and have decreased Rad51 and Dmc1 foci [49]. These phenotypes are reminiscent of the *scShu* complex mutants. Despite the similarities between RAD51 and DMC1, direct physical interactions between the

RAD51 paralogs and DMC1 have not yet been described. Therefore, it appears that the RAD51 paralogs are important during meiosis due to their role as RAD51 mediators.

1.8 Overarching hypothesis

Yeast cells with mutations in the Shu complex are primarily sensitive to MMS. However, MMS induces a complex and diverse set of DNA lesions and repair intermediates that are usually handled by the BER repair pathway. In an attempt to better understand why Shu complex mutants exhibit increased sensitivity to MMS, previous work from our laboratory studied the genetic interaction between the Shu complex and genes from the BER repair pathway [81]. Godin et al. found that the deletion of the Shu complex genes leads to an increase in the MMS sensitivity of cells with deletions of BER genes [81]. Notably, one of the strongest effects was observed when deletions of the Shu complex genes were combined with deletions of the enzymes that process abasic (AP) sites. These results suggested that the Shu complex may play a critical role in the tolerance of AP sites.

Therefore, in this thesis, I sought to validate the hypothesis that the yeast Shu complex promotes error-free tolerance of AP sites. I used a combination of the genetic and molecular biology strategies to approach this problem and our results are summarized in Chapter II.

To further explore which MMS-induced DNA lesions are tolerated by a Shu complex dependent mechanism, I analyzed genome-wide mutational patterns of Shu complex mutant cells chronically exposed to MMS. Importantly, these results confirmed the critical role of the Shu complex in the tolerance of AP sites. However, this analysis also suggested that the Shu complex

plays a role in the error-free tolerance of 3-Methylcytosines. My tests of this prediction are presented in Chapter III.

1.9 Acknowledgments

This chapter is modified from the following collaborative published work:

Bonilla, B*., S. R. Hengel*, M. K. Grundy and K. A. Bernstein (2020). "RAD51 Gene Family Structure and Function." Annu Rev Genet. * *Denotes equal contribution.*

The selected sections and the figure were written and made by B.B. with contributions from S.R.H., M.K.G., and K.A.B.

2.0 The Shu complex promotes error-free bypass of abasic sites

Accurate DNA replication is essential for genomic stability and cancer prevention. Homologous recombination is important for high-fidelity DNA damage tolerance during replication. How the homologous recombination machinery is recruited to replication intermediates is unknown. Here, we provide evidence that a Rad51 paralog-containing complex, the budding yeast Shu complex, directly recognizes and enables tolerance of predominantly lagging strand abasic sites. We show that the Shu complex becomes chromatin-associated when cells accumulate abasic sites during S-phase. Shu complex DNA binding mutants are sensitive to MMS, are not chromatin enriched, and exhibit increased mutation rates. We propose a role for the Shu complex in recognizing abasic sites at replication intermediates, where it recruits the homologous recombination machinery to mediate strand-specific damage tolerance.

2.1 Introduction

DNA is constantly damaged by endogenous and exogenous sources such as alkylating agents, reactive oxygen species, and radiation. Each type of DNA damage is recognized and repaired using a specialized repair pathway. Repair of DNA base damage by base excision repair (BER) begins with recognition and excision of the damaged base by a DNA glycosylase resulting in abasic [also known as apurinic/apyrimidinic (AP)] site formation. In mammalian cells, spontaneous depurination events and repair of endogenous DNA damage generate between 10,000-30,000 abasic sites per day [141-143], making them one of the most common genotoxic

lesions. Most abasic sites are repaired in a high-fidelity manner by the subsequent steps of BER. During replication, abasic sites are strong blocks to the replicative DNA polymerases epsilon and delta[144, 145]. When synthesis at a replication fork is blocked by an abasic site, the lesion must be bypassed. Abasic sites within the context of DNA replication are often resolved by either low-fidelity TLS[145] or high-fidelity HR[146]. How abasic sites at stalled replication forks are targeted to distinct bypass/repair pathways remains largely unknown.

The Rad51 paralogs are a highly conserved family of proteins structurally similar to the central HR protein, Rad51[147]. The Rad51 paralogs form sub-complexes that aid in Rad51 filament formation and strand invasion, two key steps in HR. Mutations in the human RAD51 paralogs are associated with predisposition to breast and ovarian cancer, as well as Fanconi anemia-like syndromes[148, 149]. The Shu complex is an evolutionarily conserved complex, which contains Rad51 paralogs. The *S. cerevisiae* Shu complex is a heterotetramer composed of Shu2 (a SWIM-domain containing protein) and the Rad51 paralogs Csm2, Psy3, and Shu1[58, 150-152]. Shu complex mutant cells are especially sensitive to the alkylating agent, MMS, which among other agents causes replication blocking lesions, suggesting that the Shu complex may help facilitate their repair[58, 66, 71, 81, 84].

Here we show that Csm2-Psy3 also aids in preventing TLS-induced mutations that arise in the lagging strand during replication of DNA templates containing abasic sites. Therefore, we propose a model whereby the Shu complex responds to abasic sites on the lagging strand of a replication fork to facilitate an error-free, strand-specific damage tolerance pathway.

2.2 Results

2.2.1 Csm2 is the primary DNA binding subunit

To determine the role of DNA binding in *S. cerevisiae* Shu complex function, we modeled the putative DNA binding loops of the Shu complex members, the Rad51 paralogs, Csm2 and Psy3 [153]. We mutated the lysine and arginine residues within these predicted DNA binding loops (for Csm2: K189A, R190A, R191A, R192A; *csm2-KRRR*) (for Psy3: K199A, R200A, K201A; *psy3-KRK*)[151] (**Figure 3a**). To assess the DNA binding capabilities of Csm2-KRRR and Psy3-KRK, we co-expressed and purified Csm2-Psy3, Csm2-Psy3-KRK, Csm2-KRRR-Psy3, and Csm2-KRRR-Psy3-KRK complexes from *E. coli* and assessed their capacity to bind their preferred DNA substrate, double-flap DNA substrate, or Y DNA[45] by fluorescence polarization anisotropy (**Figure 3b**; **Supplemental Table 1**). Whereas Csm2-Psy3 binds the double-flap DNA substrate with an equilibrium dissociation constant (K_d) of 435 ± 37 nM, Csm2-KRRR-Psy3 and Csm2-KRRR-Psy3-KRK mutant proteins exhibit minimal DNA binding, while Csm2-Psy3-KRK exhibits more than a 6-fold reduction in DNA binding affinity relative to Csm2-Psy3 (K_d > 2.8 μM; **Figure 3b; Supplemental Table 1**). These results indicate that Csm2 is the primary DNA binding subunit.

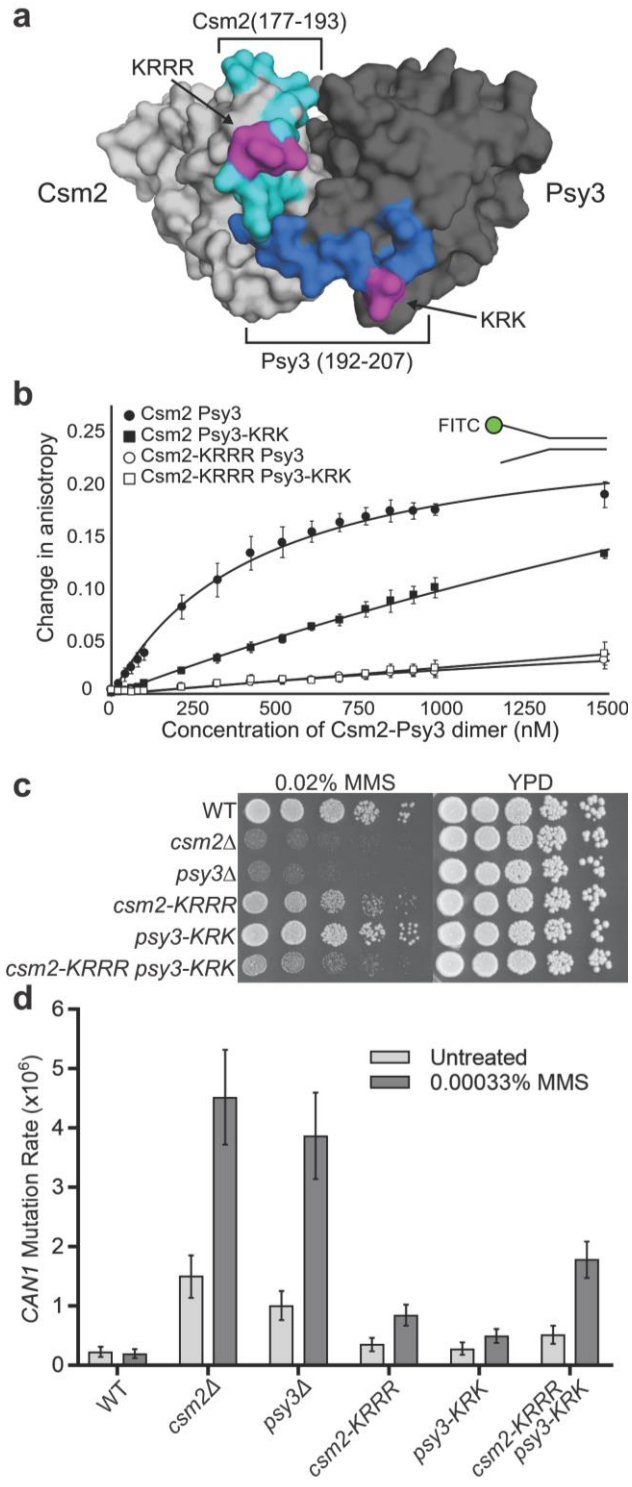

Figure 3. Csm2 and Psy3 DNA binding activities are important for Shu complex function

(a) Surface view of *S. cerevisiae* Csm2 (light grey; K189, R190, R191, R192) and Psy3 (dark grey; K199, R200, K201) with the predicted DNA binding residues highlighted in magenta and predicted DNA binding loops in light and

dark blue, respectively ([151]; Model structure derived from PDB 3VU9). (**b**) *In vitro* analysis of Csm2-Psy3 binding to a DNA fork substrate compared to Csm2-Psy3 DNA binding mutants (Csm2-K189A/R190A/R191A/R192A and/or Psy3-K199A/R200A/K201A) by fluorescence anisotropy. Increasing concentrations of Csm2-Psy3 or the indicated mutants were added to 25 nM 3' fluorescein-labeled double-flap substrate and DNA binding was assessed. Dissociation constants (K_d) and associated standard deviations from triplicate experiments were determined by non-linear curve fitting to a one-site binding model. (**c**) Cells expressing the *csm2-KRRR psy3-KRK* double mutant exhibit increased MMS sensitivity relative to *csm2-KRRR* or *psy3-KRK* cells. The DNA binding residues shown in (**a**) were mutated to alanines and integrated into the genomic *CSM2* and *PSY3* loci. Five-fold serial dilution of WT, *csm2*Δ*, psy3*Δ*, csm2-KRRR, psy3-KRK,* and *csm2-KRRR psy3-KRK* cells onto rich YPD medium or YPD medium containing 0.02% MMS were incubated for 2 days at 30˚C before being photographed. (**d**) Spontaneous and MMS-induced mutation rates at the *CAN1* locus were measured in WT, *csm2*Δ*, psy3*Δ*, csm2-KRRR, psy3-KRK*, and *csm2-KRRR psy3-KRK* cells. Error bars indicate 95% confidence intervals. This figure was published in [120].Author contribution: Panels a and b: performed by JCR; panel c: performed by BWH; panel d: performed by CAP and analyzed by BB.

2.2.2 Csm2-Psy3 DNA binding motif is necessary for repair *in vivo*

We next asked whether the Csm2-Psy3 DNA binding activity would be important for their function *in vivo*. To address this question, we analyzed *S. cerevisiae* cells expressing *csm2-KRRR* and *psy3-KRK* DNA binding mutants for MMS sensitivity. We observe very modest MMS sensitivity of *csm2-KRRR* cells, while *psy3-KRK* cells are largely insensitive to 0.02% MMS, and the *csm2-KRRR psy3-KRK* double mutant cells exhibit increased MMS sensitivity and reduced viability compared to the single mutants (**Figure 3c, Appendix A: Figure 15)**. We next examined whether Csm2 and Psy3 DNA binding would be important for suppressing mutations by measuring *CAN1* mutation rates (**Figure 3d**). Similar to the MMS sensitivity, we find that *csm2-KRRR psy3-KRK* double mutant cells exhibit increased spontaneous or MMS-induced mutation rates compared

to wild-type cells (**Figure 3d**). We next used western blot analysis to ensure that the phenotypes we observed in *csm2-KRRR* and/or *psy3-KRK* cells are not due to altered protein expression (**Appendix A: Figure 16a**). Similarly, we do not observe changes in Shu complex integrity or known protein interactions by yeast-2-hybrid or during recombinant protein purification, where the Csm2-KRRR Psy3-KRK elution profile is similar to wild-type complexes (**Appendix A: Figure 16b-d**). Therefore, Csm2 and Psy3 DNA binding residues are important for Shu complex function without affecting complex formation. Furthermore, our findings suggest that the combined DNA binding activities of Csm2 and Psy3 are critical for MMS resistance and suppressing mutations.

2.2.3 Csm2 is chromatin enriched when abasic sites accumulate

We find that disruption of the DNA binding activities of Csm2 and Psy3 leads to increased mutation rates (**Figure 3d**) and our previous work shows that when abasic sites accumulate in *csm2*Δ cells, mutation rates increase over 1000-fold[81]. Therefore, we wanted to determine if Csm2-Psy3 DNA binding is critical for MMS resistance *in vivo* when abasic sites accumulate. Abasic sites can be forced to accumulate by deleting the enzymes responsible for their processing, which include the AP endonucleases (*APN1 APN2*) and AP lyases (*NTG1 NTG2*). Suggesting that Csm2-Psy3 DNA binding activities are important when abasic sites accumulate, we observe that *csm2-KRRR psy3-KRK apn1*Δ *apn2*Δ *ntg1*Δ *ntg2*Δ cells exhibit increased MMS sensitivity that is comparable to a *csm2*Δ *apn1*Δ *apn2*Δ *ntg1*Δ *ntg2*Δ cell (**Figure 4a**).

Since we find that the Shu complex binds most tightly to double-flap DNA[45, 151] and is important for resistance to abasic sites (**Figure 4a**), we hypothesized that Csm2-Psy3 may be enriched at chromatin when abasic sites accumulate during replication. To test this hypothesis, we

performed chromatin fractionation experiments. We first arrested Csm2-6HA expressing cells (with or without *apn1*Δ *apn2*Δ *ntg1*Δ *ntg2*Δ) in G1 with alpha-factor and released these cells into 0.02% MMS for 1 hour before lysis and fractionation. We observe Csm2 chromatin association increases 4.5-fold when abasic sites accumulate and this enrichment depends on Csm2 DNA binding activity (**Figure 4b**). Moreover, our preliminary data shows that the recruitment of Csm2 to the chromatin is critical for Rad51 chromatin association (**Appendix A: Figure 17**). In contrast to Csm2, we find that RPA chromatin association occurs independently of Csm2 DNA binding activity (**Figure 5a**).

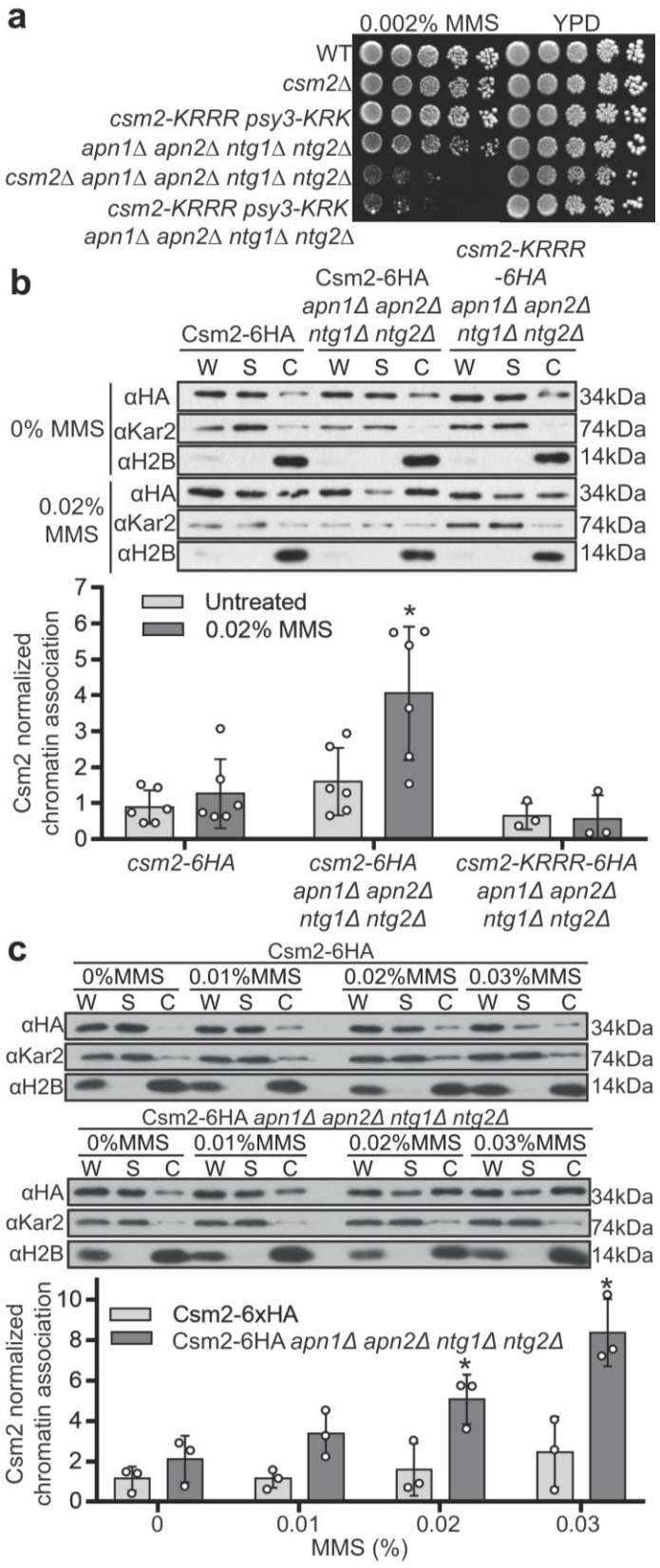

Figure 4. Csm2 is recruited to chromatin when abasic sites accumulate

(**a**) Csm2-Psy3 DNA binding motif is critical for survival when abasic sites accumulate. Five-fold serial dilutions of the indicated yeast strains on rich medium (YPD) or rich medium containing 0.002% MMS. Abasic sites accumulate by combined disruption of the AP endonucleases (*APN1, APN2*) and AP lyases (*NTG1, NTG2*) in the presence of MMS. Csm2-Psy3 double DNA binding mutant (*csm2-KRRR psy3-KRK*) exhibits similar MMS sensitivity to *csm2*Δ cells when abasic sites accumulate. (**b**) Csm2 is enriched at the chromatin when abasic sites accumulate in a DNA binding-dependent manner. Csm2-6HA expressing cells were synchronized in G1 with alpha-factor and released into YPD medium or YPD medium containing 0.02% MMS for 1 hour before cellular fractionation. Csm2 protein levels from whole-cell extract (W), supernatant (S), and chromatin (C) fractions from the indicated strains were determined by western blot using HA antibody. Kar2 and histone H2B were used as fractionation controls (S and C, respectively). The results from 3-5 experiments were plotted with standard deviations, as fold enrichment relative to the untreated WT (Csm2-6HA). The p-value between Csm2-6HA *apn1*Δ *apn2*Δ *ntg1*Δ *ntg2*Δ and WT (treated and untreated) or csm2-KRRR-6HA *apn1*Δ *apn2*Δ *ntg1*Δ *ntg2*Δ was calculated using an unpaired two-tailed Student's t-test between experimental samples and in each case was $p \leq 0.05$ (**c**) Csm2 chromatin association increases in an MMS dose-dependent manner. Same as (b) except that Csm2-6HA or Csm2-6HA *apn1*Δ *apn2*Δ *ntg1*Δ *ntg2*Δ were treated with 0%, 0.01%, 0.02%, or 0.03% MMS and results were quantified as described in (**b**). This figure was generated by BB and published in [120].

We next examined whether Csm2 chromatin association increases in an MMS dose-dependent manner. To test this, we treated Csm2-6HA expressing cells (with or without *apn1*Δ *apn2*Δ *ntg1*Δ *ntg2*Δ) with different MMS concentrations for 1 hour (0%, 0.01%, 0.02%, and 0.03%). Importantly, we observe Csm2 chromatin association increases in an MMS dose-dependent manner (~2- to 7-fold) when abasic sites accumulate (**Figure 4c;** $p = 0.02$ for 0.02% MMS and $p = 0.01$ for 0.03% MMS). We also observe a reproducible, although not statistically significant, a two-fold increase in Csm2 chromatin association in WT cells comparing untreated to 0.03% MMS (**Figure 4c**). Consistent with specificity for MMS-induced damage and abasic

sites, we do not observe Csm2 enrichment when forks are stalled with HU (**Figure 5b**). Overall, these results suggest that the Shu complex is enriched at chromatin when abasic sites accumulate.

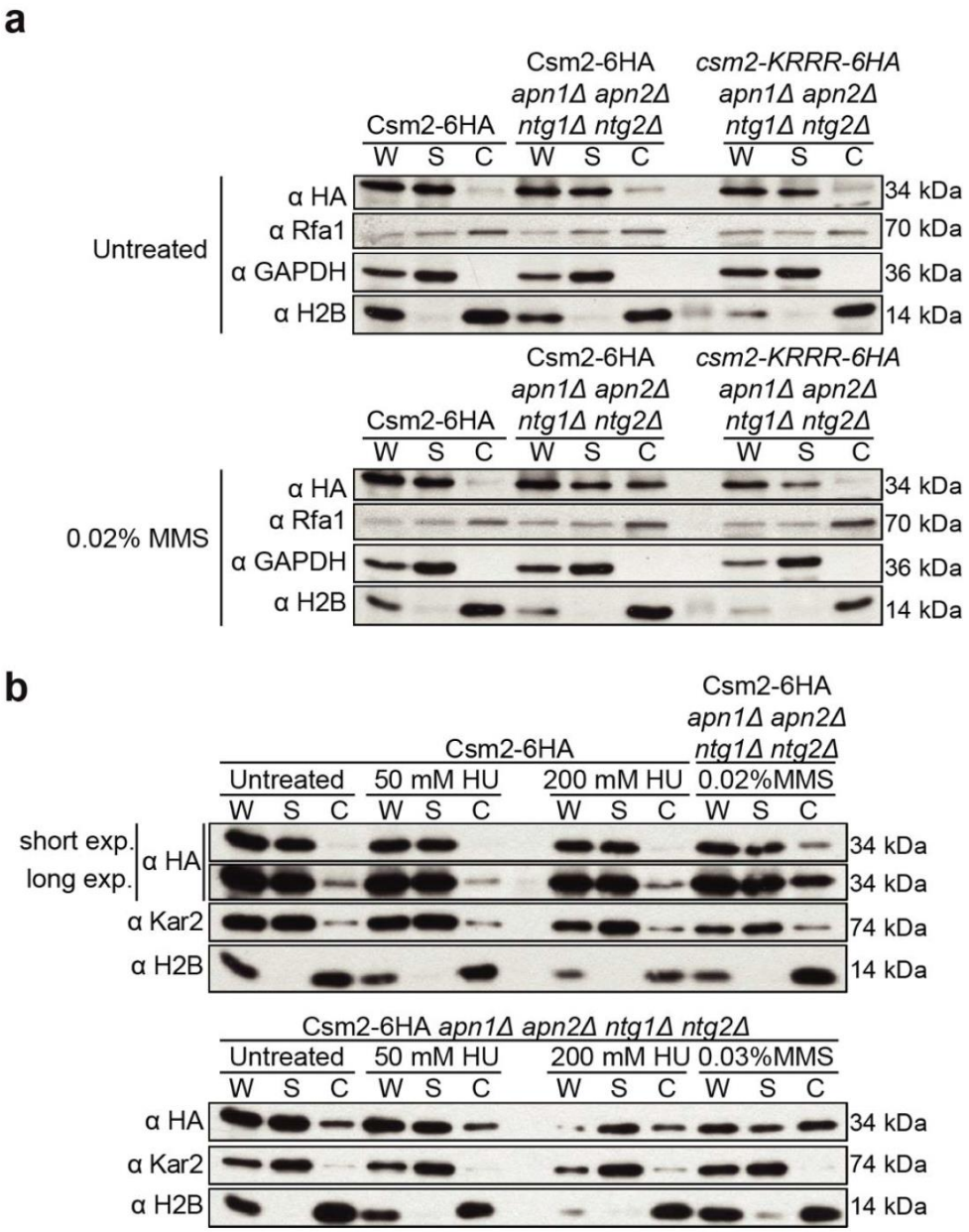

Figure 5. Csm2 chromatin enrichment is MMS specific

(**a**) Unlike Csm2, RPA chromatin association is independent of Csm2 DNA binding. Csm2-6HA expressing cells were synchronized in G1 with alpha-factor and released into YPD medium or YPD medium containing 0.02% MMS for 1 hour before cellular fractionation. Csm2 protein levels from whole-cell extract (W), supernatant (S), and chromatin (C) fractions from the indicated strains were determined by western blot using HA antibody. RPA chromatin association was assessed using a Rfa1-specific antibody. GAPDH and histone H2B were used as fractionation controls (S and C, respectively). (**b**) Csm2 is not chromatin enriched upon non-template induced replication stress. Csm2-6HA

or Csm2-6HA *apn1*Δ *apn2*Δ *ntg1*Δ *ntg2*Δ cells were synchronized in G1 with alpha-factor and released into YPD medium or YPD medium containing MMS (0.02% or 0.03%) or HU (50 mM or 200 mM) for 1 hour before cellular fractionation. Csm2 protein levels from whole-cell extract (W), supernatant (S), and chromatin (C) fractions from the indicated strains were determined by western blot using HA antibody. Kar2 and histone H2B were used as fractionation controls (S and C, respectively). This figure was generated by BB and published in [120].

2.2.4 Csm2-Psy3 suppress lagging strand abasic site mutations

To determine if Csm2 and Psy3 facilitate the bypass of abasic sites, we assessed how disruption of these genes influences the *CAN1* mutation rate and spectrum induced by the human cytidine deaminase, APOBEC3B. APOBEC family cytidine deaminases induce genomic hypermutation in human tumors[154-156]. Bioinformatic analysis of mutations in cancer genomes[157-159] and experiments in yeast[160] and bacterial systems[161] indicate APOBECs deaminate the lagging strand template during DNA replication. APOBEC3B-induced mutation rates and spectra were previously measured within yeast with *CAN1* at a location 16 kB centromere proximal to ARS216. In this setting, APOBEC-induced mutations occur primarily at G bases in leftward moving forks due to the deamination of cytidines on the lagging DNA strand[160, 162] (**Figure 6a**). Moreover, the APOBEC3B-induced dU is efficiently removed by the uracil glycosylase, Ung1, which results in the formation of synthesis-blocking abasic sites on the template of Okazaki fragments (**Figure 6a**). We used this system to determine if Csm2 and Psy3 facilitate bypass of abasic sites induced by APOBEC3B during replication of the lagging strand *in vivo*. We find that combining APOBEC3B expression with Shu complex defects results in a synergistic increase in *CAN1* mutation rates to levels observed in *ung1* deletion strains, in which all APOBEC3B-induced lesions are converted to mutations (**Figure 6b**). Importantly, *CSM2* or *PSY3* deletion in combination with *ung1*Δ results in mutation rates similar to the *ung1* single

deletion (**Figure 6b**), indicating that Shu complex genes are epistatic with *UNG1* in their ability to decrease APOBEC3B-induced mutation. Sequencing of *can1* mutants from *csm2*Δ *ung1*Δ produced nearly exclusively G to A transitions (**Figure 6c**), confirming that Ung1 operates prior to Csm2 in avoiding APOBEC3B-induced mutations. In contrast, *CAN1* mutation spectra in both *csm2*Δ and *psy3*Δ cells revealed both G to C transversions and G to A transitions, consistent with mutations caused by Rev1-mediated and A-rule polymerase-mediated TLS past abasic sites[162] generated by Ung1 glycosylase activity. Moreover, the *can1* mutations in the *csm2*Δ and *psy3*Δ strains maintained a G nucleotide strand-bias observed in wild-type and exacerbated in *ung1*Δ cells (**Figure 6d**), which is indicative of lagging strand-associated mutagenesis. Together these results indicate that the Shu complex promotes an error-free template switch mechanism to inhibit the conversion of abasic sites in the lagging strand template to mutations.

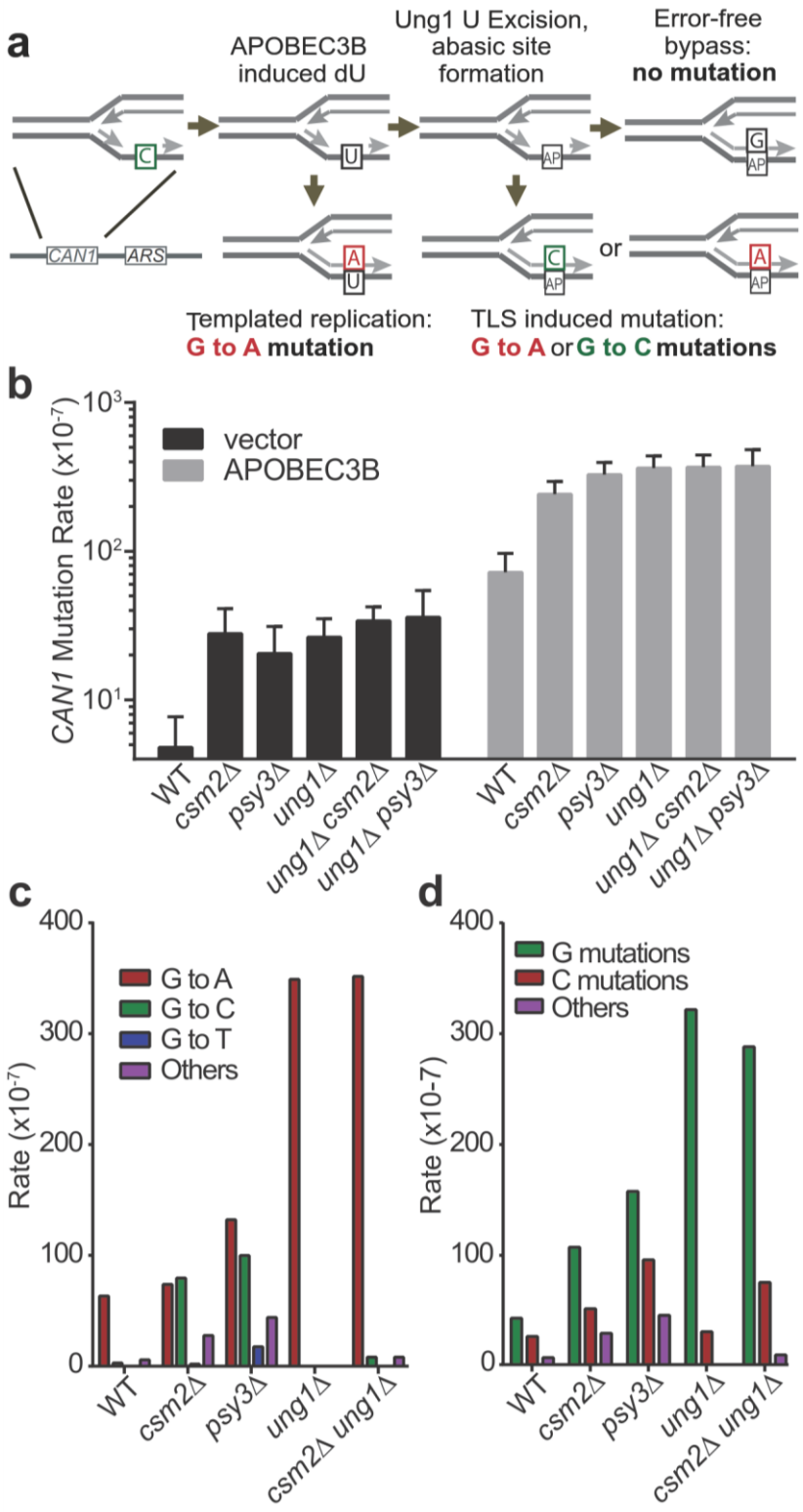

Figure 6. Shu complex proteins, Csm2 and Psy3, promote bypass of DNA replication-associated APOBEC3B-induced lesions

(**a**) APOBEC3B-induced mutation rates on the lagging strand of a replication fork measured using a *CAN1* reporter integrated 16 kb from ARS216 on chromosome II. Expression of the cytidine deaminase APOBEC3B induces primarily lagging strand mutations caused by dU templated replication (G to A transition). The uracil glycosylase Ung1 removes U resulting in abasic site formation (AP) in the lagging strand, which can be bypassed by TLS (G to A transition, G to C transversion). (**b**) *CSM2* and *PSY3* are in the same pathway as *UNG1* and their deletion results in similar mutation rates individually or in combination with each other. Mutation rates of the indicated genotypes were measured in *CAN1* reporter strains transformed with either an empty or APOBEC3B-expressing vector. Error bars indicate 95% confidence intervals. (**c**) In the absence of *CSM2* or *PSY3*, abasic sites accumulate and TLS predominates resulting in primarily G to A transitions (red) or G to C transversions (green) within the *CAN1* locus. APOBEC3B expression in WT, *ung1*Δ, or *csm2*Δ *ung1*Δ cells primarily result in G to A transitions. The rate reported represents the proportion of the Can-R mutants observed from sequencing multiplied by the mutation rate determined in (**b**). G to T substitutions are indicated in blue. "Other" mutations consisting of rare substitutions at A:T base pairs, insertions, deletions, and complex events composed of multiple mutations are depicted in purple. (**d**) The strand bias of *CAN1* mutations from APOBEC3B expression was evaluated by Sanger sequencing. APOBEC3B expression results in a mutation bias in the lagging strand from templated replication of C deaminations. *CSM2*, *PSY3*, or *UNG1* deleted cells exhibit more G mutations (green) than C mutations (red). Other mutations as defined in (**b**) are indicated in purple. Individual mutation rates were calculated as in (**c**) Statistical significance of strand bias in APOBEC3B-expressing strains was determined by a two-tailed G-test with $p < 0.05$ for all genotypes. This figure was published in [120]. Author contribution: panel a: BB; panels b-d: TMM, EM and SAR.

2.3 Discussion

DNA damage can arise from many different sources and damage that is encountered by the replication fork can result in fork stalling, collapse, and DSB formation (**Figure 7**). Our results suggest that the leading and lagging strands may be differentially recognized by specific DNA repair factors and targeted for repair through unique mechanisms. For example, the lagging strand

contains more ssDNA regions, which inherently make it more prone to spontaneous damage as well as accessible to DNA damaging agents. Here we propose that the Rad51 paralogs, Csm2-Psy3, directly recognize and tolerate abasic sites (**Figure 7**). Rad51 paralog binding to abasic sites prevents AP endonuclease cleavage and potential formation of cytotoxic DSBs [120]. This function is not unprecedented as RPA blocks APE1 cleavage of an abasic site analog on ssDNA and a double-flap substrate[163]. It is interesting to note that in mammalian cells, the HMCES protein forms protein-DNA crosslinks at abasic sites, shielding these sites from TLS or APE1-induced DSBs[164]. In contrast, Rad51 paralog binding to specific fork blocking lesions, such as an abasic site and perhaps other fork blocking lesions, would promote Rad51 filament formation enabling a template switch using the newly synthesized sister chromatid. By template switching, the lesion would be bypassed by the replication machinery in an error-free manner and could subsequently be repaired by BER after the fork progresses. At the same time, disruption of the Shu complex ability to recognize and bind to abasic sites results in error-prone repair, such as TLS and single-strand annealing[81], to predominate.

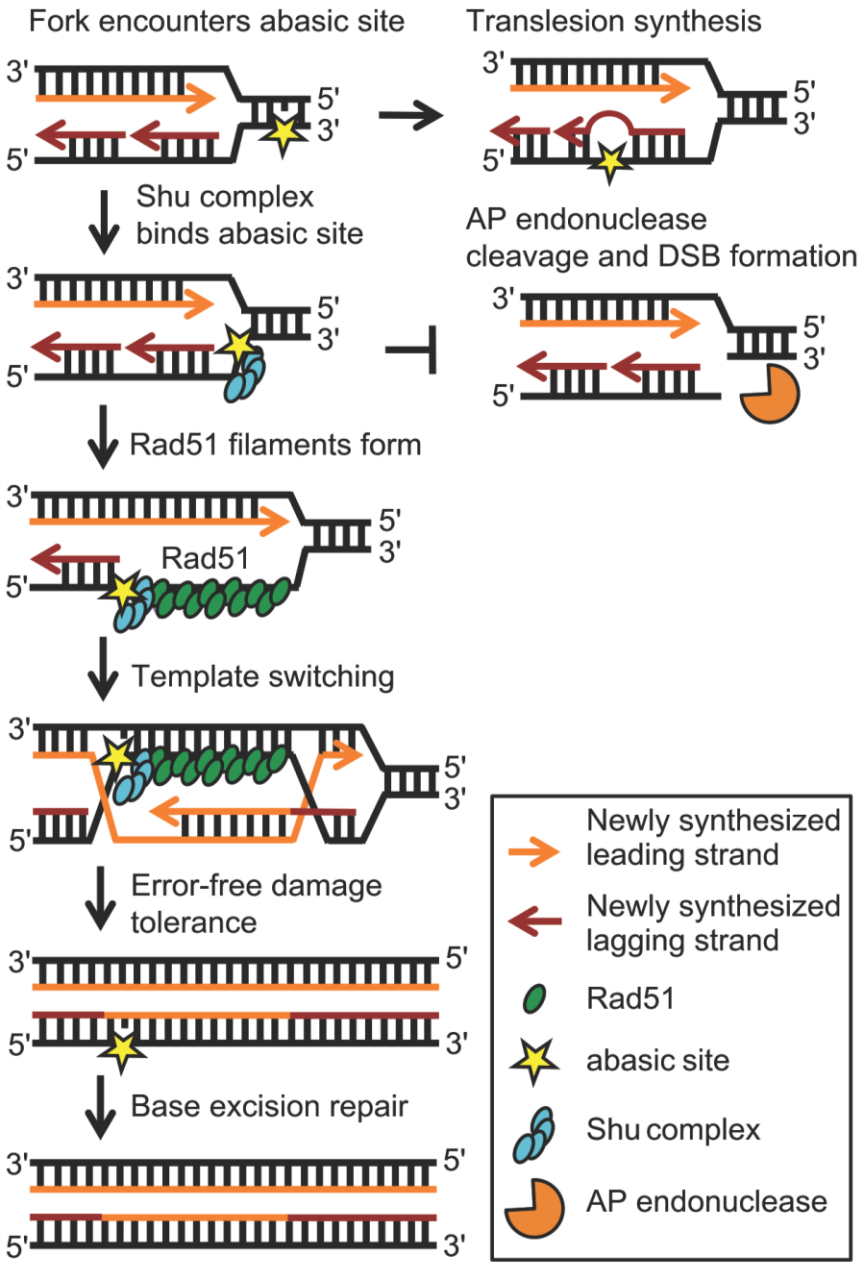

Figure 7. Model of novel Rad51 paralog-mediated DNA strand-specific damage tolerance pathway

The Shu complex DNA binding components, the Rad51 paralogs Csm2-Psy3, bind to abasic sites at a double-flap junction to promote Rad51-mediated template switching while preventing AP endonuclease cleavage. MMS-induced DNA damage is primarily repaired by the BER pathway. However, if a replication fork encounters DNA damage such as an abasic site (yellow star), then the fork can stall or collapse. The Shu complex (blue ovals) binds abasic sites on the lagging strand template proximal to the dsDNA fork stem. Shu complex DNA binding 1) promotes Rad51 filament formation (green ovals) and 2) likely prevents AP endonuclease cleavage (orange Pac-man) and DSB formation. Thus,

the Shu complex mediates a DNA strand-specific damage tolerance pathway enabling error-free lesion bypass through a template switch using the newly synthesized sister chromatid. This strand-specific lesion bypass pathway allows replication to continue efficiently in an error-free manner and the abasic site to be repaired by BER after the fork progresses. This figure was generated by BB and published in [120].

Here we present *in vitro* and *in vivo* evidence for a function of the Shu complex in the tolerance of abasic sites. We show that 1) Shu complex member Csm2 chromatin association is enriched upon abasic site accumulation but not stalled forks (**Figure 4b,c; Figure 5b**); 2) Csm2 DNA binding is required for its chromatin association when abasic sites accumulate and these mutants exhibit extreme DNA damage sensitivity and are mutagenic (**Figure 4a,b**); 3) *csm2*Δ and *psy3*Δ mutants exhibit mutation signatures consistent with abasic site repair on the lagging strand (**Figure 6**); 4) Csm2-Psy3 and Csm2-Psy3-Shu1-Shu2 bind with improved affinity to a double-flap substrate containing an abasic site analog (THF) at the junction (Not shown) [120]; lastly 5) Csm2-Psy3 protect AP6 double-flap substrates from *in vitro* endonuclease cleavage (Not shown) [120]. One interesting aspect of this study is the two-fold improved affinity observed of Csm2-Psy3 for AP6 but not AP7 (Not shown) [120]. There may be a binding pocket in the Csm2-Psy3 complex that can accommodate an abasic site analog when it is only in the AP6 position compared to the AP7 position. The nucleotide adjacent to the abasic site analog may also alter the DNA structure and therefore influence the DNA binding activity of Csm2-Psy3[165, 166]. In addition, it remains unknown how Rad51 and Rad55-Rad57, which directly interact with Csm2-Psy3, may contribute to this substrate specificity. Future atomic resolution studies will be necessary to understand the specificity differences between these two substrates. Together, the combined *in vitro* and *in vivo* complementary data described above provides the strongest evidence that the Shu complex has an important role in the tolerance of abasic sites.

Our *in vitro* findings suggest a role for the Shu complex in preventing DSB formation during replication and further studies are needed to demonstrate that DSBs are indeed increased *in vivo* upon Shu complex disruption. However, consistent with increased DSB formation, Shu complex mutant cells exhibit more Rad52 foci upon MMS exposure in S/G2/M cells compared to wild-type [58] and a delay in chromosome reconstitution upon MMS exposure in S phase synchronized culture [81]. It is interesting to note that *csm2*Δ in combination with accumulation of abasic sites (from an *apn1*Δ *apn2*Δ *ntg1*Δ *ntg2*Δ mutant), results in a 1075X increase in spontaneous mutation rates [81], which likely accounts for the extreme MMS sensitivity observed in this mutant background.

Although we find that the Shu complex exhibits improved binding affinity for double-flap structures (Not shown) [120], we previously showed that the Csm2-Psy3 heterodimer also binds to 5' and 3' DNA overhangs[45]. In this context, the Shu complex could bind to a 5' overhang that forms when a replicative polymerase stalls at a DNA lesion and then dissociates from it. It is also possible that other DNA repair factors or the replication machinery itself may also contribute to Shu complex recruitment to DNA damage at a replication fork. In this scenario, the Shu complex could recruit Rad51 to stalled replication forks to facilitate a template switch.

Our work has important clinical implications as the interdependency between DNA repair pathways needed during replication is being exploited for cancer treatment. For example, human BRCA1 and BRCA2 function during HR by promoting resection and RAD51 activity, respectively[167]. BRCA1 and BRCA2 disruption are associated with hereditary breast and ovarian cancers. PARP inhibitors are effective in the treatment of patients with BRCA1- and BRCA2-deficient tumors[168-170]. Recent studies have extended these observations and PARP inhibitors are now being used to treat patients with RAD51 paralog deficient tumors in clinical

trials[171]. Therefore, upon replication stress when early DNA repair steps are blocked by PARP inhibition, HR is required to bypass the lesion. A recent study has implicated PARP1 in ligation of Okazaki fragments where PARP inhibition prevents Okazaki fragment ligation, which would then require HR for removal[172]. In this replicative context, combined PARP inhibition with HR deficiency (due to BRCA or RAD51 paralog mutation) results in tumor cell lethality. Understanding the underlining mechanisms of how BER intermediates, such as ssDNA breaks and abasic sites, are recognized and channeled for repair through HR is critical for exploiting DNA repair interdependency in cancer therapy to ensure the most durable clinical response.

2.4 Methods

2.4.1 Protein Expression and Purification

All Csm2-Psy3 heterodimers were cloned into the dual expression plasmid pRSFDuet (EMD Millipore) which encodes a 6XHIS-TEV tag on Csm2. Transformed *E. coli* [BL21-Codon+ (DE3, RIL) Agilent] was grown at 37˚C to 0.6 OD_{600} and recombinant protein expression was induced by the addition of 0.2 mM isopropyl beta thiogalactoside (IPTG) at 18˚C overnight for 16-18 hrs. Cells were harvested by centrifugation. Approximately 10 g of cell pellet was lysed in 60 mL of lysis buffer containing 20 mM Tris (pH 8.0), 500 mM NaCl, 10% glycerol, 5 mM imidazole, and 1 mM β-mercaptoethanol supplemented with protease inhibitors (Roche) and DNAse (1 µg/ml). Cells were lysed using an emulsiflex and centrifuged at 30,000 x *g* for 1 hour at 4˚C. Csm2 and Psy3 were co-purified through nickel affinity chromatography (Qiagen) using the N-terminal His_6-tag on Csm2 in Nickel binding buffer (20 mM Tris pH 8.0, 500 mM NaCl, 10

mM Imidazole, and 1 mM beta-mercaptoethanol). Csm2-Psy3 was washed on the column with 50 mL of binding buffer containing 10, 15, and 20 mM imidazole to remove contaminating proteins. The Csm2-Psy3 was eluted from the column with elution buffer containing (20 mM Tris pH8.0, 500 mM NaCl, and 250 mM Imidazole. Wild-type Csm2-Psy3 dimers used in the abasic binding experiments were further purified using HiTrap Heparin HP (GE Healthcare) affinity chromatography. The Csm2-Psy3 protein was loaded onto the heparin column equilibrated in buffer containing (Tris pH 8.0, 1 mM beta-mercaptoethanol, and 8% glycerol). The complex was eluted with a gradient elution from 25% to 100% (Tris pH 8.0, 1 M NaCl, 1 mM beta-mercaptoethanol, and 8% glycerol) over 75 mL. The Csm2-Psy3 protein typically eluted around 400-600 mM NaCl. Since mutant Csm2-Psy3 dimers fail to bind the heparin column, wild-type Csm2-Psy3, and mutant Csm2-Psy3 constructs were purified using a HiTrap Q (GE Healthcare) anion exchange column for a direct comparison of DNA binding affinities. Note that this change in the purification scheme results in different binding affinities compared to the protein preparations that used the heparin column. All Csm2-Psy3 constructs were subsequently purified by size exclusion chromatography using a Sephacryl S200 column (GE Healthcare) in buffer (Tris pH 8.0, 1 M NaCl, 1 mM beta-mercaptoethanol, and 8% glycerol), eluting as a single peak (**Figure 16d**). Csm2-Psy3 protein concentration was determined by absorbance at A_{280} with an extinction coefficient of 54320 M^{-1} cm^{-1}. Shu1-MBP-Shu2 and Rad51 were purified as previously described[41].

2.4.2 Equilibrium binding assays using fluorescence polarization anisotropy

Anisotropy experiments were performed using a FluoroMax-3 spectrofluorometer (HORIBA Scientific) and a Cary Eclipse Spectrophotometer. For unmodified forks, fluorescein

dT was incorporated at the 5' single-stranded end of the fork (**Figure 3b**). For double-flap substrates containing abasic site analogs, the label was placed on the single-stranded end of the oligonucleotide that did not contain the abasic site analog. Anisotropy measurements were recorded in a 500 µL cuvette containing 20 mM Tris pH 8.0 and 20 nM of the fluorescein-labeled double-flap substrate as a premixed sample of purified Csm2-Psy3 protein and substrate (20 nM AP6 + 1.6 µM Csm2-Psy3 dimer in 1 M NaCl) was titrated into the cuvette. Fluorescence anisotropy measurements were recorded using the integrated polarizer and excitation and emission wavelengths of 466 nm and 512 nm, respectively with path lengths of 10 nm. Titrations were carried out until anisotropy became unchanged. At the end of each titration, the DNA substrate was competed off with 1M NaCl to confirm that the increase in anisotropy was explained by bona fide electrostatic interactions with Csm2-Psy3. All experiments were performed in triplicate with multiple preparations of the recombinant proteins. Dissociation constants (K_d) were calculated by fitting our data to a one-site binding model using the equation for a rectangular hyperbola [Y=Bmax*X/(K_d+X)], with PRISM7 software (**Supplemental Table 1**). Anisotropy experiments with 2.5 nM and 5 nM substrate concentrations were fit to a quadratic equation [Y=M* ((x+D+K_d) -sqrt(((x+D+K_d)^2) – (4*D*x))) / (2*D)], with PRISM7 software. The double flap substrate used in the equilibrium binding assay was formed by annealing of the following oligos were: 5'-/FITC/ TTT TTT TTT TTT TTT TTT TTC TTG ACA AGC TTG CGC ACT G-3' and 5'-CAG TGC CGA AGC TTG TCA AGT TTT TTT TTT TTT TTT TTT T-3'.

2.4.3 Strains and plasmids

The strains and plasmids used are listed in (**Supplemental Table 2**). The Y2H strains PJ69-4A and PJ69-4α were used as described[45, 173]. All strains are isogenic with W303 RAD5+

W1588-4C[174] and W5059-1B[175] except for the APOBEC3B-mediated mutagenesis assay. In the APOBEC3B-mediated mutagenesis, the yeast strains used for determining *CAN1* mutation rates and spectra are derived from wild-type ySR128[160], in which the *CAN1* gene is integrated approximately 16 kb to the left of ARS216. The construction of ySR128-derived *ung1*Δ, *mph1*Δ, and *ubc13*Δ strains was described[160, 162]. HygMX cassettes for creating deletions of *CSM2* and *PSY3* were generated by PCR using primers described in (**Supplemental Table 3**) and plasmid template pAG32[176]. After transformation and selection, gene deletions were confirmed by PCR using primers that flank each gene (**Supplemental Table 3**). APOBEC3B expressing and empty plasmids were created in the vectors pySR-419 and pSR-440[160]. A fragment containing the *LEU2* gene from pUG73[177] was PCR amplified using oligos oTM-74 and oTM-75. This fragment was then ligated into backbones created from PCR amplification of pySR-419 and pSR-440 with primers oTM-80 and oTM-81. The resulting plasmids, pTM-19 (empty vector) and pTM-21 (APOBEC3B expression vector) were validated by Sanger sequencing. The primers used for cloning and sequencing are found in **Supplemental Table 3**.

2.4.4 Canavanine mutagenesis assay

Five individual *CAN1* colonies of WT, *csm2*Δ, *psy3*Δ, *csm2-KRRR*, *psy3-KRK*, and *csm2-KRRR psy3-KRK* were grown in 2 mL YPD or YPD medium containing 0.00033% MMS (18 h) overnight at 30˚C. The cultures were diluted 1:10, with 250 µL plated on SC-ARG+CAN or diluted 1:60,000, with 120 µL plated on SC. The plates were then incubated for 48 hours at 30˚C. Colonies were used to measure total cell number (SC) or forward mutation rates (SC-ARG+CAN). For each condition, colony count from at least 4 independent trials was used to calculate a mutation rate using FALCOR [178], and the Lea-Coulson method of the median.

2.4.5 APOBEC3B-mediated mutation rate measurements and mutation spectra

Yeast strains were transformed with either pTM-19 (empty vector) or pTM-21 (APOBEC3B expression plasmid) and selected on synthetic complete medium lacking leucine (SC-leu). Individual isolates were plated on SC-leu at a density of approximately 50 cells per plate and grown to colony sizes of $7x10^7$ cells (for empty vector) or $7x10^6$ cells (for APOBEC3B expression plasmid). Eight independent colonies were then re-suspended in water and plated on SC or SC-arginine medium supplemented with 0.006% canavanine (SC+can) and incubated for three days at 30°C. Colonies were used to measure total cell number (SC) or forward mutation rate (SC-ARG+CAN). For each condition, data from at least three independent transformants were used to calculate a mutation rate using FALCOR [178], and the Lea-Coulson method of the median. Mutation spectra were determined for APOBEC3B-expressing strains plated on SC-leu medium at a density of about 50 cells per plate and grown until colonies reached approximately $7x10^6$ cells. The resulting colonies were replica-plated to SC+can medium and grown for 4 days. To isolate independent clonal CanR mutants, papillae derived from discrete colonies were struck to single colonies on SC+can medium and after three days one colony from each was patched onto YPDA medium. Genomic DNA was isolated from each patch and used as a template for amplification of the *CAN1* gene by PCR using primers oTM-92 and oTM-93 (**Supplemental Table 3**). The resulting PCR products were Sanger sequenced (GenScript, Piscataway, NJ), using primers oTM-94, oTM-95, and seqDG-91 (**Supplemental Table 3**), and the mutations inactivating *CAN1* were identified using the Geneious software package (Biomatters).

2.4.6 Growth Assays

Five-fold serial dilutions of the indicated yeast strains were performed as described[81] except that 5 µL of culture at OD_{600} 0.2 were 5-fold serially diluted onto YPD medium or YPD medium containing 0.02% MMS. Cell viability assays were performed by growing the indicated strains in 3 mL of YPD at 30˚C overnight, and then diluting the culture to 0.2 OD_{600} for 3-4 hours. The cultures were all diluted to 0.5 OD_{600} in 1 mL YPD and diluted either 1:10,000 or 1:20,000 and 250µL was plated onto YPD medium or YPD medium containing 0.012%, 0.02%, 0.03% MMS. The plates were incubated at 30˚C for 2 days before being counted. Representative images were taken after two days of growth at 30˚C for one of the experiments and the brightness and contrast were adjusted using Photoshop (Adobe Systems Incorporated). The experiment was performed five times with standard deviations calculated.

2.4.7 Western Blot Analysis

Five mL YPD was inoculated with the indicated cells and grown overnight at 30˚C. The cells were diluted to OD_{600} 0.2 in 5 mL YPD and grown for 3 hours at 30˚C. Whole-cell lysates of equal cell numbers (0.5 OD_{600}) were prepared by TCA precipitation[179] and 10 of 50 µL protein preparation was run on a 10% SDS-page gel where HA antibodies (sc-805; 1:500) were used to detect the 6HA tagged Csm2 and Psy3 proteins and Kar2 antibodies (Santa Cruz sc-33630; 1:200) were used as a loading control. The films were scanned and adjusted for contrast and brightness using Photoshop (Adobe Systems Incorporated).

2.4.8 Yeast-Two-Hybrids

The yeast-two-hybrid experiments using the indicated pGAD and pGBD plasmids were performed as described[45] except that both pGAD and pGBD plasmids were transformed into PJ69-4A[173]. A yeast-two-hybrid interaction is indicated by growth on synthetic complete (SC) medium lacking histidine, tryptophan, and leucine whereas equal cell loading was observed by plating the cells on SC medium lacking tryptophan and leucine to select for the pGAD (leucine) or pGBD (tryptophan) plasmids.

2.4.9 Chromatin fractionation

Chromatin fractionation was based on[180, 181] with modification. Five mL YPD was inoculated with the indicated cells and grown overnight at 30℃. The cells were diluted to 0.2 OD_{600} in 50 mL YPD and grown for 3 hours at 30℃. The cells were then diluted to 0.3 OD_{600} in 50 mL fresh YDP with 20 μM α-factor (GeneScript). After 2 hours of incubation at 30℃, the cells were pelleted and washed with 50 mL YPD. The culture was diluted to 0.5 OD_{600} in 50 mL fresh YPD or YPD containing the indicated MMS concentration (0.01%, 0.02%, or 0.03%) or HU concentration (50 mM or 200 mM). After 1 hour incubation at 30℃, 30 OD_{600} cells were washed with 50 mL ice-cold water and resuspended in 2 mL pre-spheroplast buffer (100 mM PIPES/KOH pH 9.4, 10 mM DDT, 0.1% NaN_3)[180] for 10 minutes at room temperature. The cells were pelleted and then resuspended in 3 mL spheroplast buffer (50 mM K_2HPO_4/KH_2PO_4 pH 7.5, 0.6 M Sorbitol, 10 mM DTT, 0.1 μg/mL Zymolyase 100T [amsbio])[180] and incubated for 40 minutes at 30℃ (120 rpm). The spheroplasts were pelleted and washed with ice-cold wash buffer (50 mM HEPES/KOH pH 7.5, 100 mM KCl, 2.5 mM $MgCl_2$, 0.4 M sorbitol)[180]. The

spheroplasts were pelleted and resuspended in 80 µL of extraction buffer (wash buffer with 1 % Triton X-100, 1 mM DTT, protease inhibitors, and 2 mM PMSF)[181]. The spheroplasts were lysed by vortexing for 5 minutes with intermittent incubation on ice. 80 µL of HU loading buffer (8 M urea, 5% SDS, 200 mM Tris pH 6·8, 1 mM EDTA, 0.02% w/v bromophenol blue, 0.2 M DTT)[179] was added to 20 µL of each lysate and set aside for analysis [whole cell lysate (W)]. The remaining lysate was loaded on top of a 50 µL sucrose cushion (wash buffer with 30% sucrose, 0.25% Triton X-100, 1 mM DTT, protease inhibitors, and 2 mM PMSF)[181] and centrifuged 10 minutes at 4℃ at 20000 x g. 80 µL of HU loading buffer was added to 20 µL from the top layer and set aside for analysis [non-chromatin fraction (S)]. The chromatin fraction (C) pellets were resuspended in 100 µL of HU loading buffer. 5 µL of the W, S, and C samples were run on a 12% SDS-PAGE gel and western blot analysis was performed. HA antibodies (sc-805; 1:500) were used to detect the 6HA tagged Csm2 protein, Kar2 antibodies (Santa Cruz sc-33630; 1:200), GAPDH (UBPbio Y1040; 1:10000), Rfa1 (Abcam ab221198; 1:6000) and H2B antibodies (Active Motif #39237, 1:1000) were used for controls. The films were scanned and adjusted for contrast and brightness using Photoshop (Adobe Systems Incorporated).

2.4.10 Quantification and data analysis of the chromatin fractionation assay

Each experimental condition was repeated 3-5 times. The densitometry analysis was performed using ImageJ software[182] to quantify the whole cell lysate (W), the non-chromatin fraction (S), and chromatin fraction (C). To analyze the amount of Csm2 that is chromatin-associated, the signal of Csm2 in the C fraction was divided by the W fraction. Kar2 chromatin association was also calculated by dividing the Kar2 C fraction by the W fraction. To account for chromatin extraction efficiency, the calculated Csm2 chromatin association value was then divided

by the corresponding Kar2 chromatin association value. Finally, to account for loading differences, we compared the Csm2 and Kar2 W fractions. To compare Csm2 chromatin enrichment between experiments and obtain fold changes, we set the untreated Csm2-6xHA strain chromatin signal to 1 and the averages of each trial were plotted with standard deviations and significance determined by unpaired two-tailed Student's t-test.

2.5 Acknowledgments

This chapter is modified from the following collaborative published work:

Rosenbaum, J. C.*, B. Bonilla*, S. R. Hengel*, T. M. Mertz, B. W. Herken, H. G. Kazemier, C. A. Pressimone, T. C. Ratterman, E. MacNary, A. De Magis, Y. Kwon, S. K. Godin, B. Van Houten, D. P. Normolle, P. Sung, S. R. Das, K. Paeschke, S. A. Roberts, A. P. VanDemark and K. A. Bernstein (2019). "The Rad51 paralogs facilitate a novel DNA strand-specific damage tolerance pathway." Nat Commun **10**(1): 3515. * *Denotes equal contribution.*

Author contribution is detailed in the figure legends. J.C.R., B.B., B.H., T.M.M., C.A.P., E.M. performed the experiments. J.C.R. purified recombinant proteins and performed biochemical analysis. S.K.G. created the DNA binding mutant yeast strains and plasmids. B.B., B.V.H., S.R.D., K.P., S.A.R., A.P.V., and K.A.B. designed the experiments. B.V.H, T.M.M., J.C.R., B.B., S.R.H., S.A.R., A.P.V., K.A.B. wrote the manuscript.

We thank Samuel Wilson for the APE1 enzyme. We thank William Gaines for assisting with the protein purification. This study was supported by the National Institutes of Health grant

(ES024872 to K.A.B., A.P.V.; ES019566 to B.V.H.; ES007061 to P.S.; CA218112 to S.A.R.) and the American Cancer Society (129182-RSG-16-043-01-DMC to K.A.B.). K.P. is supported by a Starting grant from the European Research Council (ERC Stg Grant: 638988-G4DSB). This project used the UPMC Hillman Cancer Center Biostatistics Facility that is supported in part by award P30CA047904.

3.0 The Shu complex promotes error-free bypass of 3meC

Three-methyl cytosines (3meCs) are replication blocking, toxic, and mutagenic lesions that can form from endogenous sources as well as alkylating agents found in the environment, such as those from tobacco smoke. In most species, 3meC are repaired by the AlkB family of enzymes. However, budding yeast does not possess an AlkB homolog. How budding yeast tolerates damage from 3meC has been a long-standing question. Mag1 was recently shown to initiate base excision repair on 3meC at double-stranded DNA. However, since 3meCs occur almost exclusively in single-stranded DNA, it remains unknown how yeast tolerates their toxicity and mutagenesis during DNA replication. Homologous recombination is responsible for error-free DNA damage bypass during replication. The yeast Shu complex is a homologous recombination mediator, primarily specialized in preventing replication-associated mutagenesis and in the tolerance of specific types of replication-associated DNA lesions. Here, we performed a genome-wide sequencing of Shu complex disrupted cells chronically exposed to the prototypical alkylating agent MMS. In Shu complex deficient cells exposed to MMS, analysis of the mutation pattern revealed 3meC as a major contributor to mutagenesis. We show that ectopic expression of the human AlkB homolog, *ALKBH2*, specifically rescues MMS-induced phenotypes observed in Shu complex mutant cells, such as growth defects and increased mutagenesis. Our results demonstrate an unexpected function for the Shu complex in mediating an error-free pathway to prevent mutagenesis and toxicity from 3meC, finally uncovering how these lesions are tolerated during replication. In light of ALKBH2 function in chemotherapy resistance, our findings have broad implications in how tumors evade chemotherapy.

3.1 Introduction

Alkylating agents such as MMS induce a diverse set of base lesions (**Supplemental Table 4**), that are primarily recognized and repaired by the base excision repair (BER) pathway [183]. However, when these lesions, or their repair intermediates, are encountered by a replisome, replication fork stalling can occur [144, 184]. In this scenario, DNA base damage is preferentially bypassed using homologous recombination (HR) or translesion synthesis (TLS), postponing its repair but allowing replication to be completed in a timely fashion. These pathways are often referred to as Post-Replicative Repair (PRR) or DNA Damage Tolerance (DDT) and have been best described in the budding yeast *S. cerevisiae* [185-187].

In yeast, HR-mediated PRR is an error-free pathway and is dependent on the polyubiquitination of PCNA by the Mms2-Rad5-Ubc13 complex [185]. Lesion bypass is achieved by Rad51 filament formation, and recombination between sister chromatids to fill the single-stranded DNA (ssDNA) gaps originated from the stalling of replicative polymerases. While HR can bypass these lesions in an error-free manner, TLS can also be used to bypass this damage. However, TLS may lead to mutations and is often referred to as error-prone lesion bypass. In yeast, TLS serves as an alternative pathway to error-free lesion bypass, as disruption of genes involved in the error-free PRR pathway leads to increased mutations that are dependent on TLS [61, 188, 189].

The Shu complex is an evolutionarily conserved HR factor that we recently discovered to have a novel function in strand-specific DNA damage tolerance during replication [18, 53, 66, 120]. In *S. cerevisiae*, the Shu complex is a heterotetramer formed by the SWIM domain-containing protein, Shu2, and the Rad51 paralogs Csm2, Psy3, and Shu1. The Shu complex promotes Rad51 filament formation, a key step for HR [18]. Consistent with their role in DSB

repair, most HR genes deletions lead to increased sensitivity to DSB-inducing agents. However, the Shu complex seems to be exceptional, as its mutants are primarily sensitive to the alkylating agent MMS, but not to the DSB inducing agents such as ionizing radiation (IR)[58, 81]. This makes the Shu complex an attractive factor to dissect the role of HR in the tolerance of replication-associated DNA damage.

Previous studies from our group and others demonstrated that the Shu complex operates in the error-free branch of the PRR to tolerate DNA damage from MMS-induced lesions [45, 83]. Despite these findings, it has remained unknown which MMS-induced lesions, or repair intermediates, the Shu complex is important for. Previous results from our lab uncovered genetic interactions between members of the BER pathway and the Shu complex upon treatment with MMS [81]. Notably, cells lacking the BER enzymes that process abasic (AP) sites show exquisite sensitivity and a 1000X increase in mutation rates when the Shu complex is also disrupted. This suggested that the Shu complex is important for the tolerance of AP sites, which we recently demonstrated [120].

Here, we address the question as to whether the Shu complex function is specific for abasic sites or if it is important for the recognition of a broader range of DNA lesions. To address this, we performed an unbiased genome-wide screen by chronically exposing Shu mutant cells, *csm2*Δ, to MMS. By performing a genome-wide mutational analysis, we identified a novel role for the Shu complex in the tolerance of 3meC, in addition to its known role in abasic site tolerance. Importantly, unlike bacteria and human cells that have an enzyme that directly repairs 3meC, this family of enzymes is absent in *S. cerevisiae* and therefore it has remained unknown how 3meC are repaired in yeast [190]. Here, we show that the expression of human *AlkBH2* specifically rescues the MMS-sensitivity of Shu complex mutant cells and alleviates their MMS-induced mutagenesis.

In contrast to Shu complex mutants, we surprisingly observe that *ALKBH2* expression very weakly rescues the MMS induced phenotypes in cells with deletion of canonical HR factors. Our findings underscore the specialized role of the Shu complex in the recognition and promotion of error-free bypass of replication-associated DNA base damage. Overall, our results uncover how yeast tolerate 3meC DNA damage despite their lack of an AlkB homolog.

3.2 Results

3.2.1 Unbiased genome-wide analysis of mutation patterns suggests that the Shu complex function in the error-free bypass of specific MMS-induced lesions

To determine the specific MMS-induced lesions that the Shu complex bypasses, we chronically exposed Shu complex deficient cells to MMS (**Figure 8a**). To do this, we plated wild-type (WT) or *csm2*Δ cells on MMS-containing medium and then transferred individual colonies every two days onto fresh medium containing MMS ten times, allowing mutations to accumulate. Finally, we extracted genomic DNA from these colonies and performed whole-genome sequencing. Consistent with previous findings, Shu complex deficient *csm2*Δ cells accumulate more mutations than WT upon MMS treatment (**Figure 8b**) [45, 81].

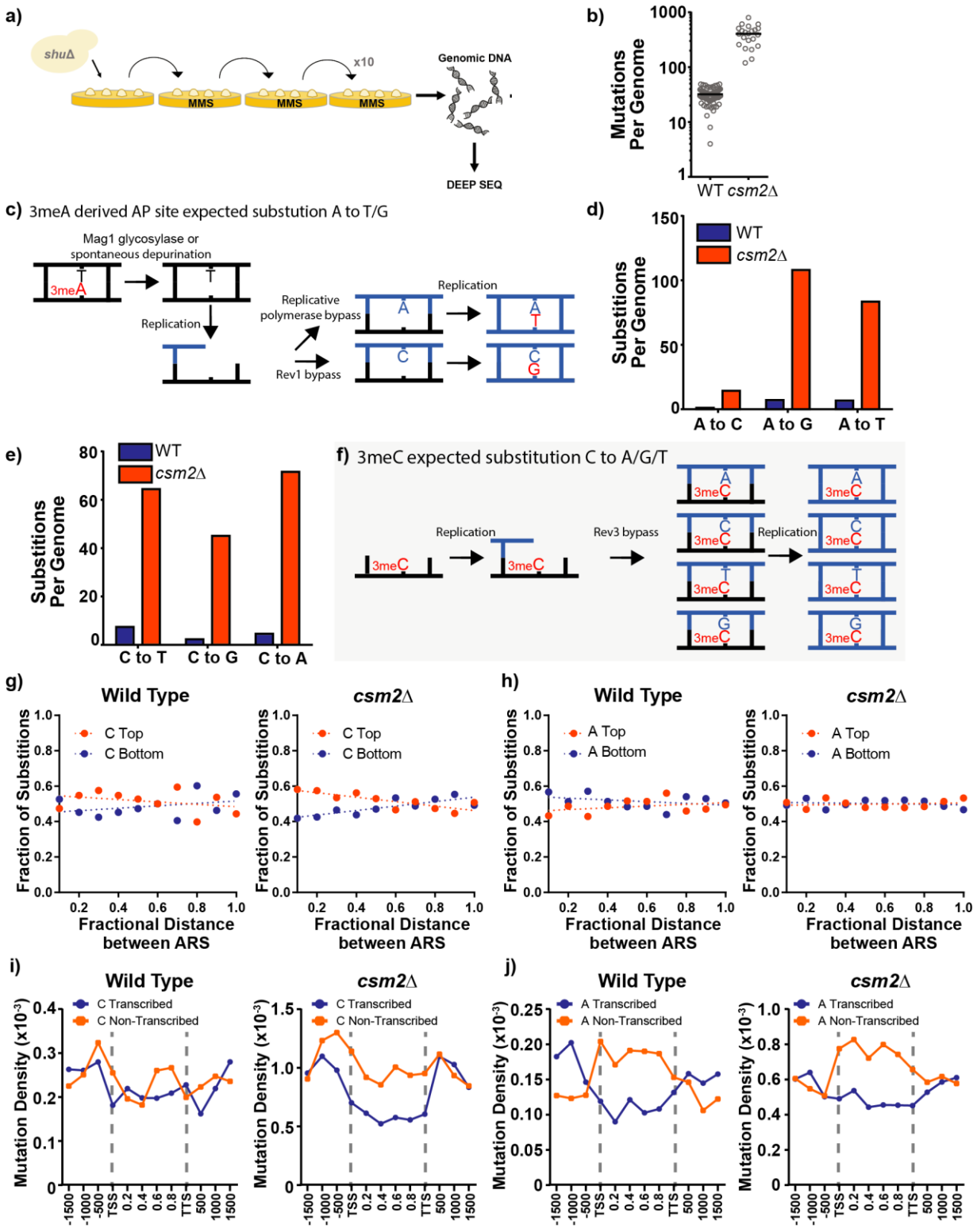

Figure 8. csm2Δ cells chronically exposed to MMS exhibit substitution patterns consistent with TLS activity on/bypass of AP sites and 3meC

(**a**) Schematic of the experiment where wild-type and *csm2*Δ cells were chronically exposed to MMS. Wild-type and *csm2*Δ cells were chronically exposed to 0.008% MMS by plating individual colonies onto rich medium containing MMS, after 2 days of growth, the colonies were plated onto fresh medium containing MMS for 10 passages. DNA was extracted from 90 colonies per genotype and deep sequenced. (**b**) The number of mutations per genome for wild-type or *csm2*Δ cells chronically MMS-exposed was determined. (**c**) Schematic of how 3meA derived AP sites result in A to T/G mutations. 3MeA is removed by the Mag1 glycosylase or may undergo spontaneous depurination resulting in an AP site. During DNA replication, the replicative polymerase bypasses the AP site resulting in a T mutation, alternatively, Rev1 bypasses the AP site resulting in a G mutation. (**d**) The mutation pattern observed in *csm2*Δ cells is consistent with a function in the error-free bypass of AP sites. The mutations at A-T base pairs for wild-type and *csm2*Δ cell cells were counted and graphed. (**e**) The mutation pattern observed in *csm2*Δ cells is consistent with a function in the error-free bypass of 3meCs. The mutations at C-G base pairs for wild-type and *csm2*Δ cells were counted and graphed. (**f**) Schematic of how 3meC results in C to A/G/T base substitutions. 3meC occurs primarily in ssDNA and during replication, Rev3 mediated bypass results in incorporation of A, T, G, or C nucleotides. (**g**) Strand bias between origins of replication for G:C base pairs of wild-type and *csm2*Δ MMS-exposed cells. "Top" is used as a lagging strand template with regards to "left" origins and a leading strand template in regards to "right" origins. "Bottom" is used as a leading strand template in regards to "left" origins and a lagging strand template with regards to "right" origins. (**h**) Similar to (g), strand bias between origins of replication for A:T base pairs of wild-type, and *csm2*Δ MMS-exposed cells. (**i**) Transcriptional strand bias for G:C base pairs of wild-type and *csm2*Δ MMS-exposed cells. (**j**) Transcriptional strand bias for A:T base pairs of wild-type and *csm2*Δ MMS-exposed cells. Author contribution as listed in section 3.5: panel a: performed by BB and CAP; panels c and f: BB; panels b, d, e, and g-j: TMM, EM, and SAR.

To infer which DNA lesions caused the mutations, we analyzed the substitution patterns considering the MMS-induced lesion profile [191-193]. In dsDNA A:T base pairs, 3meA is the most common MMS-induced lesion, accounting for approximately 10% of the total MMS-induced lesions observed in dsDNA both in *vitro* and *in vivo* [192] (**Supplemental Table 4**). 3meA can be converted to an AP site by the activity of the Mag1 glycosylase or by spontaneous depurination

(**Figure 8c**)[184]. When these AP sites are encountered by a replicative polymerase, they can lead to its stalling. However, they can be bypassed in an error-prone manner by the TLS polymerase Rev1 or the replicative polymerase δ, which typically incorporate an A or C, respectively, across the missing base (**Figure 8c**)[145, 162, 194]. The replicative polymerase δ (and to a lesser extent Polα or Polη) with the accessory subunit, Pol32, can incorporate an A across an AP site. The extension of this incorporation is performed by Polζ (Rev3, Rev7, and Pol32) (and to a lesser extent Polη), and is stimulated by Rev1 [194, 195]. Alternatively, Rev1 can catalyze the incorporation of C across abasic sites and is stimulated by Polη. The extension of this incorporation is performed by Polζ [194, 195]. Therefore, TLS activity on 3meA-derived AP sites leads to an A->G and A->T substitution pattern (**Figure 8c**). Consistent with a function for the Shu complex in the bypass of AP sites, we observe elevated A->G transitions and A->T transversions in *csm2*Δ cells (**Figure 8d**). This is consistent with our results obtained for the Shu complex disrupted cells and supports the notion that the Shu complex promotes error-free bypass of AP sites, as recently demonstrated by our group [81, 120].

At G:C base pairs, 7meG is the most common MMS-induced DNA adduct, accounting for approximately 84% of the total MMS-induced lesions observed in dsDNA both in *vitro* and *in vivo* [192] (**Supplemental Table 4**). Although not itself mutagenic, it may be subjected to spontaneous depurination, or Mag1 excision, which both lead to AP sites [184, 196, 197]. When AP sites are generated from guanines, their bypass by Rev1 is error-free because it incorporates a C across the missing base. Alternatively, bypass by the replicative polymerase results in the incorporation of A across the missing base, which leads to a G to T transversion. The mutation pattern at G:C base pairs from *csm2*Δ cells, not only include G->T mutations but also includes G->A and G->C mutations. Therefore, the mutation pattern observed in *csm2*Δ cells does not support 7meG-derived

AP sites as the main mutagenic lesion in MMS-exposed Shu complex mutant cells (**Figure 8e**). One possibility is that the observed mutational pattern represents the Shu complex-mediated tolerance of a different MMS induced lesion, such as 3meC. 3meC occurs almost exclusively at ssDNA because the N3 of cytosine is protected by the hydrogen bound [198]. It accounts for approximately 10% of the total MMS-induced lesions observed in ssDNA both in *vitro* and *in vivo* [199] (**Supplemental Table 4**). Importantly, 3meC are mutagenic DNA adducts and can block the replicative polymerase [184]. Rev3-mediated TLS bypass of 3meC leads to the incorporation of a random nucleotide across the lesion, leading to a mutational pattern consistent with the one we observed upon *CSM2* disruption (**Figure 8e,f**) [199, 200]. Our results suggest that the Shu complex promotes error-free bypass of 3meC.

ssDNA occurs naturally in the lagging strand during replication. Therefore, DNA lesions that occur primarily in ssDNA exhibit strand bias nearby replication origins [160, 201, 202]. In other words, the closer to an origin of replication, the more likely it is that a strand is going to be copied into either leading or lagging most of the times. Strand bias can be assessed by correlating the distance from origins of replication with the relative abundance of mutations at a certain base pair when one nucleotide is used as a lagging strand or leading strand template. DNA lesions that occur predominantly in ssDNA are expected to lead to increased mutation frequencies at base pairs where the target nucleotide is used as lagging strand template and decreased mutation frequencies at base pairs where the target nucleotide is used as leading strand template. Similarly, strand bias can also be observed when comparing the mutation frequency seen in nucleotides at the transcribed and the non-transcribed strands. When lesions occurring at ssDNA are a prominent source of mutations, it is expected that higher mutation frequency is observed at base pairs where the target nucleotide is at the non-transcribed strand. Since 3meCs occur primarily at ssDNA, we, therefore,

asked if the observed mutation patterns wild-type or *csm2*Δ MMS-exposed cells exhibit strand bias. We indeed observe that the substitution pattern at G:C base pairs in Shu complex deficient cells show an increased strand bias both near origins of replication and when comparing transcribed to non-transcribed strands (**Figure 8g,i**). Unlike G:C base pairs, since 3MeA occurs predominantly in dsDNA we do not observe an increased strand bias at A:T base pairs (**Figure 8h,j**)[191-193]. Our results are consistent with 3meC as a major source for mutations at G:C base pairs in MMS-exposed Shu complex mutants on the lagging strand.

3.2.2 *ALKBH2* expression rescues the MMS-induced phenotypes of Shu complex deficient cells

Based on the analysis of the mutation patterns, we hypothesized that the Shu complex promotes the error-free bypass of 3meC. 3meC can be repaired by the AlkB family of Fe(II)/α-Ketoglutarate-dependent dioxygenases [203]. This family is conserved from bacteria to humans; however, a yeast homolog has yet to be identified. Therefore, it remains unknown how yeast tolerates and repairs 3meC. In humans, there are nine AlkB homologs and *ALKBH2* and *ALKBH3* are responsible for 3meC DNA repair [203, 204]. We, therefore, reasoned that ectopic expression of AlkB homologs would rescue the MMS-induced phenotypes observed in Shu complex deficient cells. To test this hypothesis, we took advantage of the lack of an AlkB homolog in yeast by ectopically expressing human AlkB homologs, *ALKBH2*, or *ALKBH3*, in *csm2*Δ cells and analyzed their effect on MMS sensitivity. *ALKBH2* and *ALKBH3* were expressed under the constitutive GAP promoter in a CEN plasmid. We find that both *ALKBH2* and *ALKBH3* expression lead to a partial rescue of the growth defects observed in MMS-exposed *csm2Δ* cells, with *ALKBH2* showing a stronger rescue (**Figure 9a**). Therefore, we focused on ALKBH2 for the remainder of

the experiments. As expected considering the lack of enzymes that repair 3meC from ssDNA in yeast, *ALKBH2* expression very mildly rescues the MMS sensitivity of wild-type cells as well (**Figure 9a**). The rescue of the growth defect observed in MMS-treated *csm2Δ* cells is dependent on ALKBH2's enzymatic activity since the expression of an ALKBH2 catalytic dead mutant (ALKBH2-V101R,F120E herein referred to as alkbh2-CD)[205] does not rescue *csm2*Δ cell viability (**Figure 9b**). We find that these findings are not specific to *csm2*Δ as ALKBH2 rescues the MMS sensitivity of the other Shu complex members to the same extent (**Figure 9c**). Next, we analyzed the effect of *ALKBH2* expression on *csm2Δ* cells acutely exposed to MMS. To do this, we treated *ALKBH2*-expressing WT or *csm2Δ* cultures with MMS for 30 minutes. We then assessed cell survival by counting the number of viable colonies after two days of growth in a rich medium. We observe that *ALKBH2* expression leads to a dose-dependent increase in the survival of *csm2Δ* cells, whereas WT cell survival is only mildly rescued (**Figure 9d**).

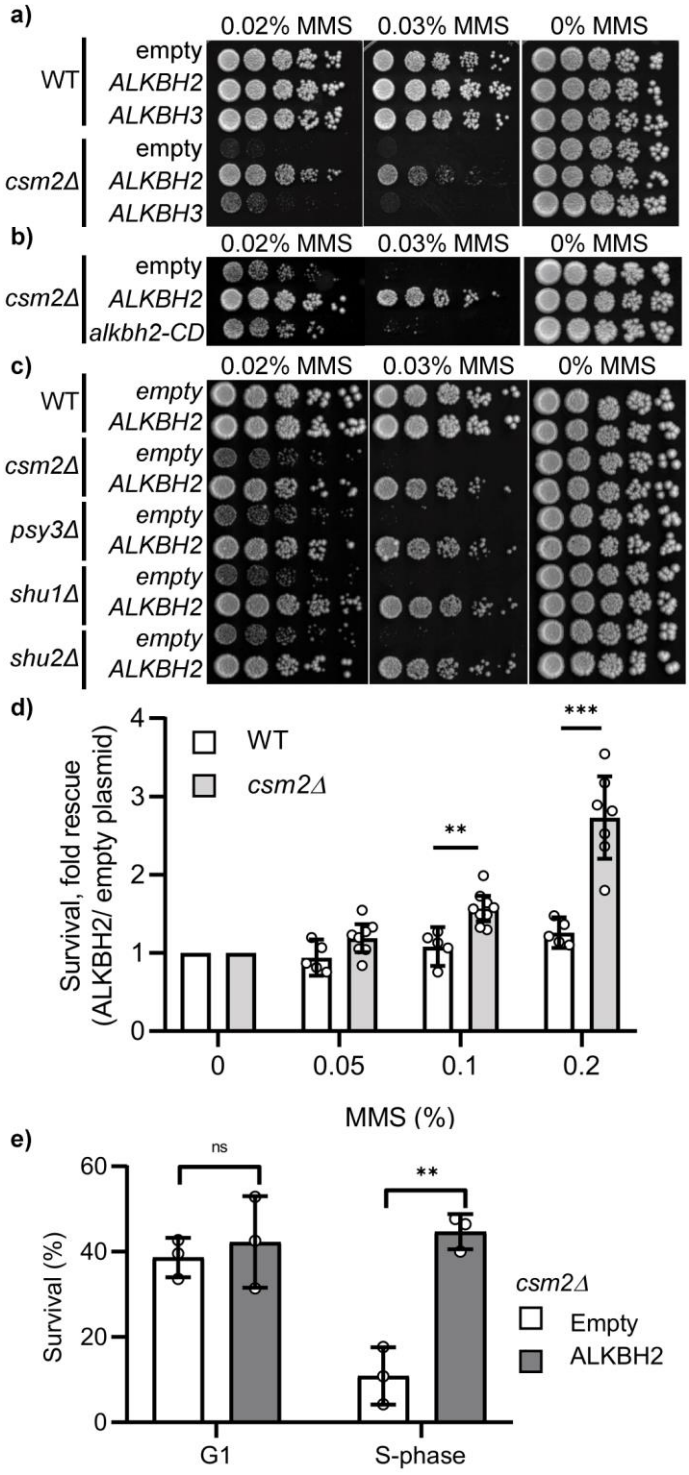

Figure 9. Expression of human *ALKBH2* rescues the MMS sensitivity of csm2Δ cells

(a) *csm2Δ* cells expressing *ALKBH2* exhibit decreased MMS sensitivity. Five-fold serial dilution of WT or *csm2*Δ cells transformed with an empty plasmid, a plasmid expressing *ALKBH2*, or a plasmid expressing *ALKBH3* onto rich

YPD medium or YPD medium containing the indicated MMS concentration were incubated for 2 days at 30 °C before being photographed. (**b**) The enzymatic activity of ALKBH2 is required for the rescue of the MMS sensitivity of *csm2*Δ cells. *csm2*Δ cells transformed with an empty plasmid, a plasmid expressing *ALKBH2*, or a plasmid expressing a catalytic dead *ALKBH2* mutant were diluted and plated as described in ***a*** and incubated for three days at 30°C before being photographed. (**c**) *ALKBH2* expression rescues the MMS sensitivity of cells with deletions of the four Shu complex genes. WT, *csm2*Δ, *psy3*Δ, *shu1*Δ, or *shu2*Δ cells transformed with an empty plasmid, or a plasmid expressing *ALKBH2* were five-fold serially diluted, plated, and analyzed as described in ***b***. (**d**) *csm2Δ* cells expressing *ALKBH2* exhibit increased survival after acute MMS treatment. YPD liquid cultures of WT or *csm2*Δ cells transformed with an empty plasmid or a plasmid expressing *ALKBH2* were treated with the indicated concentration of MMS following plating onto rich YPD medium. Colony number was assessed after incubation for two days at 30°C. Fold rescue of cellular survival represents the ratio of the survival of cells expressing *ALKBH2* relative to the survival of cells expressing the empty plasmid. Survival represents the number of colonies as a percentage of the colonies obtained without MMS treatment. The individual and mean values from five to nine experiments were plotted. Error bars indicate 95% confidence intervals. The *p*-values between WT and *csm2*Δ cells treated with 0.1% MMS and 0.2% MMS were calculated using an unpaired two-tailed Student's t-test and were $p \leq 0.01$ and $p \leq 0.001$, respectively. (**e**) S-phase *csm2*Δ cells expressing *ALKBH2* exhibit increased survival after acute MMS treatment. WT or *csm2*Δ cells were synchronized on G1 with alpha factor and either released from G1 arrest or maintained in G1 in the presence or absence of 0.1% MMS. Cells were plated after 30 minutes of treatment and the colony number was assessed after incubation for two days at 30°C. Survival is calculated as described in ***d***. The mean values from three experiments were plotted with standard deviations. The *p*-values between control (empty plasmid) and *ALKBH2* expressing cells were calculated using an unpaired two-tailed Student's t-test and were $p>0.05$ (n.s.) and $p \leq 0.001$ for the G1 and S-phase cells, respectively. Author contribution as listed in section 3.5: panels a, b, d, and e: BB; panel b: experiment designed by BB and performed by KSR.

Since 3meC only occurs at ssDNA and ssDNA is a physiological intermediate of DNA replication, we reasoned that *ALKBH2* expression would preferentially rescue the survival of cells that are progressing through S-phase and therefore more vulnerable to 3meC induced toxicity. To

test this, we compared the survival of *ALKBH2* expressing *csm2Δ* cells arrested in G1 in MMS containing media with *ALKBH2* expressing *csm2Δ* cells progressing through S-phase. Interestingly, we observe that only the cells that progressing through S-phase show increased survival when *ALKBH2* is expressed (**Figure 9e**).

3.2.3 ALBH2 expression alleviates the MMS-induced mutations observed in the Shu complex mutant, *csm2*Δ

Since 3meC is a mutagenic lesion, we asked whether *ALKBH2* expression would alleviate the mutational load of *csm2Δ* cells exposed to MMS. To do this, we utilized the *CAN1* reporter assay. The *CAN1* gene encodes for an arginine permease, therefore when cells are exposed to the toxic arginine analog canavanine, only cells that acquire mutations in the *CAN1* genes are able to grow. The number of colonies obtained correlates with the mutation frequency/mutation rates of the strain. As expected, we find that *ALKBH2* expression leads to lower mutation frequency in *csm2Δ* cells exposed to MMS, while the mutation frequencies of WT cells were unaffected (**Figure 10**). Deletion of the Shu complex leads to an increase in the spontaneous mutation frequency, which is likely due to the TLS-mediated bypass of abasic sites [58, 81, 83, 120, 184]. Therefore, we would not expect *ALKBH2* expression to rescue the spontaneous mutations observed in a Shu complex mutant. Consistent with the notion that the effect of ALKBH2 is due to the repair of MMS-induced lesions, we do not observe a decrease in the mutation frequency in untreated *csm2Δ* cells (**Figure 10**). To further examine the specificity of the ALBKH2 rescue for MMS-induced DNA damage, we analyzed the effect of *ALKBH2* expression on an MMS-independent phenotype observed in Shu complex disrupted cells. Disruption of the Shu complex in cells with mutations in the TLS polymerase polζ leads to increased UV sensitivity [84]. Consistently, *ALKBH2*

expression does not rescue the growth defect observed in UV-treated *csm2Δ rev3Δ* double mutant cells (**Figure 11**). Together, these results further support the notion that the Shu complex has a specific role in the tolerance of 3meC.

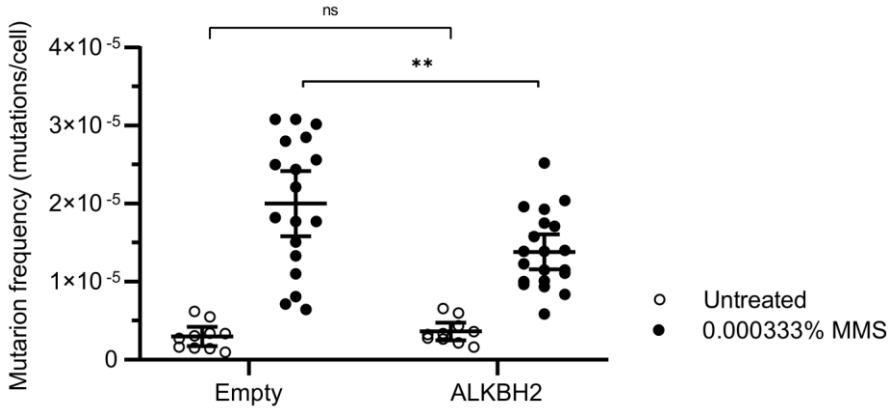

Figure 10. *ALKBH2* expression reduces the mutation frequency observed in MMS exposed *csm2Δ* cells

csm2Δ cells expressing *ALKBH2* exhibit reduced MMS-induced mutation frequencies. Spontaneous and MMS-induced mutation frequencies at the *CAN1* locus were measured in *csm2*Δ cells transformed with an empty plasmid or a plasmid expressing *ALKBH2*. The mean values of 10 to 20 experiments were plotted. Error bars indicate 95% confidence intervals. The *p*-values between control (empty plasmid) and *ALKBH2* expressing cells were calculated using an unpaired two-tailed Student's t-test and were $p>0.05$ and $p \leq 0.001$ for the untreated and MMS treated samples respectively. Author contribution as listed in section 3.5: this figure was generated by BB.

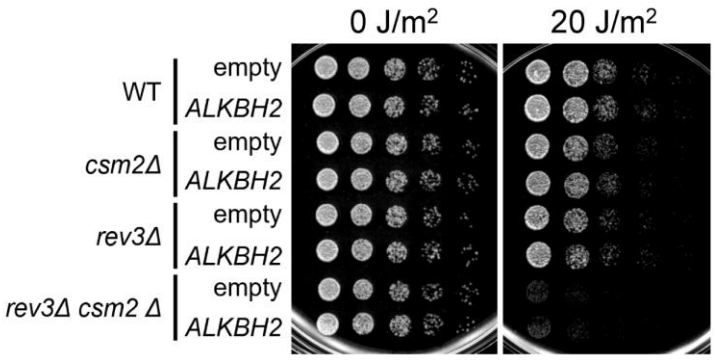

Figure 11. Expression of *ALKBH2* does not rescue the increased UV sensitivity observed in *csm2Δrev3Δ* double mutants

Five-fold serial dilution of WT, *csm2Δ*, *rev3Δ*, or *rev3Δ csm2Δ* cells were transformed with an empty plasmid or a plasmid expressing *ALKBH2* and five-fold serially diluted onto rich YPD or rich YPD medium exposed to 20 J/m^2 ultra-violet (UV), and incubated for 2 days at 30 °C before being photographed. An untreated plate (0 J/m^2) serves as a loading control. Author contribution as listed in section 3.5: this figure was generated by BB.

3.2.4 3meC repair in yeast is channeled through error-free post-replicative repair.

The Shu complex directly functions with the canonical Rad51 paralogs, Rad55-Rad57, and Rad52 to promote HR through Rad51 filament formation [41, 45]. The Shu complex function occurs in the context of error-free post-replicative repair downstream of poly-ubiquitination of PCNA by the Rad5-Ubc13-Mms2 complex [84]. Therefore, we asked whether the rescue of the MMS-induced phenotypes by *ALKBH2* would be specific for Shu complex mutants. To do this, we ectopically expressed *ALKBH2* in cells with deletions of *CSM2*, *RAD51*, *RAD52*, *RAD55*, and *UBC13* and performed serial dilutions upon increasing MMS doses (**Figure 12a**). Surprisingly, we find that *rad51*Δ, *rad52*Δ, and *rad55*Δ MMS sensitivity is not rescued by *ALKBH2* expression to the same extent as a *csm2*Δ cell. In contrast, *ubc13*Δ cell's MMS sensitivity is largely rescued by *ALKBH2* expression. Unlike Shu complex mutant cells, deletion of the canonical HR genes

would leave the cells vulnerable to toxic DSBs induced by MMS through clustered lesions. In this scenario, *ALKBH2* function would be dispensable as the DSB repair machinery would be required to repair the break. This toxicity in turn prevents *ALKBH2* rescue. These results underscore the specificity for the Shu complex in replication-associated DNA damage and the more general function for Rad55-Rad57 and Rad52 in DSB repair in multiple contexts.

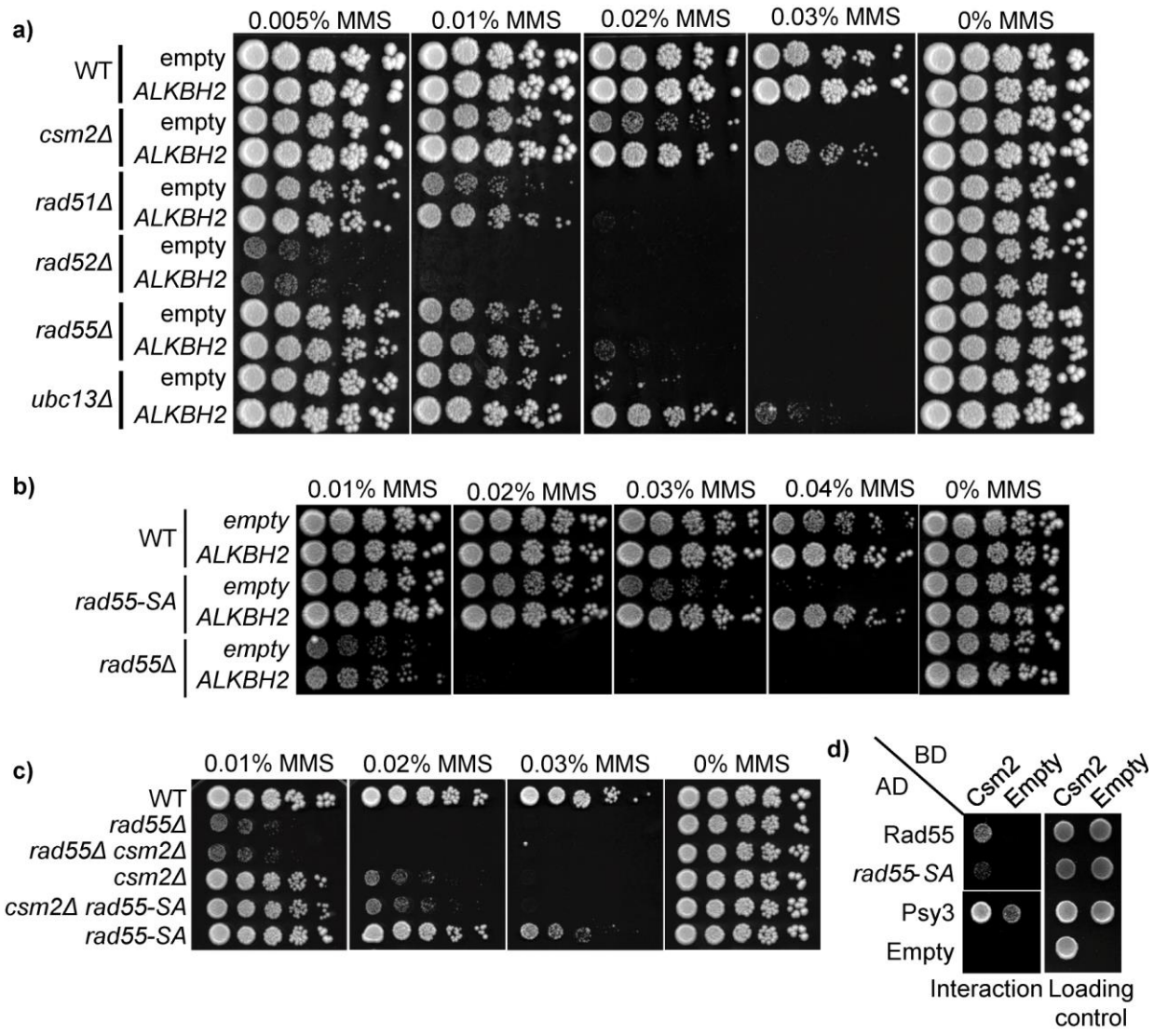

Figure 12. 3meC are bypassed by the error-free post replicative repair (PRR) pathway

(a) Unlike PRR mutant *UBC13*, expression of *ALKBH2* mildly rescues the MMS sensitivity of HR factors, *RAD51*, *RAD52*, and *RAD55*. Five-fold serial dilution of WT, *csm2Δ*, *rad51Δ*, *rad52Δ*, *rad55Δ*, or *ubc13Δ* cells were transformed with an empty plasmid or a plasmid expressing *ALKBH2* onto rich YPD medium or YPD medium containing the indicated MMS concentration and incubated for 3 days at 30°C before being photographed. (**b**) *rad55-S2,8,14A* cells expressing *ALKBH2* exhibit decreased MMS sensitivity. WT, *rad55-S2,8,14A*, or *rad55Δ* cells transformed with an empty plasmid or a plasmid expressing *ALKBH2* were five-fold serially diluted, plated, and analyzed as described in ***a***. (**c**) *csm2Δ* is epistatic to *rad55-S2,8,14A* for MMS damage. Cells with the indicated genotypes were five-fold serially diluted and plated as described in **a)**, and incubated for 2 days at 30°C before being photographed (**d**) rad55-S2,8,14A exhibit an impaired yeast-2-hybrid (Y2H) interaction with Csm2. Y2H analysis of

pGAD-*RAD55*, *rad55-S2,8,14,S*, *PSY3*, or pGAD-C1 (Empty) with pGBD-*RAD57*, *CSM2*, pGBD-C1 (Empty). A Y2H interaction is indicated by plating equal cell numbers on SC medium lacking histidine, tryptophan, and leucine. Equal cell loading is determined by plating on SC medium lacking tryptophan and leucine used to select for the pGAD (AD) and pGBD (BD) plasmids. Author contribution as listed in section 3.5: panels a and b: experiment designed by BB and performed by KSR; panels c and d: BB.

To explore this idea further, we investigated the effect of *ALKBH2* in a *RAD55* phosphorylation mutant that is MMS sensitive while being DSB repair proficient [119]. In this *RAD55* mutant, three serine residues (2,8,14) are mutated to alanines (*rad55-S2,8,14A*). Since the *rad55-S2,8,14A* mutant cell largely phenocopies the defects observed in a Shu complex mutant [119], we asked whether Rad55 function in MMS-induced DNA damage may be uncoupled from its role in canonical DSB repair. Unlike *rad55*Δ cells, the *rad55-S2,8,14A* mutant MMS sensitivity is largely rescued by *ALKBH2* expression (**Figure 12b**). To further investigate the genetic relationship between the Shu complex and Rad55, we combined either *rad55*Δ or *rad55-S2,8,14A* with a *csm2*Δ mutant cell. As previously reported, *csm2*Δ *rad55*Δ double mutants exhibit the same MMS sensitivity as a *rad55*Δ mutant cell [45]. In contrast, a *csm2*Δ *rad55-S2,8,14A* double mutant exhibits the same MMS sensitivity as a *csm2*Δ mutant cell (**Figure 12c**). This result is surprising since the Shu complex is thought to function downstream of Rad55. However, this result is consistent with the specificity of the Shu complex in enabling tolerance of MMS induced DNA lesions [120].

Rad55 directly interacts with Csm2-Psy3 [41, 45]. While *rad55-S2,8,14A* mutant maintains its protein interactions with Rad57, Rad51, and Rad52, its interaction with the Shu complex was not determined[119]. Therefore, one possibility is that the Shu complex helps to recruit Rad55 to specific MMS-induced DNA lesions through interaction with phosphorylated Rad55 or at the

interface where Rad55 is phosphorylated. To test this, we performed an Y2H analysis of Rad55 or *rad55-S2,8,14S* with Csm2 (**Figure 12d**). We observe a reduced interaction between *rad55-S2,8,14S* with Csm2 (**Figure 12d**). These results suggest that Rad55 phosphorylation may stimulate its interaction with Csm2 or that Csm2 interacts with Rad55 in that region. Overall, the loss of Rad55-Shu complex interaction may contribute to Rad55 MMS sensitivity.

3.3 Discussion

3meC's are cytotoxic and mutagenic DNA lesions [184, 191, 206]. In eukaryotes, they can arise endogenously from S-adenosyl methionine (SAM), and from the enzymatic activity of DNA methyltransferases or exogenously from alkylating agents such as nitrosamines, which are present in the tobacco smoke, temozolomide, or MMS [207-210]. 3meCs occur primarily in ssDNA and can lead to the stalling of replicative polymerases. Unlike bacteria and higher eukaryotes, yeast does not encode for an enzyme capable of repairing 3meC from ssDNA [190, 211]. Therefore, yeast cells rely on bypass mechanisms to complete DNA replication. Here, we utilized the budding yeast model to demonstrate that the Shu complex facilitates an HR-mediated error-free bypass of 3meC to prevent the mutagenesis and toxicity of this lesion.

The Shu complex is primarily involved in tolerance of replicative base template damage, being dispensable for DSB repair [81, 83]. This makes the Shu complex ideal to dissect the role of HR during bypass of specific base lesions. The major phenotypes observed in MMS-exposed Shu complex disrupted cells are decreased cell survival and elevated mutation frequency [18, 58, 83]. We observe that *ALKBH2* expression specifically alleviates the MMS-induced phenotypes of cells when the Shu complex is disrupted (**Figure 9-11**). The Shu complex rescue by ALKBH2 is partial,

which is consistent with our recent finding that the Shu complex is also involved in the tolerance of the mutagenesis and toxicity from another MMS-induced lesion, an abasic site [120, 212]. Although it is not possible to specifically induce 3meC, it is possible to regulate the occurrence of its template, by controlling the amount of ssDNA in MMS-exposed cells. It would be interesting to observe how the rescue by expression of *ALKBH2* correlates with the amount of ssDNA. Consistently, our results show that ALKBH2 is only able to rescue the MMS sensitivity of Shu complex mutant cells that are progressing through S-phase and therefore exhibit ssDNA intermediates (**Figure 9e**).

Although *ALKBH2* expression leads to a robust rescue of the MMS-induced phenotypes seen in Shu complex deficient cells, *ALKBH3* expression only mildly rescues the MMS sensitivity of *csm2Δ* cells (**Figure 9a**). This can be explained by the fact that ALKBH3 depends on the helicase ASCC3 to perform its repair activity [209], a factor that seems it is also absent in yeast.

The error-free PRR pathway requires polyubiquitination of PCNA by Mms2-Ubc13-Rad5 and the activity of the core HR machinery [91, 213]. Interestingly, the deletions of other HR factors, such as *RAD51*, are only partially rescued by *ALKBH2* expression (**Figure 12a**). This can be explained by their critical role in DSB repair, an activity for which the Shu complex is thought to be dispensable. Together, these results are consistent with 3meC being bypassed by the HR branch of the PRR pathway (**Figure 13**) and the notion that the Shu complex is an HR factor specialized for replication-damage.

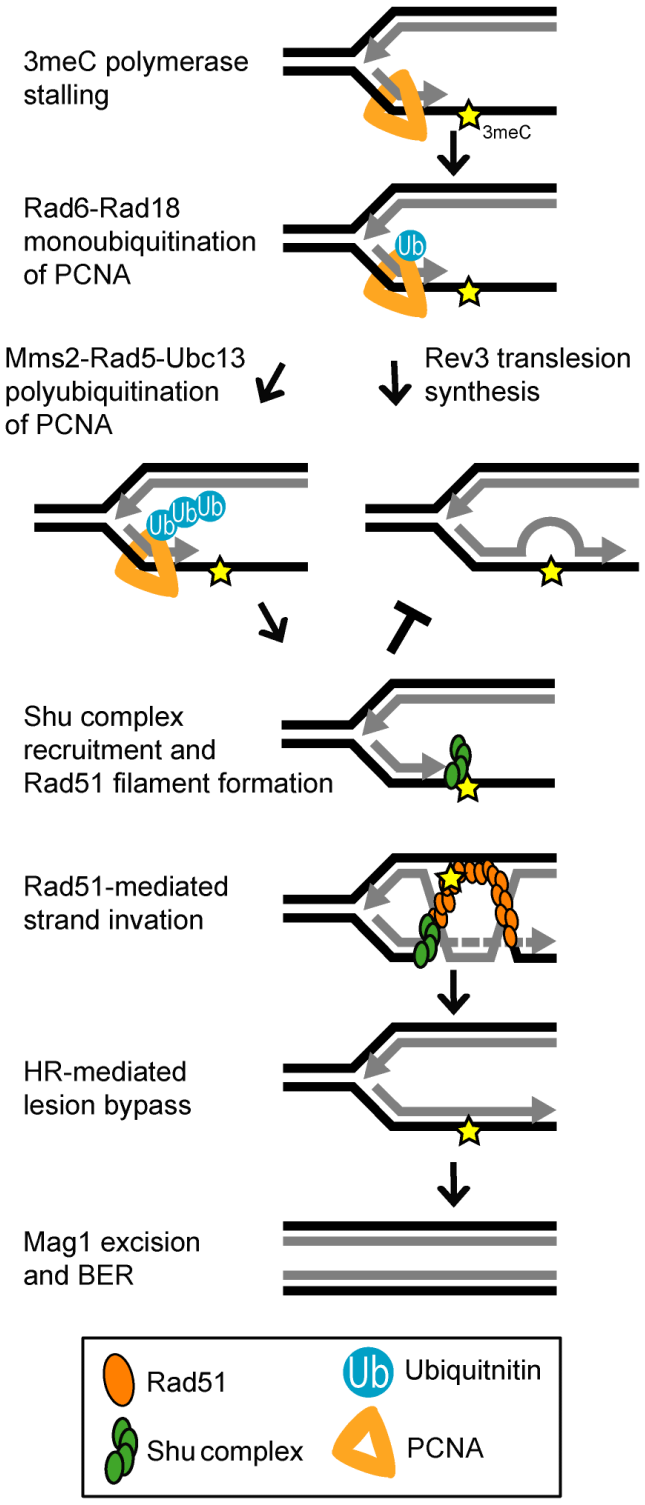

Figure 13. Model of Shu complex-mediated error-free bypass of 3meC

MMS-induced 3meC (yellow star) arising at DNA replication intermediates at ssDNA can stall the replicative polymerase. Replication fork stalling leads to PCNA (orange triangle) K63–linked polyubiquitination of lysine 164

(K164) by the sequential activities of the Rad6-Rad18 and Mms2-Rad5-Ubc18 complexes. The Shu complex (green ovals) through its DNA-binding components, Csm2-Psy3, binds to 3meC at a double-flap DNA junction to promote Rad51 filament formation (orange ovals) enabling Rad51-mediated HR with the newly synthesized sister chromatid. Importantly, the Shu complex activity prevents mutagenesis from the TLS-mediated error-prone bypass of 3meC. After DNA synthesis using the undamaged sister chromatid as a template, the HR intermediates are resolved. The error-free bypass of 3meC enables S-phase completion in a timely manner. Finally, after replication is completed, 3meCs are likely recognized and excised by the Mag1 glycosylase, which initiates the BER-mediated repair. Author contribution as listed in section 3.5: this figure was generated by BB.

It is important to note that TLS can also bypass 3meA directly and can also contribute to the mutation pattern that we observe for both wild-type and *csm2*Δ cells. Direct TLS bypass of 3meA leads to a mutation pattern of elevated A->T substitutions [184]. Therefore, we cannot rule out the contribution of direct TLS bypass of 3meA to the mutation pattern observed in our sequence analysis. However, previous work from our group has provided genetic, *in vivo*, and *in vitro* evidence of the Shu complex role in the error-free bypass of AP sites specifically [18, 81, 120].

AlkB proteins are also able to repair 1meA, which primarily occurs at ssDNA [203]. Like 3meC, 1meA is a toxic and mutagenic adduct [184]. It possible that this lesion is also bypassed by the Shu complex and the error-free PRR pathway. Hence, we cannot rule out that ALKBH2 repair of 1meA can also contribute to the rescue of MMS-induced phenotypes that we observed. However, it is evident from our sequence analysis that the Shu complex contributes to the bypass of lesions occurring at G:C base pairs, which excludes 1meA. Moreover, 3meC is thought to be the main lesion contributing to mutagenesis from MMS at ssDNA [199, 200].

A previous study claimed that yeast *TPA1* is an AlKB homolog [214]. However, in our hands, and consistent with a recent report [211], *tpa1Δ* cells show no increased sensitivity to MMS. Furthermore, unlike other genes that are involved in repairing MMS-induced lesions, we find that

TPA1 does not exhibit a synthetic sick phenotype when Shu complex mutants upon MMS exposure (**Figure 14**). Recently, the Mag1 glycosylase was shown to excise 3meC in dsDNA; therefore, initiating their repair through BER [211]. However, this work also demonstrated that Mag1 is not able to excise 3meCs from ssDNA [211]. This highlights the need for a mechanism to bypass this lesion 3meC from ssDNA to avoid mutagenesis and cytotoxicity (**Figure 13**). We propose here that the Shu complex enables bypass of ssDNA 3meC to enable repair by Mag1 after replication is completed (**Figure 13**).

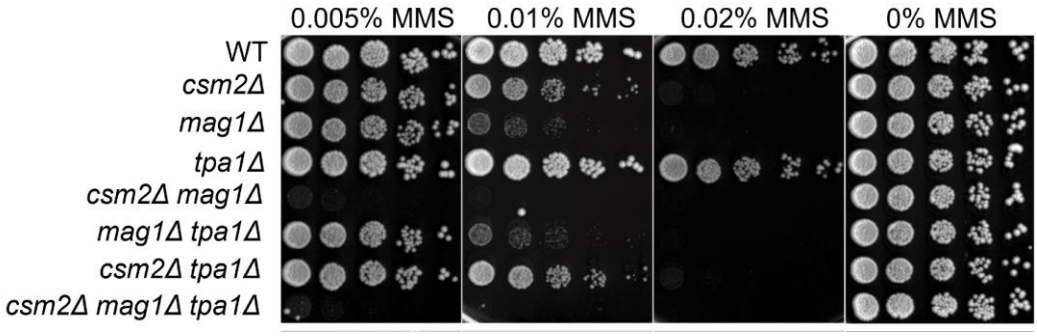

Figure 14. *TPA1* does not interact genetically with *CSM2* or *MAG1* for MMS damage

Five-fold serial dilutions of cells with the indicated genotypes were plated onto rich YPD medium or rich YPD medium containing the indicated MMS concentration were incubated for two days at 30°C before being photographed. Author contribution as listed in section 3.5: experiment designed by BB and performed by KSR.

Previous work from our group and others show that the Shu complex role is functionally conserved in humans and mice [49, 50, 53]. Therefore, future studies to address whether the human Shu complex can act as a back-up of the ALKBH enzymes in tolerating mutagenesis and toxicity from 3meC. This is of particular importance since both *ALKBH2* and *ALKBH3* have been proposed as tumor suppressors, being silenced in various tumors, including gastric and breast cancer [203, 215-217]. On the other hand/conversely, ALKBH3 is often overexpressed in different cancers and inhibition of ALKBH2 and ALKBH3 can sensitize cancer cells to DNA chemotherapy [218-222].

Moreover, *ALKBH2* and *ALKBH3* upregulation mediate resistance to chemotherapeutic agents such as temozolomide and ALKBH3 loss leads to endogenous 3meC accumulation in tumor cell lines [209, 223, 224]. The role of the Shu complex promoting tolerance of 3meC could provide a new avenue for therapeutic approaches to target these tumors.

3.4 Methods

3.4.1 Yeast strains, plasmids, and oligos

The Y2H strains PJ69-4A and PJ69-4α were used as described [45, 173]. All strains are isogenic with W303 RAD5+ W1588-4C [174] and W5059-1B [175]. KBY-1088-3C (rad55-S2,8,14A) was generated by the transformation of a cassette containing the 50 bp homology upstream of the *RAD55* start codon and the rad55-S2,8,14A ORF fused to a kanMX6 resistance cassette and the 50 bp homology downstream of the *RAD55* stop codon. This fused cassette was obtained using Gibson Assembly® Master Mix (NEB) following the manufacturer's instructions and the primers used to generate the assembly fragments were designed using NEBuilder Assembly Tool (https://nebuilder.neb.com). The *rad55-S2,8,14A* gene fragment was commercially synthesized whereas the kanMX6 cassette was amplified from the pFA6a-kanMX6 plasmid [225]. Before transformation, the fused product was PCR amplified using the RAD55.S1 and RAD55.S2 primers as described [225]. All yeast transformations were performed as described [226]. pAG416GPD-ccdB-ALKBH2-CD was generated by site-directed mutagenesis of the pAG416GPD-ccdB-ALKBH2 plasmid as described by [227] with minor adaptations according to the manufacturer's recommendations for PCR using Phusion High-Fidelity PCR Master Mix with

HF Buffer (Thermo). The pAG416GPD-ccdB-ALKBH2, pAG416GPD-ccdB-ALKBH3, and pAG416GPD-ccdB plasmids were a gift from Hani Zaher and Nima Mosammaparast. All plasmids and strains were verified by DNA sequencing.

3.4.2 Chronic MMS exposure and DNA sequencing

Individual colonies of WT or *csm2Δ* cells were grown overnight at 30˚C. The cultures were then pinned onto a YPD medium containing 0.008% MMS using a yeast pinning robot from S&P Robotics. After a 2-day incubation at 30˚C, the plates were replica-plated onto YPD plates containing 0.008% MMS using a robotic pinner and then replated onto fresh YPD medium containing 0.008% MMS a total of 10 times. The MMS-exposed yeasts were then separated into single colonies (96 per strain). These colonies were inoculated in YPD cultures and grown overnight at 30˚C and genomic DNA extracted. The genome-wide deep sequencing was performed as described [160].

3.4.3 Growth assays

Individual colonies of the indicated strains were transformed with an empty plasmid or a plasmid expressing ALKKBH2 when indicated. The cultures were grown in 3ml YPD or SC-URA medium overnight at 30˚C. Five-fold serial dilutions were performed as described [81] except that 5 µL of culture at 0.2 OD_{600} were 5-fold serially diluted onto YPD medium or YPD medium containing the indicated MMS concentration. UV treatment was performed using Stratagene Stratalinker 2400 UV Crosslinker. The plates were imaged after 48 h or 72 h of incubation at 30˚C

and the brightness and contrast were globally adjusted using Photoshop (Adobe Systems Incorporated).

3.4.4 Survival assays

Individual colonies of WT or csm2Δ cells were transformed with an empty plasmid or a plasmid expressing *ALKBH2* were grown in 3ml SC-URA medium at 30˚C overnight. The cultures were then diluted to OD600 = 0.2 in 50 ml SC-URA medium and grown for 3-4 h at 30˚C. The cultures were all diluted back to OD600 = 0.2 in YPD or YPD containing 0.05%, 0.1% or 0.2% MMS and incubated for 30 minutes at 30˚C and 220 rpm. After the treatment, the cultures were washed twice with YPD and resuspended to OD600 = 0.2 in fresh YPD. The cultures were then diluted 1/10000 (untreated and 0.05% MMS) or 1/1000 (0.1% and 0.2% MMS) and 150 ul were plated in YPD medium plates in duplicate. The plates were incubated at 30˚C for 2 days before being imaged. The colonies were counted using OpenCFU [228]. Data from 5 to 9 colonies from at least 3 independent transformants was used.

3.4.5 Canavanine mutagenesis assay

Individual colonies of the indicated strains were transformed with an empty plasmid or a plasmid expressing *ALKBH2* and grown in 3ml SC-URA medium or SC-URA medium containing 0.00033% MMS for 20 h at 30˚C. The cultures were diluted to 3.0 OD_{600}. 150 ul were plated on SC-ARG+CAN (0.006% canavanine) medium in duplicate or 150 ul of a 1:10,000 dilution were plated on SC medium in duplicate. The plates were then incubated for 48 hours at 30˚C before being imaged. Colonies were used to measure total cell number (SC) or forward mutation rates

(SC-ARG+CAN). The colonies were counted using OpenCFU [228]. The mutation frequency was obtained by dividing colony number in SC-ARG+CAN by the number obtained in the SC plates times the dilution factor. Data from 10 to 20 colonies from at least three independent transformants were used.

3.4.6 Yeast-Two-Hybrid assays

The yeast-two-hybrid experiments using the indicated pGAD and pGBD plasmids were performed as described [45] except that both pGAD and pGBD plasmids were transformed into PJ69-4A [173]. A yeast-two-hybrid interaction is indicated by growth on synthetic complete (SC) medium lacking histidine, tryptophan, and leucine whereas equal cell loading was observed by plating the cells on SC medium lacking tryptophan and leucine to select for the pGAD (leucine) or pGBD (tryptophan) plasmids.

3.5 Acknowledgments

This chapter is modified from the following collaborative in preparation manuscript:

Bonilla, B., T.M. Mertz, K.S. Rapchak, E. MacNary, C.A. Pressimone, H. Zaher, N. Mosammaparast, S.A. Roberts, K.A. Bernstein. “The yeast Shu complex promotes error-free bypass of 3-methylcytosines”.

Author contribution is detailed in the figure legends. B.B., K.S.R., and C.A.P. performed the experiments. T.M.M., E.M., and S.A.R. performed and analyzed the sequencing. B.B., S.A.R.,

N.M., and K.A.B. designed the experiments. B.B. wrote the manuscript with the contribution of K.A.B.

4.0 Discussion

In this work, we broadened our understanding of the molecular function of yeast Shu complex during repair of alkylation-induced DNA damage. We found that disruption of the Shu complex leads to a mutational pattern that is consistent with a role in error-free tolerance of AP sites and 3meC arising from chronic MMS exposure. We also found that, during replication, the Shu complex is recruited to the chromatin in response to AP site accumulation through a direct DNA interaction. Moreover, we show that Shu complex DNA binding activity is critical for the Rad51 association to the chromatin and cell survival upon AP site accumulation. Importantly, we also found that the Shu complex prevents mutagenesis from APOBEC-induced AP sites. This demonstrates that the Shu complex specifically responds to AP sites arising at the lagging strand of replication intermediates independently from MMS-induced DNA damage. One implication of these results is that the Shu complex is likely involved in preventing mutagenesis from spontaneous AP sites and that spontaneous AP sites are the major contribution of the mutagenesis observed in undamaged Shu complex disrupted cells.

In addition to the Shu complex function in bypassing AP sites, we uncovered a novel and unexpected role for the yeast Shu complex in error-free tolerance of 3meC. In most organisms, 3meC are usually repaired by the AlkB family of enzymes. However, since budding yeast does not encode for an AlkB homolog, how yeast repairs 3meC has been a long-standing question in the field. Suggesting a function for the yeast Shu complex in the processing of 3meC, we find that the ectopic expression of human *ALKBH2* specifically rescues the MMS-induced phenotypes observed in cells with deletion of the Shu complex. Moreover, *ALKBH2* expression alleviates the MMS-induced mutations primarily occurring at G:C base pairs. Interestingly, we also find that

ALKBH2 mediated rescue of the MMS sensitivity is weak or absent in cells with deletion of other HR factors. This further supports the specialized role of the Shu complex in replication-associated DNA base damage. Finally, we observe that *ALKBH2* expression does, in turn, rescue the MMS-induced sensitivity of *UBC13* deleted cells. This is consistent with the idea that 3meCs are tolerated by the error-free post-replicative repair pathway. Overall, our findings help to seal the long-standing gap of knowledge on how yeast tolerates 3meC.

In this chapter, we will discuss the outstanding questions and broader implications of our findings on understanding the complex function of the Shu complex.

4.1 Is the role of the Shu complex in lesion bypass conserved in humans?

As described in the introduction, there are several lines of evidence pointing to the evolutionary conservation of the Shu complex from yeast to humans. This evidence includes sequence conservation and phylogenetic analyses based on the SWIM domain in SWS1 [21, 66]. Godin et al. performed evolutionary analysis using SWS1 and Shu2, which led to the discovery of Shu2/SWS1 homologs in different organisms across the Eukaryotic domains such as *D. melanogaster*, *C. elegans*, *G. lambia,* and *Arabidopsis thaliana* [66]. Importantly, deletion of Shu complex members in different model organisms such as *C. elegans*, mice, and human cell lines have shown remarkably similar phenotypes such as excessive anti-recombinase activity, MMS sensitivity, defects in RAD51 foci formation, replication stress response defects, and meiotic defects [21, 24, 49, 50, 53, 54, 67]. This body of work strongly suggests functional conservation for the Shu complex across eukaryotic lineages. It is therefore logical to hypothesize a role for the

human Shu complex in the error-free bypass of specific DNA lesions and future studies will address this phenomenon.

4.1.1 Role of the human Shu complex in AP sites tolerance

Here, we uncovered a novel and unexpected role for the yeast Shu complex in the error-free bypass of AP sites [229]. Abasic sites are one of the most common DNA lesions in mammalian cells and are generated spontaneously, by DNA damaging agents, and as byproducts of DNA repair pathways [230]. It is estimated that there are 10,000-30,000 AP sites generated each day in a mammalian cell [141, 142]. As in yeast, AP sites are a major source of mutation and replication stress [143, 231, 232]. Therefore, uncovering a role for the human Shu complex in the tolerance of AP sites would be of great relevance in understanding broader mechanisms of genome maintenance.

One of the first approaches to investigate the role of the human Shu complex in the tolerance of the AP sites would be to study the genetic interaction between the Shu complex and the enzymes responsible for AP site processing in mammalians. APE1 is the major AP endonuclease in mammalian cells and plays an essential role in the processing of AP sites by BER [233]. Our laboratory has recently generated SWS1 and SWSAP1 CRISPR-Cas9-based knock-out RPE-1 cell lines [50]. These cell lines could be treated with one or more of the several commercially available small molecule APE1 inhibitors, such as APE1 Inhibitor III (Calbiochem) or Aurintricarboxylic Acid [234]. Upon MMS treatment, MMS sensitivity can be assessed using cell viability, cell proliferation, and/or colony formation as read-outs. If the human Shu complex functions as a back-up for AP site tolerance, we would expect a synergistic effect on the MMS sensitivity when Shu complex knock-out cells are treated with APE1 inhibitor. Importantly, this effect should be

suppressed by ectopic expression of the Shu complex genes. Although the use of an APE1 small molecule inhibitor allows precise control over the APE1 activity enabling better characterization of the genetic interaction, they may exhibit off-target effects. To account for this, a different APE1 inhibitor could be used. Alternatively, the results can be recapitulated with an shRNA knockdown of APE1, which enables the use of ectopic expression of shRNA-resistant APE1 as control for the specificity of the effect.

As previously discussed, MMS induces a diverse set of lesions and repair intermediates and does not directly induce AP sites. Therefore, a complementary approach should aim to validate the observations using a different mechanism to induce AP sites other than MMS. One option is to interrogate the genetic interaction of the human Shu complex with the APOBEC cytidine deaminases. The APOBEC enzymes catalyze the deamination of cytidines in ssDNA resulting in deoxyuridine (dU). dU is then excised by the UNG2 glycosylase leading to AP sites in the DNA. The APOBEC enzymes are most common and diverse among vertebrates with some mammals, like humans, encoding 11 variants/paralogs. The APOBEC enzymes have roles in RNA editing, and defense against viral infection and retrotransposons [235]. For instance, their cytidine deaminase activity targets the viral genomes, or their replication intermediates inducing deoxyuridines that result in mutations upon replication [236]. Besides their role in limiting viral replication, the APOBEC enzymes have gained interest due to their role in cancer. Genome-wide sequences analysis showed that dysregulated APOBEC activity is a source of mutagenesis in 15% of cancers [154-156, 237]. Mutagenesis by the APOBEC enzymes arises from DNA replication of dU-containing DNA and the AP sites generated when the uracils are excised by the UNG2 glycosylase [238, 239].

In this work, we demonstrate that the yeast Shu complex promotes error-free tolerance of APOBEC3B-induced AP sites. Therefore, is it possible to hypothesize that the human Shu complex would similarly be involved in the processing of APOBEC-induced AP sites. To demonstrate this, one could first analyze if APOBEC overexpression leads to S-phase arrest, DNA damage, and increased markers of HR activity such as RAD51 foci and sister chromatid exchanges. Importantly, these phenotypes should not be observed when a catalytically dead APOBEC is expressed; and should be suppressed by UNG2 inhibition by expression of a uracyl glycosylase inhibitor (UGi) from the *B. subtilis* bacteriophage, PBS2 [240]. If the human Shu complex promotes error-free tolerance of APOBEC-induced AP sites, the absence of the Shu complex may lead to increased DNA damage and/or mutagenesis when APOBEC enzymes are overexpressed. For instance, DSB occurrence in APOBEC-overexpressing SWS1 and SWSAP1 knock-out RPE-1 cell lines [50] can be assessed by neutral comet assay. Moreover, APOBEC-induced mutagenesis in these cells can be analyzed by performing whole-genome sequencing analysis of these cells. It is expected that in the absence of the Shu complex, APOBEC-induced AP sites would lead to an increase in TLS-mediated mutagenesis. Importantly, this APOBEC-induced mutagenesis exhibits a specific pattern due to APOBEC sequence motif specificity and the nucleotide biases from the TLS activity [156]. Finally, if the human Shu complex prevents DNA damage and/or mutagenesis from APOBEC activity, depletion of the Shu complex would lead to increased cell death or growth arrest in cells that exhibit APOBEC mutagenesis. To approach this, one could identify cell lines with different levels of APOBEC activity by analyzing exome databases and APOBEC expression levels. The Shu complex can be downregulated in the selected cell lines and its effect on cell death can be assessed by clonogenic survival assays. It is expected that we would observe a correlation between the cells' sensitivity to Shu complex

depletion and their levels of APOBEC activity. Again, this effect should be suppressed by the expression of UGi. One potential caveat of this approach is that resistance may occur from increased TLS activity, to overcome this, the cells can be treated with TLS inhibitors or *REV3* could be downregulated by shRNA or siRNA.

4.1.2 Role of the human Shu complex in 3meC tolerance

Here, we also uncovered a novel role for the yeast Shu complex in the error-tolerance of 3meC. 3meC is a toxic and mutagenic DNA lesion that is repaired by members of the AlkB enzyme family [203]. Members of this family are present in the genome of most organisms, including *E. coli* and humans. However, a budding yeast AlkB homolog has yet to be identified [203, 211]. A recent publication proposes that the yeast glycosylase Mag1 is responsible for 3meC removal from dsDNA, channeling 3meC repair to the BER pathway [211]. However, considering that this DNA lesion predominantly arises at ssDNA replication intermediates, it is still crucial to elucidate how yeast handle 3meC during replication. Here, we found that the yeast Shu complex promotes the error-bypass of 3meC.

ALKBH2 and *ALKBH3* have been proposed as tumor suppressors, being silenced in various tumors, including gastric and breast cancer [203, 215-217]. On the other hand, *ALKBH3* is overexpressed in different cancers and inhibition of ALKBH2 and ALKBH3 can sensitize cancer cells to DNA chemotherapy [218-222]. Moreover, *ALKBH2* and *ALKBH3* upregulation mediate resistance to chemotherapeutic agents such as temozolomide and *ALKBH3* loss leads to endogenous 3meC accumulation in tumor cell lines [209, 223, 224]. Therefore if the human Shu complex promotes the tolerance of 3meC, the Shu complex could play a role in cancers with aberrant ALKBH2 or ALKBH3 expression.

Considering the functional conservation of the Shu complex from yeast to humans, future experiments should address the role of the Shu complex in the error-free tolerance of 3meC. An analogous strategy to the one proposed to interrogate the role of the human Shu complex in the tolerance of AP sites can be envisioned. Firstly, it is important to determine whether HR serves as a back-up tolerance strategy for ALKBH2 and ALKBH3 repair of 3meC. To answer this, ALKBH2 and/or ALKBH3 could be downregulated by shRNA or inhibited by Rhein or 2-Hydroxyglutarate treatment [241, 242]. It is expected that when ALKBH2 and/or ALKBH3 activity is impaired, an increase in markers for HR activity would be observed upon MMS treatment when. This increased reliance on HR can be observed by more RAD51 foci, polyubiquitination of PCNA, and sister chromatid exchanges. Moreover, since 3meC can be detected by immunofluorescence [243], it is possible to analyze whether 3meCs colocalize to MMS-induced Rad51 foci during S-phase. Importantly, the effects observed when ALKBH2/3 are knocked-down by shRNA should be suppressed by expression of shRNA-resistant ALKBH2/3 but not by expression of catalytic dead ALKBH2/3.

Complementary evidence for the role of the Shu complex and HR as in the error-free tolerance of 3meC could come from the analysis of mutation patterns upon MMS treatment. In humans, 3meC can be bypassed by TLS polymerases which leads to a mutational pattern that includes mostly C->A and C->T [244, 245]. Therefore, if the Shu complex is involved in error-free tolerance of 3meC, it is expected that cell lines with KO of the Shu complex genes (such as the ones generated by our laboratory [50]), would show an increase in C->A and C->T mutations upon MMS treatment. Importantly, since ALKBH2 mediates resistance to alkylation damage [223, 245], this effect would be rescued by overexpression of *ALKBH2* and/or *ALKBH3*.

Furthermore, it would be important to assess whether the downregulation of the Shu complex would sensitize ALKBH2 and ALKBH3 deficient cells to alkylating DNA damage. To approach this, the Shu complex genes can be knocked down by shRNA in cell lines where ALKBH2 repair is impaired. For instance, ALKBH2 repair is impaired in commercially available cell lines with specific *IDH1* or *IDH2* mutations [218, 241]. IDH1 and IDH2 catalyze the formation of α-ketoglutarate, a substrate for ALKBH enzymes. Some cancer-associated mutations in *IDH1* or *IDH2* lead to the production of 2-Hydroxyglutarate instead of α-ketoglutarate. This alternative product acts as a competitive inhibitor of the ALKBH enzymes [241]. Alternatively, ALKBH2 can be downregulated by shRNA or inhibited by Rhein treatment [242]. MMS or Temozolomide (TMZ) sensitivity can be evaluated by clonogenic survival assays.

One limitation of both the sequencing analysis and the genetic approaches stems from the diversity of lesions and repair intermediates that both TMZ and MMS induce. It is technically challenging to selectively induce 3meC, however, there are a couple of approaches that may mitigate this potential limitation. Since 3meC arises exclusively at ssDNA, the damage incidence of 3meC can be enhanced by inducing ssDNA. Therefore, HU treatment or S-phase synchronization would increase the amount of ssDNA.

One recent work demonstrated that ALKBH3 is recruited to sites of damage by direct physical interaction with the RAD51 paralog, RAD51C [243]. This surprising observation opens the possibility that a similar interaction between the human Shu complex members and ALKBH2 or ALKBH3 could take place. We can easily test this possibility by Y2H analysis or co-IP.

4.2 What are the events that lead to the recruitment of the Shu complex to DNA damage?

Early work from the Rothstein and Xiao groups revealed that the yeast Shu complex is a member of the error-free PRR pathway [58, 83]. Several results from these groups lead to this conclusion, most importantly: 1) deletion of the Shu complex members leads to increased spontaneous and DNA damage-induced mutagenesis that is dependent on Rev3 [58]; 2) deletion of the Shu complex leads to a synergistic increase in the MMS sensitivity when combined with deletions of the TLS genes [83]; 3) The Shu complex deletions are epistatic to deletion of genes controlling the error-free PRR pathway, such as *MMS2* and *UBC13*, with respect to MMS-induced damage [58]; 4) Deletion of the Shu complex genes rescues the MMS sensitivity conferred by deletions of genes involved in resolving HR intermediates, such as *SGS1* and *TOP3 [58]*; 5) deletion of the Shu complex genes leads to delayed S-phase progression [83]; 6) deletion of the anti-recombinase *SRS2* rescues the MMS sensitivity seen in Shu complex mutant cells [83]. Despite this compelling evidence, our understanding of the Shu complex function has been limited in part due to the lack of approaches that can directly detect the Shu complex at DNA damage sites.

In this work, we optimized a cell fractionation protocol that enabled us to monitor the recruitment of the Shu complex to the chromatin fraction upon MMS treatment. Using this approach, we showed that the Shu complex is recruited to chromatin upon AP site accumulation through direct interaction with the DNA (**Figure 4b**). We also showed that the Shu complex chromatin association is proportional to the amount of DNA damage. These results represent the first direct detection of the Shu complex responding to DNA damage.

We believe that the expansion of this approach holds great promise for the advancement of our understanding of the Shu complex role during the error-free PRR pathway. In fact, by

combining this approach with simple deletions, one could envision several important questions that could be readily answered. For example, the poly-ubiquitination of PCNA by the Rad5-Mms2-Ubc13 complex is regarded as the key step controlling the error-free PRR pathway [113, 185, 213, 246]. However, its precise role remains unclear. It would be informative to know the poly-ubiquitination of PCNA is required for the recruitment of the Shu complex to the chromatin. This can be answered by studying the effect of the deletion of *MMS2* or *UBC13* on the Shu complex recruitment to the chromatin upon MMS damage. Similarly, it would be interesting to explore if the deletion of *RAD52* leads to impaired recruitment of the Shu complex to the chromatin. Rad52 is the main Rad51 mediator, as it physically interacts with Rad51 and is critical for its recruitment to DNA damage sites [30]. However, it is not known whether Rad52 is also important for the recruitment of the Rad51 paralogs.

DNA lesions that block DNA synthesis do not usually lead to replisome stalling thanks to the naturally occurring re-priming at the lagging strand and the re-priming activity from the Polα/primase complex at the leading strand [117]. However, these activities lead to the accumulation of ssDNA gaps behind the advancing replication fork. Recent work has revealed that these ssDNA gaps are bidirectionally expanded by the coordinated activities of the nucleases Exo1 and Mre11, the helicase Pif1, and the PCNA and 9-1-1 clamp complexes [247, 248]. This expansion is needed for the activation of the Rad9-Rad53 DNA damage checkpoint and sister chromatid invasion [247, 249]. However, it is not known if any of these events precede or are needed for the recruitment of the Shu complex.

In yeast, Srs2 is a helicase that binds SUMOylated PCNA during replication and is responsible for preventing unscheduled/unwanted HR at replication intermediates [77, 250-253]. Srs2 is often regarded as an anti-recombinase for its ability to stimulate Rad51 filament

disassembly. Srs2 physically interacts with Shu1 and Shu2 [46, 80]. This interaction is conserved since the Shu2 homolog in fission yeast, Sws1, also interacts with Srs2 [21]. From a functional point of view, the deletion of the Shu complex leads to elevated Srs2 foci while *SRS2* deletion rescues the MMS sensitivity seen in *REV3 SHU* complex double mutant cells [46, 83]. Therefore, the Shu complex is thought to promote Rad51 filament formation in part by inhibiting Srs2. Interestingly, the human Shu complex inhibits the RAD51-anti-recombinase of FIGNL1 [42, 54]. However, it is not known if, conversely, Srs2 affects the Shu complex recruitment to DNA damage sites. To answer this, it is possible to overexpress Srs2 and analyze its effect on the recruitment of the Shu complex to the chromatin upon MMS treatment.

An alternative technique that could be implemented to monitor the recruitment of the Shu complex to the chromatin upon DNA damage is iPOND (isolation of proteins on nascent DNA). This technique allows temporal analysis of protein recruitment to replication forks by labeling the newly synthesized DNA with EdU, and subsequently cross-linking the DNA to proteins. This allows the Edu labeled DNA to can be conjugated to biotin and following streptavidin purification the proteins-of-interest can then be identified by western blot [254-256]. Therefore, we could analyze how the recruitment Shu complex to newly synthesized DNA upon MMS treatment is affected by the deletion of the above-mentioned factors. Interestingly, the use of APOBEC and a thymidine chase stage could allow differentiating whether the Shu complex is recruited to the replication fork or ssDNA gaps left behind the moving fork. However, iPOND has been largely used in mammalian and mostly with HU treatment, therefore its application in yeast and with an MMS treatment would likely require optimization.

Overall, answering these questions will greatly expand our understanding of the precise circumstances and signals that lead to the engagement of the Shu complex-mediated bypass.

Additionally, the specialization of the Shu complex in the error-free PRR makes it the ideal read-out for monitoring HR activity at this pathway.

4.3 Does the phosphorylation of S2,8,14 in Rad55 play a role in the interaction with Csm2?

The Shu complex physically interacts with the Rad51 paralog Rad55 through its member Csm2 [45, 84]. Early work by the Heyer group showed that Rad55 is phosphorylated on Serine residues 2, 8, and 14 (Rad55-pS2,pS8,pS14) in response to MMS [119]. Interestingly, when challenged with a myriad of DNA damaging agents, cells with non-phosphorylatable mutant Rad55 (phospho-deficient Rad55 - rad55-S2,8,14A) showed sensitivity primarily to MMS [119]. This contrasts with the phenotypes seen in cells with a deletion in *RAD55*, which include increased sensitivity to a broad range of DNA damaging agents including HU and IR [119, 136, 257]. However, the phenotypes exhibited by *rad55-S2,8,14A* cells are reminiscent of the ones exhibited by cells with deletions of the Shu complex [18, 58, 81]. Furthermore, similar to cells lacking the Shu complex, the phospho-deficient Rad55 mutant leads to synthetic sickness when combined with a TLS mutant upon exposure MMS [18, 81, 83, 119]. Interestingly, in an attempt to explain the MMS sensitivity seen in cells expressing phospho-deficient Rad55, Herzberg et al. analyzed the known Rad55 interactions, and they found that this mutant is proficient to interact with all its known protein partners [119]. However, the interaction with Csm2 had not been described at that time.

Here, we found that similar to a deletion of the Shu complex, but unlike a deletion of *RAD55*, the MMS sensitivity of cells expressing rad55-S2,8,14A is strongly rescued by expression *ALKBH2*. This is can be explained by the fact that cells with deletions of the Shu complex or

expressing *rad55-S2,8,14A* are proficient for DSB repair while cells lacking *RAD55* are not. To further explore if there is a functional relationship between the deletion of the Shu complex and the phospho-deficient Rad55 mutant, we compared the MMS sensitivity of the double mutant to each single mutant. Surprisingly, we observe that the MMS sensitivity of a *csm2Δ rad55-S2,8,14A* mutant is the same as the one observed in *CSM2* null cells. This suggests that the defects seen in the *rad55-S2,8,14A* mutant, are related to the Shu complex. Furthermore, in a Y2H analysis under untreated conditions, we found that the interaction between Csm2 and rad55-S2,8,14A. is impaired compared to WT Rad55. Even though these results do not completely rule out an effect of Rad55 phosphorylation, they do support the notion that the growth defects seen in cells expressing the *rad55-S2,8,14A* mutant are likely due to an impaired interaction with the Shu complex rather than its inability to be phosphorylated.

Previous work by our group mapped *csm2-F46A*, a mutation that disrupts the interaction with Rad55 [41]. Importantly, csm2-F46A is incapable of promoting Rad51 filament formation *in vitro* and leads to a similar growth defect as the deletion of Csm2 *in vivo* [41]. These results show that this interaction is critical for the Shu complex activity. In contrast, our sensitivity assay shows that cells expressing the *rad55-S2,8,14A* mutant are less sensitive to MMS than cells with deletions in the Shu complex. One simple scenario to explain this discrepancy is that the rad55-S2,8,14A mutant and Csm2 still retain partial interaction. To confirm our findings and further explore the relationship between Rad55 and the Shu complex, several approaches can be pursued.

First, it would be important to characterize the interaction defect between rad55-S2,8,14A and Csm2. This can be done by performing *in vitro* pulldowns with purified GST-tagged WT Csm2-Psy3 and purified 9-MYC-tagged phospho-deficient Rad55-Rad57 heterodimer. To evaluate this in a more physiological setting, we can perform co-immunoprecipitation (co-IP) with

endogenously expressed 6HA-tagged Csm2, 9MYC-tagged phospho-deficient Rad55, and also WT proteins from MMS treated or control cultures, in the presence of Benzoase. Finally, to study the effect of *rad55-S2,8,14A in situ*, we can perform proximity ligation assay (PLA) using the cells described for co-IP. It is important to note that the Shu complex members have not been localized to DNA repair centers (observed as fluorescent foci) potentially due to their low abundance. This prevents us from studying their interactions with other DNA repair proteins using fluorescent tags.

To further describe the genetic interactions between *rad55-S2,8,14A* and the Shu complex, we can evaluate the mutation frequencies and gene conversion frequency. To analyze mutation frequencies, we can use the previously mentioned canavanine forward-mutation assay (2.4.4 Canavanine mutagenesis assay, page 46; and 3.4.5 Canavanine mutagenesis assay, page 77). To evaluate the gene conversion frequency, it is possible to use a direct repeat recombination assay, which allows the identification of DSB-independent HR events based on the expression of reporter genes [258]. In this assay, strains harbor a pair of differentially mutated reporter genes in direct orientation (heteroallelic repeat, *leu2-1*, and *leu2-2*) with a functional reporter gene in between (*URA3*). In this context, functional Leu+ auxotrophs (colonies able to grow in media lacking Leucine) can be generated through recombination between the mutated alleles. Importantly, Ura+ Leu+ clones (colonies able to grow in medium lacking Leucine and Uracil) can only be generated through Rad51-mediated gene conversion. Conversely, Leu+ ura- colonies (colonies able to grow in media lacking Leucine but not Uracil) are originated mainly from homology-directed annealing of ssDNA between directly repeated *leu2* alleles, which also results in deletion of the intervening *URA3* marker. Since this mechanism does not involve strand invasion, it is independent of Rad51.

Overall, if rad55-S2,8,14A and Csm2 have indeed impaired interaction, the absence of phosphorylation is not the only potential explanation for the phenotypes seen in *rad55-S2,8,14A*

expressing cells. A traditional approach to test the role of phosphorylation is the use of phosphomimetic mutations, usually changing the Serine residues to Aspartic acid or Glutamic acid. Unfortunately, Herzberg et al. did not include said mutants in their work. Another important player to study the role of phosphorylation is the kinase responsible for the modification. Unfortunately, this has yet to be identified. It still possible that the phosphorylation observed by the Heyer group was an artifact due to the overexpression of the Rad55-Rad57 heterodimer and sample processing.

On the other hand, our protein-protein interaction results with rad55-S2,8,14A may inform about which are the residues in Rad55 that are responsible for its interaction with Csm2. An approach involving truncations and mutations at Rad55 N-terminal domain will likely uncover/identify which residues are important for its interaction with Csm2. Identifying a Rad55 interaction mutant would add a valuable tool for future studies that aim to answer questions reading the biological role of the Rad55-Csm2 interaction. For example, is the Rad55-Csm2 interaction important for the role of the Rad51 paralogs during Srs2 inhibition? Is the Rad55-Csm2 interaction important during meiosis? And, is this interaction important for the recruitment of the complexes to damage sites?

4.4 Concluding remarks

In this work, we present evidence suggesting that the yeast Shu complex promotes an HR mediated error-free bypass of two mutagenic and toxic DNA lesions: AP sites and 3meC. Considering the functional conservation of the Shu complex across eukaryotes, our findings have implications on future approaches to understanding the role of the human Shu complex. Although

the canonical human Rad51 paralogs have been implicated in cancer, the role of the Shu complex in cancer has remained elusive. Importantly, our result dissecting the DNA lesion specificity of the Shu complex (and its potential genetic interactions with cancer-relevant factors such as APOBEC and ALKBH enzymes), could inform the different scenarios where the Shu complex may play a role in tumorigenesis or even chemoresistance.

Appendix A Supplemental figures

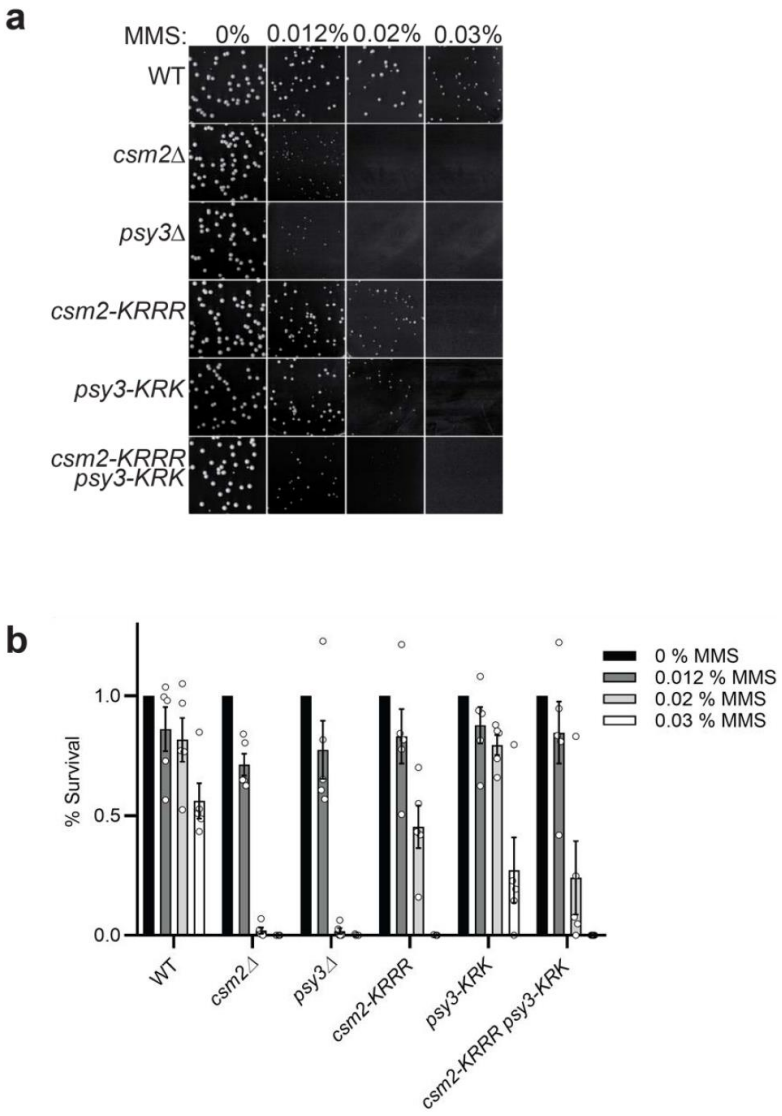

Figure 15. Viability of Csm2 and Psy3 DNA binding mutants upon MMS exposure

(**a**) Representative images of the indicated genotypes used for serial dilution viability assays. All strains were exposed to MMS for 2 days at 30˚C. (**b**) Viability as determined by cell counts on three plates for Csm2 and Psy3 DNA binding mutants per condition. The experiment was repeated five times with standard deviations plotted. This figure was generated by BWH and published in [120].

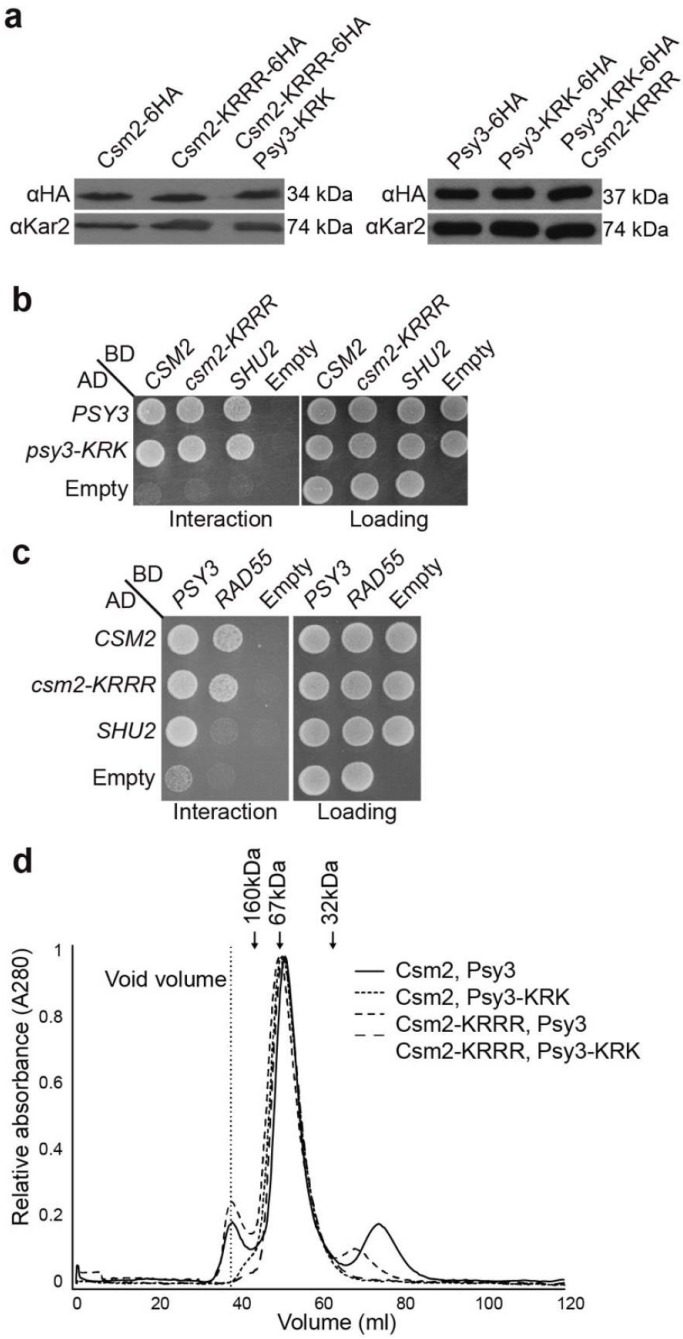

Figure 16. Csm2-Psy3 DNA binding mutants express normally and retain their protein-protein interactions

(**a**) Mutating the DNA binding residues in Csm2 and Psy3 does not affect protein expression. Protein was extracted from equal cell numbers and protein expression levels of the indicated 6HA tagged strains were determined by protein blot using an HA antibody. Expression of Kar2 was used as a loading control. (**b**) Csm2 and Psy3 DNA binding mutants exhibit wild-type yeast-2-hybrid (Y2H) interactions. Y2H analysis of pGAD-*PSY3*, pGAD-*psy3-KRK*, or pGAD-C1 (Empty) with pGBD-*CSM2*, *csm2-KRRR*, *SHU2*, or pGBD-C1 (Empty). A Y2H interaction is indicated by

plating equal cell numbers on SC medium lacking histidine, tryptophan, and leucine. Equal cell loading is determined by plating on SC medium lacking tryptophan and leucine used to select for the pGAD (AD) and pGBD (BD) plasmids. (**c**) Y2H interactions performed as in (**b**), with analysis of pGAD-*CSM2*, pGAD-*csm2-KRRR*, pGAD-*SHU2*, or pGAD-C1 (Empty) with pGBD-*PSY3*, pGBD-*RAD55*, or pGBD-C1 (Empty). (**d**) Csm2 and Psy3 DNA binding mutants form a stable heterodimer with similar properties as wild-type. Overlaid chromatograms show the elution profile of Csm2-Psy3 heterodimers for wild-type and DNA binding mutant combinations resolved using size exclusion chromatography. This figure was published in [120]. Author contribution: panel a: BB and BWH; panels b and c: BWH; panel d: JCR.

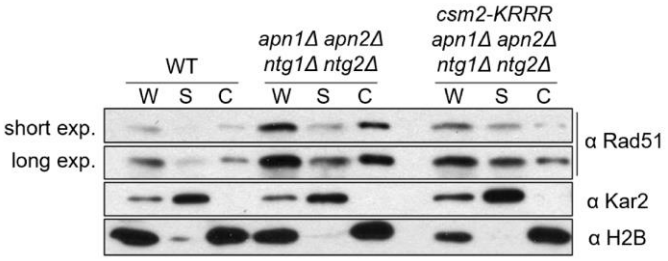

Figure 17. Csm2-Psy3 DNA binding motif is critical for Rad51 chromatin association upon AP site accumulation

Cells with the indicated genotype were synchronized in G1 with alpha-factor and released into YPD medium or YPD medium containing 0.02% MMS for 1 hour before cellular fractionation. Rad51 protein levels from whole-cell extract (W), supernatant (S), and chromatin (C) fractions were determined by western blot. Kar2 and histone H2B were used as fractionation controls (S and C, respectively). This figure was generated by BB.

Appendix B Supplemental tables

Supplemental Table 1. Dissociation constants for Csm2-Psy3 DNA binding mutants

Name	Dissociation constant (K_d)	B_{max}
WT (3' strand)	435 +/- 37	0.28 +/- 0.01
Csm2 Psy3-KRK	2828 +/- 512	0.4 +/- 0.0
Csm2-KRRR Psy3	N.D.	N.D.
Csm2-KRRR Psy3	N.D.	N.D.

Supplemental Table 2. Yeast strains and plasmids

Yeast strains				
Simplified genotype used in figures and text	Strain ID	Genotype	Strain Background	Reference
WT (wild-type)	W9100-17D	*MAT*a *ADE2 leu2-3,112 his3-11,15 ura3-1 TRP1 lys2*Δ *RAD5*	W303	Godin et al, 2015. Genetics
csm2Δ	KBY107-2D	*MAT*a *csm2Δ::KanMX LYS2*	W303	Godin et al, 2015. Genetics
psy3Δ	KBY108-3D	*MAT*a *psy3Δ::KanMX4 trp1-1 LYS2*	W303	Godin et al, 2016. Nucleic Acids Res
csm2-KRRR	KBY820-1	*MAT*a *csm2-K189A,R190A,R191A,R192A trp1-1 LYS2*	W303	This study
psy3-KRK	KBY909-1	*MATα psy3-K199A,R200A,R201A trp1-1 LYS2*	W303	This study
csm2-KRRR psy3-KRK	KBY945-3A	*MATa psy3-K199A,R200A,K201A csm2-K189A,R190A,R191A,R192A LYS2 trp1-1*	W303	This study
csm2-6xHA	KBY530-1	*MATα CSM2-6HA-k.i.TRP1 LYS2 trp1-1*	W303	This study
csm2-KRRR-6xHA	KBY1106-1	*MATa csm2-K189A,R190A,R191A,R192A-6HA-k.i.TRP1 LYS2 trp1-1*	W303	This study
csm2-KRRR-6xHA psy3-KRK	KBY1108-1	*MATa psy3-K199A,R200A,K201A csm2-K189A,R190A,R191A,R192A-6HA-k.i.TRP1 LYS2 trp1-1*	W303	This study
psy3-6xHA	KBY565-1A	*MATa PSY3-6HA-k.i.TRP1 trp1-1*	W303	This study
psy3-KRK-6xHA	KBY1105-1	*MATa psy3-K199A,R200A,K201A-6HA-k.i.TRP1*	W303	This study

Supplemental Table 2 continued

psy3-KRK-6xHA csm2-KRRR	KBY1107-1	*MATa psy3-K199A,R200A,K201A-6HA-k.i.TRP1 csm2-K189A,R190A,R191A,R192A LYS2 trp1-1*	W303	This study
	PJ69-4A*	*MATa trp1-901 leu2-3,112 ura3-52 his3-200 gal4Δ gal80Δ GAL2-ADE2 LYS2::GAL1-HIS3 met2::GAL7-lacZ*	W303	James et al, 1996. Genetics
	PJ69-4α*	*MATα trp1-901 leu2-3,112 ura3-52 his3-200 gal4Δ gal80Δ GAL2-ADE2 LYS2::GAL1-HIS3 met2::GAL7-lacZ*	W303	James et al, 1996. Genetics
WT	ySR_128	*MATα lys2Δ(Chr.II) ura3Δ(Chr.V) can1Δ(Chr.V) ade2Δ(Chr.XV) leu2-3,112 trp1-289 his7-2 Chr.II 488694::lys2::ADE2-URA3-CAN1*	CG379	Roberts et al. 2012. Mol Cell
ung1Δ	ySR_616	*MATα ung1::NatMX*	CG379	Hoopes et al. 2016.Cell Rep
csm2Δ	yTM_62	*MATα csm2::HygMX*	CG379	This study
psy3Δ	yTM_54	*MATα psy3::HygMX*	CG379	This study
ung1Δ csm2Δ	yTM_70	*MATα ung1::NatMX csm2::HygMX*	CG379	This study
ung1Δ psy3Δ	yTM_52	*MATα ung1::NatMX psy3::HygMX*	CG379	This study
WT	KBY869-1C	*MATa CAN1 trp1-1 LYS2*	W303	Godin et al, 2016. Nucleic Acids Res
csm2Δ	KBY869-8A	*MATα csm2::KanMX4 CAN1 trp1-1 LYS2*	W303	Godin et al, 2016. Nucleic Acids Res
psy3Δ	KBY758-11A	*MATa psy3::KanMX4 CAN1 LYS2 trp1-1*	W303	Godin et al, 2016. Nucleic Acids Res
csm2-KRRR	KBY1080-1B	*MATa psm2-K189A,R190A,R191A,R192A LYS2 CAN1*	W303	This study
psy3-KRK	KBY1081-4B	*MATα psy3-K199A,R200A,K201A CAN1*	W303	This study

Supplemental Table 2 continued

csm2-KRRR psy3-KRK	KBY1101-2D	*MATa psy3-K199A,R200A,K201A csm2-K189A,R190A,R191A,R192A CAN1*	W303	This study
apn1Δ apn2Δ ntg1Δ ntg2Δ	KBY698-4A	*MATα ntg1::NatMX, ntg2::NatMX ,apn1::HygMX apn2::HygMX LYS2*	W303	Godin et al, 2016. Nucleic Acids Res
apn1Δ apn2Δ ntg1Δ ntg2Δ csm2Δ	KBY745-17C	*MATa csm2::KanMX ntg1::NatMX ntg2::NatMX apn1::HygMX apn2::HygMX LYS2*	W303	This study
apn1Δ apn2Δ ntg1Δ ntg2Δ csm2-KRRR psy3-KRK-6HA	KBY1187-41D	*MATα psy3-K199A,R200A,K201A-6HA-k.i.TRP1 csm2-K189A,R190A,R191A,R192A ntg1::NatMX ntg2::Nat apn1::HygMX apn2::HygMX LYS2*	W303	This study
Plasmids				
Name	Purpose	Backbone	Selection marker	
pAG32	HYG knock out cassette	pFA6	Ampicillin	Goldstein & McCusker, 1999. Yeast
pTM-19	empty vactor/ APOBEC3B mutagenesis	pySR-419	Ampicillin/LEU2	This study
pTM-21	APOBEC3B expression/ APOBEC3B mutagenesis	pSR-440	Ampicillin/LEU2	This study
pGAD-csm2-K189A,R190A,R191A,R192A	Y2H	pGAD-C1	Ampicillin/LEU2	This study
pGBD-csm2-K189A,R190A,R191A,R192A	Y2H	pGBD-C1	Ampicillin	This study
pGAD-PSY3-K199A-R200A-K201A	Y2H	pGAD-C1	Ampicillin/LEU2	This study
pGBD-psy3-K199A,R200A,K201A	Y2H	pGBD-C1	Ampicillin	This study

Supplemental Table 2 continued

pGAD-SHU2	Y2H	pGAD	Ampicillin/LEU2	Gaines et al. 2015. Nat Commun
pGBK-SHU2	Y2H	pGBK	Kanamicin	Godin et al, 2015. Genetics
pGAD-CSM2	Y2H	pGAD	Ampicillin/LEU2	Gaines et al. 2015. Nat Commun
pGBK-CSM2	Y2H	pGBK	Kanamicin	Gaines et al. 2015. Nat Commun
pGAD-PSY3	Y2H	pGAD	Ampicillin/LEU2	Gaines et al. 2015. Nat Commun
pGBK-PSY3	Y2H	pGBK	Kanamicin	Gaines et al. 2015. Nat Commun
pGBD-RAD55	Y2H	pGBD	Ampicillin	Gaines et al. 2015. Nat Commun
pGAD-C2	Y2H empty vector	N/A	Ampicillin/LEU2	
pGBD-C1	Y2H empty vector	N/A	Ampicillin	
YIplac211-csm2-K189A,K190A,R191A,R192A	Yeast integration	YIplac211	Ampicillin/URA3	This study
YIplac211-psy3-K199A,R200A,R201A	Yeast integration	YIplac211	Ampicillin/URA3	This study
pRSF-Duet-CSM2-PSY3	Protein expression	pRSF-Duet	Kanamicin	This study
pRSF-Duet-csm2-K189A,K190A,R191A,R192A-PSY3	Protein expression	pRSF-Duet	Kanamicin	This study
pRSF-Duet-CSM2-psy3-K199A,R200A,R201A	Protein expression	pRSF-Duet	Kanamicin	This study
pRSF-Duet-csm2-K189A,K190A,R191A,R192A-psy3-K199A,R200A,R201A	Protein expression	pRSF-Duet	Kanamicin	This study

Unless noted, all W303 strains are RAD5+ and isogenic to W9100-17D (Thomas & Rothstein, 1989) which is derived from W1588 (Zhao et al, 1998).

All CG379 strains are isogenic to ySR_128

* Strains derivative from DGY63::171 (James et al, 1996)

Supplemental Table 3. PCR oligos

Name	Description	Sequence
oTM-550	*CSM2* deletion cassette generation (forward)	AATAAAAAAAAAATGGAGAGAAGAGACTG CTAGCGGCAAAGGATGCAGCTGAAGCTTCG TACGC
oTM-551	*CSM2* deletion cassette generation (reverse)	GGTGTTACATGGTGTACCGATGCTTTAATTG CACTTATGTAGTCAGCATAGGCCACTAGTG GATCTG
oTM-556	*PSY3* deletion cassette generation (forward)	AAATTCTTAGGAAAAGAGAAAGGAAGTAG CGAATGGAATGGGATGCAGCTGAAGCTTCG TACGC
oTM-557	*PSY3* deletion cassette generation (reverse)	ATTTATGTATCTGAGTTTTTAATGTTTTTTTT CCTTCTCTTATCAGCATAGGCCACTAGTGGA TCTG
oTM-546	confirmation of *csm2*Δ::HygMX (forward)	ATTACAAAGAACTCAACTCACTGGC
oTM-549	confirmation of *csm2*Δ::HygMX (reverse)	AATTATTATTACACAGCAGCCCAAG
oTM-552	confirmation of *psy3*Δ::HygMX (forward)	AATCTTCTATTTGGTTGGGTTCTTC
oTM-555	confirmation of *psy3*Δ::HygMX (reverse)	AACTCCACCTTAATACAATTGGACA
oTM-074	Amplification of LEU2 from pUG73 (forward)	CCGCAGGCTAACCGGAACCTGTATT
oTM-075	Amplification of LEU2 from pUG73 (reverse)	GAGCTCGCTGTGAAGATCCCAGCAAAG
oTM-080	Amplification of pySR419 and pySR440 plasmid backbones (forward)	GTTTCTTAGACGTCAGGTGGCACTTT
oTM-081	Amplification of pySR419 and pySR440 plasmid backbones (reverse)	GCCAGAAAATGTTGGTGATGCGC
oTM-092	Amplification of *CAN1* for creation of mutation spectra (forward)	TATGAGGGTGAGAATGCGAAATGGCG
oTM-093	Amplification of *CAN1* for creation of mutation spectra (reverse)	AAGAGTGGTTGCGAACAGAGTAAACC
oTM-094	Sequencing of *CAN1* for creation of mutation spectra	TTGCCACATATCTTCAACGCTGTT

Supplemental Table 3 continued

oTM-095	Sequencing of *CAN1* for creation of mutation spectra	AAACTTTGTCACCACCAGTAGATGT
seqDG-91	Sequencing of *CAN1* for creation of mutation spectra	TTTGACAGGGAACAAGTT
Psy3.K199A.Forward	Psy3 site-directed mutagenesis at DNA binding residues (forward)	GATAAGTGGTCAATCGCGAGGAAAAGCGGCG
Psy3.K199A.Reverse	Psy3 site-directed mutagenesis at DNA binding residues (reverse)	CGCCGCTTTTCCTCGCGATTGACCACTTATC
Psy3.K199A.Add.R200A.Forward	Psy3 site-directed mutagenesis at DNA binding residues (forward)	GATAAGTGGTCAATCGCGGCGAAAAGCGGCGTTACAC
Psy3.K199A.Add.R200A.Reverse	Psy3 site-directed mutagenesis at DNA binding residues (reverse)	GTGTAACGCCGCTTTTCGCCGCGATTGACCACTTATC
Psy3.K199A.R200A.Add.R201A.Forward	Psy3 site-directed mutagenesis at DNA binding residues (forward)	GATAAGTGGTCAATCGCGGCGGCAAGCGGCGTTACACTGTACC
Psy3.K199A.R200A.Add.R201A.Reverse	Psy3 site-directed mutagenesis at DNA binding residues (reverse)	GGTACAGTGTAACGCCGCTTGCCGCCGCGATTGACCACTTATC
Csm2.K189A.Forward	Csm2 site-directed mutagenesis at DNA binding residues (forward)	GAACGTCATCTGTGCGTAGCGCAAGAAGGCGGATTAAAAATG
Csm2.K189A.Reverse	Csm2 site-directed mutagenesis at DNA binding residues (reverse)	CATTTTTAATCCGCCTTCTTGCGCTACGCACAGATGACGTTC
Csm2.K189A.Add.R190A.Forward	Csm2 site-directed mutagenesis at DNA binding residues (forward)	CATCTGTGCGTAGCGCAGCAAGGCGGATTAAAAATG
Csm2.K189A.Add.R190A.Reverse	Csm2 site-directed mutagenesis at DNA binding residues (reverse)	CATTTTTAATCCGCCTTGCTGCGCTACGCACAGATG
Csm2.K189A.R190A.Add.R191A.Forward	Csm2 site-directed mutagenesis at DNA binding residues (forward)	GTGCGTAGCGCAGCAGCGCGGATTAAAAATG

Supplemental Table 3 continued

Csm2.K189A.R190A.Add.R191A.Reverse	Csm2 site-directed mutagenesis at DNA binding residues (reverse)	CATTTTTAATCCGCGCTGCTGCGCTACGCAC
Csm2.K189A.R190A.R191A.ADDR191A.Forward	Csm2 site-directed mutagenesis at DNA binding residues (forward)	CGTAGCGCAGCAGCGGCGATTAAAAATGGAG
Csm2.K189A.R190A.R191A.ADDR191A.Reverse	Csm2 site-directed mutagenesis at DNA binding residues (reverse)	CTCCATTTTTAATCGCCGCTGCTGCGCTACG
Csm2.S2	Csm2 6xHA tagging cassette generation (forward)	GTACTGGTGTTACATGGTGTACCGATGCTTTAATTGCACTTATGTAGTCAATCGATGAATTCGAGCTCG
Csm2.S3	Csm2 6xHA tagging cassette generation (reverse)	ATTCCCTTGCTGAATATATCTGGAAGTATTATGCAGATTCATTATTCGAACGTACGCTGCAGGTCGAC
Csm2.CKF2	Csm2 6xHA tagging confirmation (forward)	AATGGAGAGAAGAGACTGCTAGCG
Csm2.CKR2	Csm2 6xHA tagging confirmation (reverse)	AGTCTAGCATCGGGGTAGTTTTCC
Psy3.S2	Psy3 6xHA tagging cassette generation (forward)	ATTTAATTTATGTATCTGAGTTTTTAATGTTTTTTTTCCTTCTCTTATCAATCGATGAATTCGAGCTCG
Psy3.S3	Psy3 6xHA tagging cassette generation (reverse)	AAGTTGTTGACGGCAGGCCACAGTACAGAAGGATAGCCGCACTTGAAGAACGTACGCTGCAGGTCGAC
Psy3.CKF2	Psy3 6xHA tagging confirmation (forward)	TGTGTACCGTAAGCATTACTCC
Psy3.CKR2	Psy3 6xHA tagging confirmation (reverse)	TCCTGGTAGATGTAAGCATTGC
KanHisNat	6xHA tagging confirmation sequencing	GACTGTCAAGGAGGGTATTCTG

Supplemental Table 4. Relative abundance of the MMS-induced lesions *in vitro*

	dsDNA occurrence (%)	ssDNA occurrence (%)
1-methyladenine (1meA)	3.8	18
3-methyladenine (3meA)	10	1.4
7-methyladenine (7meA)	1.8	3.8
3-methylguanine (3meG)	0.6	1
7-methylguanine (7meG)	85	68
O6-methylguanine (O6meG)	0.3	0
3-methylcytosine (3meC)	<1	10
methylphosphotriesters	0.80	1

N3-methylthymine, O2-methylthymine, and O4-methylthymine combined account for less than 1% occurrence in dsDNA.

This table is adapted from [192], [193], and [199]

Bibliography

1. Pannunzio, N.R., G. Watanabe, and M.R. Lieber, *Nonhomologous DNA end-joining for repair of DNA double-strand breaks.* J Biol Chem, 2018. **293**(27): p. 10512-10523.

2. Karanam, K., et al., *Quantitative live cell imaging reveals a gradual shift between DNA repair mechanisms and a maximal use of HR in mid S phase.* Molecular Cell, 2012. **47**(2): p. 320-329.

3. Her, J. and S.F. Bunting, *How cells ensure correct repair of DNA double-strand breaks.* The Journal of Biological Chemistry, 2018. **293**(27): p. 10502-10511.

4. Symington, L.S. and J. Gautier, *Double-strand break end resection and repair pathway choice.* Annual Review of Genetics, 2011. **45**: p. 247-271.

5. Liu, T. and J. Huang, *DNA end resection: facts and mechanisms.* Genomics, proteomics & bioinformatics / Beijing Genomics Institute, 2016. **14**(3): p. 126-130.

6. Chen, H., M. Lisby, and L.S. Symington, *RPA coordinates DNA end resection and prevents formation of DNA hairpins.* Molecular Cell, 2013. **50**(4): p. 589-600.

7. Haber, J.E., *DNA repair: the search for homology.* Bioessays: News and Reviews in Molecular, Cellular and Developmental Biology, 2018. **40**(5): p. e1700229.

8. Zapotoczny, G. and J. Sekelsky, *Human Cell Assays for Synthesis-Dependent Strand Annealing and Crossing over During Double-Strand Break Repair.* G3 (Bethesda), 2017. **7**(4): p. 1191-1199.

9. Andersen, S.L. and J. Sekelsky, *Meiotic versus mitotic recombination: two different routes for double-strand break repair: the different functions of meiotic versus mitotic DSB repair are reflected in different pathway usage and different outcomes.* Bioessays, 2010. **32**(12): p. 1058-66.

10. Verma, P. and R.A. Greenberg, *Noncanonical views of homology-directed DNA repair.* Genes Dev, 2016. **30**(10): p. 1138-54.

11. Bonilla, B., et al., *RAD51 Gene Family Structure and Function.* Annu Rev Genet, 2020. **54**: p. 25-46.

12. Moran, N.A. and A. Mira, *The process of genome shrinkage in the obligate symbiont Buchnera aphidicola.* Genome Biology, 2001. **2**(12): p. RESEARCH0054.

13. Shigenobu, S., et al., *Genome sequence of the endocellular bacterial symbiont of aphids Buchnera sp. APS.* Nature, 2000. **407**(6800): p. 81-86.

14. Wu, D., et al., *Stalking the fourth domain in metagenomic data: searching for, discovering, and interpreting novel, deep branches in marker gene phylogenetic trees.* Plos One, 2011. **6**(3): p. e18011.

15. Lin, Z., et al., *Origins and evolution of the recA/RAD51 gene family: evidence for ancient gene duplication and endosymbiotic gene transfer.* Proceedings of the National Academy of Sciences of the United States of America, 2006. **103**(27): p. 10328-10333.

16. Chintapalli, S.V., et al., *Reevaluation of the evolutionary events within recA/RAD51 phylogeny.* BMC Genomics, 2013. **14**: p. 240.

17. Andriuskevicius, T., O. Kotenko, and S. Makovets, *Putting together and taking apart: assembly and disassembly of the Rad51 nucleoprotein filament in DNA repair and genome stability.* Cell stress, 2018. **2**(5): p. 96-112.

18. Godin, S.K., M.R. Sullivan, and K.A. Bernstein, *Novel insights into RAD51 activity and regulation during homologous recombination and DNA replication.* Biochemistry and Cell Biology (Biochimie et Biologie Cellulaire), 2016. **94**(5): p. 407-418.

19. Sullivan, M.R. and K.A. Bernstein, *RAD-ical New Insights into RAD51 Regulation.* Genes, 2018. **9**(12).

20. Khasanov, F.K., et al., *Identification and characterization of the rlp1+, the novel Rad51 paralog in the fission yeast Schizosaccharomyces pombe.* DNA Repair, 2004. **3**(10): p. 1363-1374.

21. Martín, V., et al., *Sws1 is a conserved regulator of homologous recombination in eukaryotic cells.* The EMBO Journal, 2006. **25**(11): p. 2564-2574.

22. Sasanuma, H., et al., *A new protein complex promoting the assembly of Rad51 filaments.* Nature Communications, 2013. **4**: p. 1676.

23. Zhang, S., et al., *Structural basis for the functional role of the Shu complex in homologous recombination.* Nucleic Acids Research, 2017. **45**(22): p. 13068-13079.

24. Liu, T., et al., *hSWS1·SWSAP1 is an evolutionarily conserved complex required for efficient homologous recombination repair.* The Journal of Biological Chemistry, 2011. **286**(48): p. 41758-41766.

25. Taylor, M.R.G., et al., *Rad51 Paralogs Remodel Pre-synaptic Rad51 Filaments to Stimulate Homologous Recombination.* Cell, 2015. **162**(2): p. 271-286.

26. Lopes, A., et al., *Detection of novel recombinases in bacteriophage genomes unveils Rad52, Rad51 and Gp2.5 remote homologs.* Nucleic Acids Research, 2010. **38**(12): p. 3952-3962.

27. Cooper, D.L. and S.T. Lovett, *Recombinational branch migration by the RadA/Sms paralog of RecA in Escherichia coli.* eLife, 2016. **5**.

28. Haldenby, S., M.F. White, and T. Allers, *RecA family proteins in archaea: RadA and its cousins.* Biochemical Society Transactions, 2009. **37**(Pt 1): p. 102-107.

29. Prakash, R., et al., *Homologous recombination and human health: the roles of BRCA1, BRCA2, and associated proteins.* Cold Spring Harb. Perspect. Biol., 2015. **7**(4): p. a016600.

30. Sung, P., *Function of yeast Rad52 protein as a mediator between replication protein A and the Rad51 recombinase.* The Journal of Biological Chemistry, 1997. **272**(45): p. 28194-28197.

31. Sugiyama, T. and S.C. Kowalczykowski, *Rad52 protein associates with replication protein A (RPA)-single-stranded DNA to accelerate Rad51-mediated displacement of RPA and presynaptic complex formation.* The Journal of Biological Chemistry, 2002. **277**(35): p. 31663-31672.

32. Yang, H., et al., *BRCA2 function in DNA binding and recombination from a BRCA2-DSS1-ssDNA structure.* Science, 2002. **297**(5588): p. 1837-48.

33. Wong, A.K., et al., *RAD51 interacts with the evolutionarily conserved BRC motifs in the human breast cancer susceptibility gene brca2.* J Biol Chem, 1997. **272**(51): p. 31941-4.

34. Carreira, A., et al., *The BRC repeats of BRCA2 modulate the DNA-binding selectivity of RAD51.* Cell, 2009. **136**(6): p. 1032-43.

35. Carreira, A. and S.C. Kowalczykowski, *Two classes of BRC repeats in BRCA2 promote RAD51 nucleoprotein filament function by distinct mechanisms.* Proc Natl Acad Sci U S A, 2011. **108**(26): p. 10448-53.

36. Buisson, R., et al., *Cooperation of breast cancer proteins PALB2 and piccolo BRCA2 in stimulating homologous recombination.* Nat Struct Mol Biol, 2010. **17**(10): p. 1247-54.

37. Dray, E., et al., *Enhancement of RAD51 recombinase activity by the tumor suppressor PALB2.* Nat Struct Mol Biol, 2010. **17**(10): p. 1255-9.

38. Zhao, W., et al., *BRCA1-BARD1 promotes RAD51-mediated homologous DNA pairing.* Nature, 2017. **550**(7676): p. 360-365.

39. Subramanyam, S., et al., *Tyrosine phosphorylation stimulates activity of human RAD51 recombinase through altered nucleoprotein filament dynamics.* Proceedings of the National Academy of Sciences of the United States of America, 2016. **113**(41): p. E6045-E6054.

40. Bayer, F.E., et al., *Drosophila Xrcc2 regulates DNA double-strand repair in somatic cells.* DNA Repair (Amst), 2020. **88**: p. 102807.

41. Gaines, W.A., et al., *Promotion of presynaptic filament assembly by the ensemble of S. cerevisiae Rad51 paralogues with Rad52.* Nat. Commun., 2015. **6**: p. 7834.

42. Liu, J., et al., *Rad51 paralogues Rad55-Rad57 balance the antirecombinase Srs2 in Rad51 filament formation.* Nature, 2011. **479**(7372): p. 245-8.

43. Sung, P., *Yeast Rad55 and Rad57 proteins form a heterodimer that functions with replication protein A to promote DNA strand exchange by Rad51 recombinase.* Genes Dev., 1997. **11**(9): p. 1111-21.

44. Symington, L.S., *Role of RAD52 epistasis group genes in homologous recombination and double-strand break repair.* Microbiol. Mol. Biol. Rev., 2002. **66**(4): p. 630-670.

45. Godin, S., et al., *The Shu complex interacts with Rad51 through the Rad51 paralogues Rad55-Rad57 to mediate error-free recombination.* Nucleic Acids Res., 2013. **41**(8): p. 4525-4534.

46. Bernstein, K.A., et al., *The Shu complex, which contains Rad51 paralogues, promotes DNA repair through inhibition of the Srs2 anti-recombinase.* Mol. Biol. Cell, 2011. **22**(9): p. 1599-607.

47. Taylor, M.R., et al., *Rad51 Paralogs Remodel Pre-synaptic Rad51 Filaments to Stimulate Homologous Recombination.* Cell, 2015. **162**(2): p. 271-286.

48. Garcin, E.B., et al., *Differential Requirements for the RAD51 Paralogs in Genome Repair and Maintenance in Human Cells.* bioRxiv, 2019.

49. Abreu, C.M., et al., *Shu complex SWS1-SWSAP1 promotes early steps in mouse meiotic recombination.* Nat Commun, 2018. **9**(1): p. 3961.

50. Martino, J., et al., *The human Shu complex functions with PDS5B and SPIDR to promote homologous recombination.* Nucleic Acids Res, 2019. **47**(19): p. 10151-10165.

51. Baldock, R.A., et al., *RAD51D splice variants and cancer-associated mutations reveal XRCC2 interaction to be critical for homologous recombination.* DNA Repair, 2019. **76**: p. 99-107.

52. Masson, J.Y., et al., *Identification and purification of two distinct complexes containing the five RAD51 paralogs.* Genes Dev., 2001. **15**(24): p. 3296-3307.

53. Martino, J. and K.A. Bernstein, *The Shu complex is a conserved regulator of homologous recombination.* FEMS Yeast Res., 2016. **16**(6).

54. Matsuzaki, K., et al., *Human RAD51 paralogue SWSAP1 fosters RAD51 filament by regulating the anti-recombinase FIGNL1 AAA+ ATPase.* Nat Commun, 2019. **10**(1): p. 1407.

55. Mishra, A., et al., *RAD51C/XRCC3 Facilitates Mitochondrial DNA Replication and Maintains Integrity of the Mitochondrial Genome.* Mol Cell Biol, 2018. **38**(3).

56. Sage, J.M., O.S. Gildemeister, and K.L. Knight, *Discovery of a novel function for human Rad51: maintenance of the mitochondrial genome.* J Biol Chem, 2010. **285**(25): p. 18984-90.

57. Sasaki, M.S., et al., *Recombination repair pathway in the maintenance of chromosomal integrity against DNA interstrand crosslinks.* Cytogenet Genome Res, 2004. **104**(1-4): p. 28-34.

58. Shor, E., J. Weinstein, and R. Rothstein, *A genetic screen for top3 suppressors in Saccharomyces cerevisiae identifies SHU1, SHU2, PSY3 and CSM2: four genes involved in error-free DNA repair.* Genetics, 2005. **169**(3): p. 1275-89.

59. Rabitsch, K.P., et al., *A screen for genes required for meiosis and spore formation based on whole-genome expression.* Curr Biol, 2001. **11**(13): p. 1001-9.

60. Wu, H.I., et al., *Genome-wide identification of genes conferring resistance to the anticancer agents cisplatin, oxaliplatin, and mitomycin C.* Cancer Res, 2004. **64**(11): p. 3940-8.

61. Huang, M.E., et al., *A genomewide screen in Saccharomyces cerevisiae for genes that suppress the accumulation of mutations.* Proc. Natl. Acad. Sci. U S A, 2003. **100**(20): p. 11529-34.

62. Begley, T.J., et al., *Damage recovery pathways in Saccharomyces cerevisae revealed by genomic phenotyping and interactome mapping.* Mol. Cancer Res., 2002. **1**(2): p. 103-112.

63. Hanway, D., et al., *Previously uncharacterized genes in the UV- and MMS-induced DNA damage response in yeast.* Proc Natl Acad Sci U S A, 2002. **99**(16): p. 10605-10.

64. Ito, T., et al., *A comprehensive two-hybrid analysis to explore the yeast protein interactome.* Proceedings of the National Academy of Sciences of the United States of America, 2001. **98**(8): p. 4569-74.

65. Makarova, K.S., L. Aravind, and E.V. Koonin, *SWIM, a novel Zn-chelating domain present in bacteria, archaea and eukaryotes.* Trends Biochem. Sci., 2002. **27**: p. 384-386.

66. Godin, S.K., et al., *Evolutionary and Functional Analysis of the Invariant SWIM Domain in the Conserved Shu2/SWS1 Protein Family from Saccharomyces cerevisiae to Homo sapiens.* Genetics, 2015. **199**(4): p. 1023-33.

67. McClendon, T.B., et al., *Promotion of Homologous Recombination by SWS-1 in Complex with RAD-51 Paralogs in Caenorhabditis elegans.* Genetics, 2016. **203**(1): p. 133-145.

68. Tao, Y., et al., *Structural analysis of Shu proteins reveals a DNA binding role essential for resisting damage.* The Journal of Biological Chemistry, 2012. **287**(24): p. 20231-20239.

69. She, Z., et al., *Structural and SAXS analysis of the budding yeast SHU-complex proteins.* FEBS Letters, 2012. **586**(16): p. 2306-2312.

70. Matsuo, Y., et al., *Roles of the human Rad51 L1 and L2 loops in DNA binding.* The FEBS Journal, 2006. **273**(14): p. 3148-3159.

71. Mankouri, H.W., H.P. Ngo, and I.D. Hickson, *Shu proteins promote the formation of homologous recombination intermediates that are processed by Sgs1-Rmi1-Top3.* Mol. Biol. Cell, 2007. **18**: p. 4062-4073.

72. Branzei, D., et al., *Ubc9- and mms21-mediated sumoylation counteracts recombinogenic events at damaged replication forks.* Cell, 2006. **127**(3): p. 509-22.

73. Giannattasio, M., et al., *Visualization of recombination-mediated damage bypass by template switching.* Nat Struct Mol Biol, 2014. **21**(10): p. 884-92.

74. Fortin, G.S. and L.S. Symington, *Mutations in yeast Rad51 that partially bypass the requirement for Rad55 and Rad57 in DNA repair by increasing the stability of Rad51-DNA complexes.* EMBO J., 2002. **21**(12): p. 3160-3170.

75. Sugawara, N., X. Wang, and J.E. Haber, *In vivo roles of Rad52, Rad54, and Rad55 proteins in Rad51-mediated recombination.* Mol. Cell, 2003. **12**(1): p. 209-219.

76. Krejci, L., et al., *DNA helicase Srs2 disrupts the Rad51 presynaptic filament.* Nature, 2003. **423**: p. 305-309.

77. Veaute, X., et al., *The Srs2 helicase prevents recombination by disrupting Rad51 nucleoprotein filaments.* Nature, 2003. **423**(6937): p. 309-12.

78. Martin, V., et al., *Sws1 is a conserved regulator of homologous recombination in eukaryotic cells.* EMBO J., 2006. **25**: p. 2564-2574.

79. Uetz, P., et al., *A comprehensive analysis of protein-protein interactions in Saccharomyces cerevisiae.* Nature, 2000. **403**(6770): p. 623-7.

80. Ito, T., et al., *A comprehensive two-hybrid analysis to explore the yeast protein interactome.* Proc. Natl. Acad. Sci. U S A, 2001. **98**: p. 4569-4574.

81. Godin, S.K., et al., *The Shu complex promotes error-free tolerance of alkylation-induced base-excision repair products.* Nucleic Acids Res., 2016. **30**(44): p. 8199-8215.

82. Hoege, C., et al., *RAD6-dependent DNA repair is linked to modification of PCNA by ubiquitin and SUMO.* Nature, 2002. **419**(6903): p. 135-41.

83. Ball, L.G., et al., *The yeast Shu complex couples error-free post-replication repair to homologous recombination.* Mol. Microbiol., 2009. **73**(1): p. 89-102.

84. Xu, X., et al., *The yeast Shu complex utilizes homologous recombination machinery for error-free lesion bypass via physical interaction with a Rad51 paralogue.* PloS One, 2013. **8**(12): p. e81371.

85. Zeman, M.K. and K.A. Cimprich, *Causes and consequences of replication stress.* Nature cell biology, 2014. **16**(1): p. 2-9.

86. Neelsen, K.J. and M. Lopes, *Replication fork reversal in eukaryotes: from dead end to dynamic response.* Nat Rev Mol Cell Biol, 2015. **16**(4): p. 207-20.

87. Higgins, N.P., K. Kato, and B. Strauss, *A model for replication repair in mammalian cells.* J Mol Biol, 1976. **101**(3): p. 417-25.

88. Bhat, K.P. and D. Cortez, *RPA and RAD51: fork reversal, fork protection, and genome stability.* Nat Struct Mol Biol, 2018. **25**(6): p. 446-453.

89. Zellweger, R., et al., *Rad51-mediated replication fork reversal is a global response to genotoxic treatments in human cells.* J. Cell Biol., 2015. **208**(5): p. 563-579.

90. Bugreev, D.V., M.J. Rossi, and A.V. Mazin, *Cooperation of RAD51 and RAD54 in regression of a model replication fork.* Nucleic Acids Res, 2011. **39**(6): p. 2153-64.

91. Branzei, D. and B. Szakal, *Building up and breaking down: mechanisms controlling recombination during replication.* Crit Rev Biochem Mol Biol, 2017. **52**(4): p. 381-394.

92. Kolinjivadi, A.M., et al., *Smarcal1-Mediated Fork Reversal Triggers Mre11-Dependent Degradation of Nascent DNA in the Absence of Brca2 and Stable Rad51 Nucleofilaments.* Mol Cell, 2017. **67**(5): p. 867-881 e7.

93. Mason, J.M., et al., *Non-enzymatic roles of human RAD51 at stalled replication forks.* Nat Commun, 2019. **10**(1): p. 4410.

94. Mijic, S., et al., *Replication fork reversal triggers fork degradation in BRCA2-defective cells.* Nat Commun, 2017. **8**(1): p. 859.

95. Higgs, M.R., et al., *BOD1L Is Required to Suppress Deleterious Resection of Stressed Replication Forks.* Mol Cell, 2015. **59**(3): p. 462-77.

96. Lemacon, D., et al., *MRE11 and EXO1 nucleases degrade reversed forks and elicit MUS81-dependent fork rescue in BRCA2-deficient cells.* Nat Commun, 2017. **8**(1): p. 860.

97. Taglialatela, A., et al., *Restoration of Replication Fork Stability in BRCA1- and BRCA2-Deficient Cells by Inactivation of SNF2-Family Fork Remodelers.* Mol Cell, 2017. **68**(2): p. 414-430 e8.

98. Schlacher, K., et al., *Double-strand break repair-independent role for BRCA2 in blocking stalled replication fork degradation by MRE11.* Cell, 2011. **145**(4): p. 529-542.

99. Schlacher, K., H. Wu, and M. Jasin, *A distinct replication fork protection pathway connects Fanconi anemia tumor suppressors to RAD51-BRCA1/2.* Cancer Cell, 2012. **22**(1): p. 106-116.

100. Wang, A.T., et al., *A Dominant Mutation in Human RAD51 Reveals Its Function in DNA Interstrand Crosslink Repair Independent of Homologous Recombination.* Mol. Cell, 2015. **59**(3): p. 478-490.

101. Zadorozhny, K., et al., *Fanconi-Anemia-Associated Mutations Destabilize RAD51 Filaments and Impair Replication Fork Protection.* Cell Rep, 2017. **21**(2): p. 333-340.

102. Berti, M., et al., *Human RECQ1 promotes restart of replication forks reversed by DNA topoisomerase I inhibition.* Nat Struct Mol Biol, 2013. **20**(3): p. 347-54.

103. Betous, R., et al., *Substrate-selective repair and restart of replication forks by DNA translocases.* Cell Rep, 2013. **3**(6): p. 1958-69.

104. Thangavel, S., et al., *DNA2 drives processing and restart of reversed replication forks in human cells.* J Cell Biol, 2015. **208**(5): p. 545-62.

105. Ait Saada, A., S.A.E. Lambert, and A.M. Carr, *Preserving replication fork integrity and competence via the homologous recombination pathway.* DNA Repair (Amst), 2018. **71**: p. 135-147.

106. Petermann, E., et al., *Hydroxyurea-stalled replication forks become progressively inactivated and require two different RAD51-mediated pathways for restart and repair.* Mol. Cell, 2010. **37**(4): p. 492-502.

107. Teixeira-Silva, A., et al., *The end-joining factor Ku acts in the end-resection of double strand break-free arrested replication forks.* Nat Commun, 2017. **8**(1): p. 1982.

108. Cortez, D., *Replication-Coupled DNA Repair.* Mol Cell, 2019. **74**(5): p. 866-876.

109. Kramara, J., B. Osia, and A. Malkova, *Break-Induced Replication: The Where, The Why, and The How.* Trends in Genetics, 2018. **34**(7): p. 518-531.

110. Mayle, R., et al., *DNA REPAIR. Mus81 and converging forks limit the mutagenicity of replication fork breakage.* Science, 2015. **349**(6249): p. 742-7.

111. Hashimoto, Y., F. Puddu, and V. Costanzo, *RAD51- and MRE11-dependent reassembly of uncoupled CMG helicase complex at collapsed replication forks.* Nat Struct Mol Biol, 2011. **19**(1): p. 17-24.

112. Costantino, L., et al., *Break-induced replication repair of damaged forks induces genomic duplications in human cells.* Science, 2014. **343**(6166): p. 88-91.

113. Prado, F., *Homologous recombination: to fork and beyond.* Genes, 2018. **9**(12).

114. Taylor, M.R.G. and J.T.P. Yeeles, *The Initial Response of a Eukaryotic Replisome to DNA Damage.* Mol Cell, 2018. **70**(6): p. 1067-1080 e12.

115. Bianchi, J., et al., *PrimPol bypasses UV photoproducts during eukaryotic chromosomal DNA replication.* Mol Cell, 2013. **52**(4): p. 566-73.

116. Garcia-Gomez, S., et al., *PrimPol, an archaic primase/polymerase operating in human cells.* Mol Cell, 2013. **52**(4): p. 541-53.

117. Fumasoni, M., et al., *Error-free DNA damage tolerance and sister chromatid proximity during DNA replication rely on the Polalpha/Primase/Ctf4 Complex.* Mol Cell, 2015. **57**(5): p. 812-823.

118. Unk, I., et al., *Role of yeast Rad5 and its human orthologs, HLTF and SHPRH in DNA damage tolerance.* DNA Repair (Amst), 2010. **9**(3): p. 257-67.

119. Herzberg, K., et al., *Phosphorylation of Rad55 on serines 2, 8, and 14 is required for efficient homologous recombination in the recovery of stalled replication forks.* Mol. Cell. Biol., 2006. **26**(22): p. 8396-8409.

120. Rosenbaum, J.C., et al., *The Rad51 paralogs facilitate a novel DNA strand specific damage tolerance pathway.* Nat Commun, 2019. **10**(1): p. 3515.

121. Somyajit, K., et al., *Mammalian RAD51 paralogs protect nascent DNA at stalled forks and mediate replication restart.* Nucleic Acids Res., 2015. **43**(20): p. 9835-9855.

122. Somyajit, K., et al., *ATM- and ATR-mediated phosphorylation of XRCC3 regulates DNA double-strand break-induced checkpoint activation and repair.* Molecular and Cellular Biology, 2013. **33**(9): p. 1830-1844.

123. Saxena, S., K. Somyajit, and G. Nagaraju, *XRCC2 Regulates Replication Fork Progression during dNTP Alterations.* Cell reports, 2018. **25**(12): p. 3273-3282.e6.

124. Keeney, S., *Spo11 and the Formation of DNA Double-Strand Breaks in Meiosis.* Genome Dyn Stab, 2008. **2**: p. 81-123.

125. Lao, J.P. and N. Hunter, *Trying to avoid your sister.* PLoS Biol, 2010. **8**(10): p. e1000519.

126. Hunter, N., *Meiotic recombination: the essence of heredity.* Cold Spring Harbor Perspectives in Biology, 2015. **7**(12).

127. Cloud, V., et al., *Rad51 is an accessory factor for Dmc1-mediated joint molecule formation during meiosis.* Science, 2012. **337**(6099): p. 1222-5.

128. Brown, M.S. and D.K. Bishop, *DNA strand exchange and RecA homologs in meiosis.* Cold Spring Harb Perspect Biol, 2014. **7**(1): p. a016659.

129. Busygina, V., et al., *Hed1 regulates Rad51-mediated recombination via a novel mechanism.* Genes Dev, 2008. **22**(6): p. 786-95.

130. Shinohara, A., et al., *Saccharomyces cerevisiae recA homologues RAD51 and DMC1 have both distinct and overlapping roles in meiotic recombination.* Genes Cells, 1997. **2**(10): p. 615-29.

131. Crickard, J.B., et al., *Spontaneous self-segregation of Rad51 and Dmc1 DNA recombinases within mixed recombinase filaments.* J Biol Chem, 2018. **293**(11): p. 4191-4200.

132. Brown, M.S., et al., *Small Rad51 and Dmc1 Complexes Often Co-occupy Both Ends of a Meiotic DNA Double Strand Break.* PLoS Genet, 2015. **11**(12): p. e1005653.

133. Borgogno, M.V., et al., *Tolerance of DNA Mismatches in Dmc1 Recombinase-mediated DNA Strand Exchange.* J Biol Chem, 2016. **291**(10): p. 4928-38.

134. Steinfeld, J.B., et al., *Defining the influence of Rad51 and Dmc1 lineage-specific amino acids on genetic recombination.* Genes & Development, 2019. **33**(17-18): p. 1191-1207.

135. Crickard, J.B., et al., *Meiosis-specific recombinase Dmc1 is a potent inhibitor of the Srs2 antirecombinase.* Proc Natl Acad Sci U S A, 2018. **115**(43): p. E10041-E10048.

136. Game, J.C. and R.K. Mortimer, *A genetic study of X-ray sensitive mutants in yeast.* Mutation Research/Fundamental and Molecular Mechanisms of Mutagenesis, 1974. **24**(3): p. 281-292.

137. Hong, S. and K.P. Kim, *Shu1 promotes homolog bias of meiotic recombination in Saccharomyces cerevisiae.* Mol. Cells, 2013. **36**(5): p. 446-454.

138. Schwacha, A. and N. Kleckner, *Interhomolog bias during meiotic recombination: meiotic functions promote a highly differentiated interhomolog-only pathway.* Cell, 1997. **90**(6): p. 1123-35.

139. Grishchuk, A.L. and J. Kohli, *Five RecA-like proteins of Schizosaccharomyces pombe are involved in meiotic recombination.* Genetics, 2003. **165**(3): p. 1031-43.

140. Charlot, F., et al., *RAD51B plays an essential role during somatic and meiotic recombination in Physcomitrella.* Nucleic Acids Res, 2014. **42**(19): p. 11965-78.

141. Swenberg, J.A., et al., *Endogenous versus exogenous DNA adducts: their role in carcinogenesis, epidemiology, and risk assessment.* Toxicol. Sci., 2011. **120 Suppl 1**: p. S130-45.

142. Lindahl, T. and B. Nyberg, *Rate of depurination of native deoxyribonucleic acid.* Biochemistry, 1972. **11**(19): p. 3610-8.

143. Boiteux, S. and M. Guillet, *Abasic sites in DNA: repair and biological consequences in Saccharomyces cerevisiae.* DNA Repair, 2004. **3**(1): p. 1-12.

144. Sobol, R.W., et al., *Base excision repair intermediates induce p53-independent cytotoxic and genotoxic responses.* J. Biol. Chem., 2003. **278**(41): p. 39951-39959.

145. Haracska, L., et al., *Roles of yeast DNA polymerases delta and zeta and of Rev1 in the bypass of abasic sites.* Genes Dev., 2001. **15**(8): p. 945-954.

146. Swanson, R.L., et al., *Overlapping specificities of base excision repair, nucleotide excision repair, recombination, and translesion synthesis pathways for DNA base damage in Saccharomyces cerevisiae.* Mol Cell Biol, 1999. **19**(4): p. 2929-35.

147. Lin, Z., et al., *Origins and evolution of the recA/RAD51 gene family: evidence for ancient gene duplication and endosymbiotic gene transfer.* Proc. Natl. Acad. Sci. U S A, 2006. **103**(27): p. 10328-10333.

148. Godin, S.K., M.R. Sullivan, and K.A. Bernstein, *Novel insights into RAD51 activity and regulation during homologous recombination and DNA replication.* Biochem. Cell Biol., 2016. **94**(5): p. 407-418.

149. Suwaki, N., K. Klare, and M. Tarsounas, *RAD51 paralogs: roles in DNA damage signalling, recombinational repair and tumorigenesis.* Sem. Cell Dev. Biol., 2011. **22**(8): p. 898-905.

150. Sasanuma, H., et al., *A new protein complex promoting the assembly of Rad51 filaments.* Nat. Commun., 2013. **4**: p. 1676.

151. Tao, Y., et al., *Structural analysis of Shu proteins reveals a DNA binding role essential for resisting damage.* J. Biol. Chem., 2012. **287**(24): p. 20231-20239.

152. Zhang, S., et al., *Structural basis for the functional role of the Shu complex in homologous recombination.* Nucleic Acids Res., 2017. **45**(22): p. 13068-13079.

153. Lopez-Blanco, J.R., et al., *RCD+: Fast loop modeling server.* Nucleic Acids Res., 2016. **44**(W1): p. W395-400.

154. Alexandrov, L.B., et al., *Signatures of mutational processes in human cancer.* Nature, 2013. **500**(7463): p. 415-421.

155. Burns, M.B., N.A. Temiz, and R.S. Harris, *Evidence for APOBEC3B mutagenesis in multiple human cancers.* Nat Genet., 2013. **45**(9): p. 977-983.

156. Roberts, S.A., et al., *An APOBEC cytidine deaminase mutagenesis pattern is widespread in human cancers.* Nat. Genet., 2013. **45**(9): p. 970-976.

157. Haradhvala, N.J., et al., *Mutational Strand Asymmetries in Cancer Genomes Reveal Mechanisms of DNA Damage and Repair.* Cell, 2016. **164**(3): p. 538-549.

158. Morganella, S., et al., *The topography of mutational processes in breast cancer genomes.* Nat. Commun., 2016. **7**: p. 11383.

159. Seplyarskiy, V.B., et al., *APOBEC-induced mutations in human cancers are strongly enriched on the lagging DNA strand during replication.* Genome Res., 2016. **26**(2): p. 174-182.

160. Hoopes, J.I., et al., *APOBEC3A and APOBEC3B Preferentially Deaminate the Lagging Strand Template during DNA Replication.* Cell Rep., 2016. **14**(6): p. 1273-1282.

161. Bhagwat, A.S., et al., *Strand-biased cytosine deamination at the replication fork causes cytosine to thymine mutations in Escherichia coli.* Proc. Natl. Acad. Sci. U S A, 2016. **113**(8): p. 2176-2181.

162. Hoopes, J.I., et al., *Avoidance of APOBEC3B-induced mutation by error-free lesion bypass.* Nucleic Acids Res., 2017. **45**(9): p. 5243-5254.

163. Fan, J., Y. Matsumoto, and D.M. Wilson, 3rd, *Nucleotide sequence and DNA secondary structure, as well as replication protein A, modulate the single-stranded abasic endonuclease activity of APE1.* J. Biol. Chem., 2006. **281**(7): p. 3889-98.

164. Mohni, K.N., et al., *HMCES Maintains Genome Integrity by Shielding Abasic Sites in Single-Strand DNA.* Cell, 2019. **176**(1-2): p. 144-153 e13.

165. Kalnik, M.W., et al., *NMR studies of abasic sites in DNA duplexes: deoxyadenosine stacks into the helix opposite the cyclic analogue of 2-deoxyribose.* Biochemistry, 1988. **27**(3): p. 924-931.

166. Beger, R.D. and P.H. Bolton, *Structures of apurinic and apyrimidinic sites in duplex DNAs.* J. Biol. Chem., 1998. **273**(25): p. 15565-15573.

167. Gudmundsdottir, K. and A. Ashworth, *The roles of BRCA1 and BRCA2 and associated proteins in the maintenance of genomic stability.* Oncogene, 2006. **25**(43): p. 5864-5874.

168. Bryant, H.E., et al., *Specific killing of BRCA2-deficient tumours with inhibitors of poly(ADP-ribose) polymerase.* Nature, 2005. **434**(7035): p. 913-7.

169. Farmer, H., et al., *Targeting the DNA repair defect in BRCA mutant cells as a therapeutic strategy.* Nature, 2005. **434**(7035): p. 917-921.

170. Fong, P.C., et al., *Inhibition of poly(ADP-ribose) polymerase in tumors from BRCA mutation carriers.* N. Engl. J. Med., 2009. **361**(2): p. 123-134.

171. Kondrashova, O., et al., *Secondary Somatic Mutations Restoring RAD51C and RAD51D Associated with Acquired Resistance to the PARP Inhibitor Rucaparib in High-Grade Ovarian Carcinoma.* Cancer Discov., 2017. **7**(9): p. 984-998.

172. Hanzlikova, H., et al., *The Importance of Poly(ADP-Ribose) Polymerase as a Sensor of Unligated Okazaki Fragments during DNA Replication.* Mol. Cell, 2018. **71**(2): p. 319-331 e3.

173. James, P., J. Halladay, and E.A. Craig, *Genomic libraries and a host strain designed for highly efficient two-hybrid selection in yeast.* Genetics, 1996. **144**(4): p. 1425-36.

174. Thomas, B.J. and R. Rothstein, *Elevated recombination rates in transcriptionally active DNA.* Cell, 1989. **56**(4): p. 619-30.

175. Zhao, X., E.G. Muller, and R. Rothstein, *A suppressor of two essential checkpoint genes identifies a novel protein that negatively affects dNTP pools.* Mol. Cell, 1998. **2**(3): p. 329-40.

176. Goldstein, A.L. and J.H. McCusker, *Three new dominant drug resistance cassettes for gene disruption in Saccharomyces cerevisiae.* Yeast, 1999. **15**(14): p. 1541-1553.

177. Gueldener, U., et al., *A second set of loxP marker cassettes for Cre-mediated multiple gene knockouts in budding yeast.* Nucleic Acids Res., 2002. **30**(6): p. e23.

178. Hall, B.M., et al., *Fluctuation analysis CalculatOR: a web tool for the determination of mutation rate using Luria-Delbruck fluctuation analysis.* Bioinformatics, 2009. **25**(12): p. 1564-5.

179. Knop, M., et al., *Epitope tagging of yeast genes using a PCR-based strategy: more tags and improved practical routines.* Yeast, 1999. **15**(10B): p. 963-72.

180. Liang, C. and B. Stillman, *Persistent initiation of DNA replication and chromatin-bound MCM proteins during the cell cycle in cdc6 mutants.* Genes Dev., 1997. **11**(24): p. 3375-3386.

181. Wang, A.Y., et al., *Asf1-like structure of the conserved Yaf9 YEATS domain and role in H2A.Z deposition and acetylation.* Proc. Natl. Acad. Sci. U S A, 2009. **106**(51): p. 21573-21578.

182. Schneider, C.A., W.S. Rasband, and K.W. Eliceiri, *NIH Image to ImageJ: 25 years of image analysis.* Nat. Methods, 2012. **9**(7): p. 671-675.

183. Fu, D., J.A. Calvo, and L.D. Samson, *Balancing repair and tolerance of DNA damage caused by alkylating agents.* Nat. Rev. Cancer, 2012. **12**(2): p. 104-120.

184. Shrivastav, N., D. Li, and J.M. Essigmann, *Chemical biology of mutagenesis and DNA repair: cellular responses to DNA alkylation.* Carcinogenesis, 2010. **31**(1): p. 59-70.

185. Arbel, M., B. Liefshitz, and M. Kupiec, *DNA damage bypass pathways and their effect on mutagenesis in yeast.* FEMS Microbiol Rev, 2020.

186. Boiteux, S. and S. Jinks-Robertson, *DNA repair mechanisms and the bypass of DNA damage in Saccharomyces cerevisiae.* Genetics, 2013. **193**(4): p. 1025-1064.

187. Ulrich, H.D., *Conservation of DNA damage tolerance pathways from yeast to humans.* Biochem Soc Trans, 2007. **35**(Pt 5): p. 1334-7.

188. Swanson, R.L., et al., *Overlapping specificities of base excision repair, nucleotide excision repair, recombination, and translesion synthesis pathways for DNA base damage in Saccharomyces cerevisiae.* Molecular and Cellular Biology, 1999. **19**(4): p. 2929-2935.

189. Broomfield, S., B.L. Chow, and W. Xiao, *MMS2, encoding a ubiquitin-conjugating-enzyme-like protein, is a member of the yeast error-free postreplication repair pathway.* Proc Natl Acad Sci U S A, 1998. **95**(10): p. 5678-83.

190. Sedgwick, B., et al., *Repair of alkylated DNA: recent advances.* DNA Repair (Amst), 2007. **6**(4): p. 429-42.

191. Sikora, A., et al., *Lethal and mutagenic properties of MMS-generated DNA lesions in Escherichia coli cells deficient in BER and AlkB-directed DNA repair.* Mutagenesis, 2010. **25**(2): p. 139-47.

192. Beranek, D.T., *Distribution of methyl and ethyl adducts following alkylation with monofunctional alkylating agents.* Mutat. Res., 1990. **231**(1): p. 11-30.

193. Wyatt, M.D. and D.L. Pittman, *Methylating agents and DNA repair responses: Methylated bases and sources of strand breaks.* Chem Res Toxicol, 2006. **19**(12): p. 1580-94.

194. Chan, K., M.A. Resnick, and D.A. Gordenin, *The choice of nucleotide inserted opposite abasic sites formed within chromosomal DNA reveals the polymerase activities participating in translesion DNA synthesis.* DNA Repair (Amst), 2013. **12**(11): p. 878-89.

195. Zhao, B., et al., *Role of DNA polymerase eta in the bypass of abasic sites in yeast cells.* Nucleic Acids Res, 2004. **32**(13): p. 3984-94.

196. Bjoras, M., et al., *Purification and properties of the alkylation repair DNA glycosylase encoded the MAG gene from Saccharomyces cerevisiae.* Biochemistry, 1995. **34**(14): p. 4577-4582.

197. Wyatt, M.D., et al., *3-methyladenine DNA glycosylases: structure, function, and biological importance.* Bioessays, 1999. **21**(8): p. 668-76.

198. Bodell, W.J. and B. Singer, *Influence of hydrogen bonding in DNA and polynucleotides on reaction of nitrogens and oxygens toward ethylnitrosourea.* Biochemistry, 1979. **18**(13): p. 2860-3.

199. Yang, Y., D.A. Gordenin, and M.A. Resnick, *A single-strand specific lesion drives MMS-induced hyper-mutability at a double-strand break in yeast.* DNA repair, 2010. **9**(8): p. 914-21.

200. Saini, N., et al., *Mutation signatures specific to DNA alkylating agents in yeast and cancers.* Nucleic Acids Res, 2020. **48**(7): p. 3692-3707.

201. Saini, N. and D.A. Gordenin, *Hypermutation in single-stranded DNA.* DNA Repair (Amst), 2020. **91-92**: p. 102868.

202. Roberts, S.A., et al., *Clustered mutations in yeast and in human cancers can arise from damaged long single-strand DNA regions.* Mol Cell, 2012. **46**(4): p. 424-35.

203. Fedeles, B.I., et al., *The AlkB Family of Fe(II)/alpha-Ketoglutarate-dependent Dioxygenases: Repairing Nucleic Acid Alkylation Damage and Beyond.* J Biol Chem, 2015. **290**(34): p. 20734-42.

204. Yi, C. and C. He, *DNA repair by reversal of DNA damage.* Cold Spring Harb Perspect Biol, 2013. **5**(1): p. a012575.

205. Monsen, V.T., et al., *Divergent ss-hairpins determine double-strand versus single-strand substrate recognition of human AlkB-homologues 2 and 3.* Nucleic Acids Res, 2010. **38**(19): p. 6447-55.

206. Nieminuszczy, J., et al., *Mutagenic potency of MMS-induced 1meA/3meC lesions in E. coli.* Environ Mol Mutagen, 2009. **50**(9): p. 791-9.

207. Pataillot-Meakin, T., N. Pillay, and S. Beck, *3-methylcytosine in cancer: an underappreciated methyl lesion?* Epigenomics, 2016. **8**(4): p. 451-4.

208. Rosic, S., et al., *Evolutionary analysis indicates that DNA alkylation damage is a byproduct of cytosine DNA methyltransferase activity.* Nat Genet, 2018. **50**(3): p. 452-459.

209. Dango, S., et al., *DNA unwinding by ASCC3 helicase is coupled to ALKBH3-dependent DNA alkylation repair and cancer cell proliferation.* Mol Cell, 2011. **44**(3): p. 373-84.

210. Chatterjee, N. and G.C. Walker, *Mechanisms of DNA damage, repair, and mutagenesis.* Environ Mol Mutagen, 2017. **58**(5): p. 235-263.

211. Admiraal, S.J., et al., *Expansion of base excision repair compensates for a lack of DNA repair by oxidative dealkylation in budding yeast.* J Biol Chem, 2019. **294**(37): p. 13629-13637.

212. Godin, S.K., et al., *Tryptophan biosynthesis is important for resistance to replicative stress in Saccharomyces cerevisiae.* Yeast, 2016. **33**(5): p. 183-9.

213. Xu, X., et al., *Error-free DNA-damage tolerance in Saccharomyces cerevisiae.* Mutat Res Rev Mutat Res, 2015. **764**: p. 43-50.

214. Shivange, G., et al., *A role for Saccharomyces cerevisiae Tpa1 protein in direct alkylation repair.* J Biol Chem, 2014. **289**(52): p. 35939-52.

215. Gao, W., et al., *Frequent down-regulation of hABH2 in gastric cancer and its involvement in growth of cancer cells.* J Gastroenterol Hepatol, 2011. **26**(3): p. 577-84.

216. Stefansson, O.A., et al., *CpG promoter methylation of the ALKBH3 alkylation repair gene in breast cancer.* BMC Cancer, 2017. **17**(1): p. 469.

217. Knijnenburg, T.A., et al., *Genomic and Molecular Landscape of DNA Damage Repair Deficiency across The Cancer Genome Atlas.* Cell Rep, 2018. **23**(1): p. 239-254 e6.

218. Wang, P., et al., *Oncometabolite D-2-Hydroxyglutarate Inhibits ALKBH DNA Repair Enzymes and Sensitizes IDH Mutant Cells to Alkylating Agents.* Cell Rep, 2015. **13**(11): p. 2353-2361.

219. Koike, K., et al., *anti-tumor effect of AlkB homolog 3 knockdown in hormone- independent prostate cancer cells.* Curr Cancer Drug Targets, 2012. **12**(7): p. 847-56.

220. Tasaki, M., et al., *ALKBH3, a human AlkB homologue, contributes to cell survival in human non-small-cell lung cancer.* Br J Cancer, 2011. **104**(4): p. 700-6.

221. Choi, S.Y., J.H. Jang, and K.R. Kim, *Analysis of differentially expressed genes in human rectal carcinoma using suppression subtractive hybridization.* Clin Exp Med, 2011. **11**(4): p. 219-26.

222. Wu, S.S., et al., *Down-regulation of ALKBH2 increases cisplatin sensitivity in H1299 lung cancer cells.* Acta Pharmacol Sin, 2011. **32**(3): p. 393-8.

223. Johannessen, T.C., et al., *The DNA repair protein ALKBH2 mediates temozolomide resistance in human glioblastoma cells.* Neuro Oncol, 2013. **15**(3): p. 269-78.

224. Cetica, V., et al., *Pediatric brain tumors: mutations of two dioxygenases (hABH2 and hABH3) that directly repair alkylation damage.* J Neurooncol, 2009. **94**(2): p. 195-201.

225. Longtine, M.S., et al., *Additional modules for versatile and economical PCR-based gene deletion and modification in Saccharomyces cerevisiae.* Yeast, 1998. **14**(10): p. 953-61.

226. Sherman, F., G.R. Fink, and J.B. Hicks, *Methods in Yeast Genetics*. 1986, Cold Spring Harbor, NY: Cold Spring Harbor Laboratory Press.

227. Zheng, L., U. Baumann, and J.L. Reymond, *An efficient one-step site-directed and site-saturation mutagenesis protocol.* Nucleic Acids Res, 2004. **32**(14): p. e115.

228. Geissmann, Q., *OpenCFU, a new free and open-source software to count cell colonies and other circular objects.* PLoS One, 2013. **8**(2): p. e54072.

229. Rosenbaum, J.C., et al., *The Rad51 paralogs facilitate a novel DNA strand specific damage tolerance pathway.* Nat. Comm., 2019. **Under Revision**.

230. Dianov, G.L., et al., *Repair of abasic sites in DNA.* Mutat Res, 2003. **531**(1-2): p. 157-63.

231. Loeb, L.A. and B.D. Preston, *Mutagenesis by apurinic/apyrimidinic sites.* Annu Rev Genet, 1986. **20**: p. 201-30.

232. Kidane, D., D.L. Murphy, and J.B. Sweasy, *Accumulation of abasic sites induces genomic instability in normal human gastric epithelial cells during Helicobacter pylori infection.* Oncogenesis, 2014. **3**: p. e128.

233. McNeill, D.R., et al., *Functions of the major abasic endonuclease (APE1) in cell viability and genotoxin resistance.* Mutagenesis, 2020. **35**(1): p. 27-38.

234. Wilson, D.M., 3rd and A. Simeonov, *Small molecule inhibitors of DNA repair nuclease activities of APE1.* Cell Mol Life Sci, 2010. **67**(21): p. 3621-31.

235. Smith, H.C., et al., *Functions and regulation of the APOBEC family of proteins.* Semin Cell Dev Biol, 2012. **23**(3): p. 258-68.

236. Refsland, E.W. and R.S. Harris, *The APOBEC3 family of retroelement restriction factors.* Curr Top Microbiol Immunol, 2013. **371**: p. 1-27.

237. Kuong, K.J. and L.A. Loeb, *APOBEC3B mutagenesis in cancer.* Nat Genet, 2013. **45**(9): p. 964-5.

238. Krokan, H.E., et al., *Error-free versus mutagenic processing of genomic uracil--relevance to cancer.* DNA Repair (Amst), 2014. **19**: p. 38-47.

239. Burns, M.B., B. Leonard, and R.S. Harris, *APOBEC3B: pathological consequences of an innate immune DNA mutator.* Biomed J, 2015. **38**(2): p. 102-10.

240. Wang, Z. and D.W. Mosbaugh, *Uracil-DNA glycosylase inhibitor gene of bacteriophage PBS2 encodes a binding protein specific for uracil-DNA glycosylase.* J Biol Chem, 1989. **264**(2): p. 1163-71.

241. Xu, W., et al., *Oncometabolite 2-hydroxyglutarate is a competitive inhibitor of alpha-ketoglutarate-dependent dioxygenases.* Cancer Cell, 2011. **19**(1): p. 17-30.

242. Li, Q., et al., *Rhein Inhibits AlkB Repair Enzymes and Sensitizes Cells to Methylated DNA Damage.* J Biol Chem, 2016. **291**(21): p. 11083-93.

243. Mohan, M., et al., *Human RAD51 paralogue RAD51C fosters repair of alkylated DNA by interacting with the ALKBH3 demethylase.* Nucleic Acids Res, 2019. **47**(22): p. 11729-11745.

244. Furrer, A. and B. van Loon, *Handling the 3-methylcytosine lesion by six human DNA polymerases members of the B-, X- and Y-families.* Nucleic Acids Res, 2014. **42**(1): p. 553-66.

245. Nay, S.L., et al., *Alkbh2 protects against lethality and mutation in primary mouse embryonic fibroblasts.* DNA Repair (Amst), 2012. **11**(5): p. 502-10.

246. Branzei, D. and B. Szakal, *DNA damage tolerance by recombination: Molecular pathways and DNA structures.* DNA Repair (Amst), 2016. **44**: p. 68-75.

247. Garcia-Rodriguez, N., et al., *Spatial separation between replisome- and template-induced replication stress signaling.* EMBO J, 2018. **37**(9).

248. Garcia-Rodriguez, N., R.P. Wong, and H.D. Ulrich, *The helicase Pif1 functions in the template switching pathway of DNA damage bypass.* Nucleic Acids Res, 2018. **46**(16): p. 8347-8356.

249. Karras, G.I., et al., *Noncanonical role of the 9-1-1 clamp in the error-free DNA damage tolerance pathway.* Mol Cell, 2013. **49**(3): p. 536-46.

250. Antony, E., et al., *Srs2 disassembles Rad51 filaments by a protein-protein interaction triggering ATP turnover and dissociation of Rad51 from DNA.* Mol. Cell, 2009. **35**(1): p. 105-115.

251. Rong, L., et al., *The hyper-gene conversion hpr5-1 mutation of Saccharomyces cerevisiae is an allele of the SRS2/RADH gene.* Genetics, 1991. **127**(1): p. 75-85.

252. Ulrich, H.D., *PCNA^{SUMO} and Srs2: a model SUMO substrate-effector pair.* Biochem. Soc. Trans., 2007. **35**(6): p. 1385-1388.

253. Burgess, R.C., et al., *Localization of recombination proteins and Srs2 reveals anti-recombinase function in vivo.* J. Cell Biol., 2009. **185**(6): p. 969-81.

254. Sirbu, B.M., et al., *Identification of proteins at active, stalled, and collapsed replication forks using isolation of proteins on nascent DNA (iPOND) coupled with mass spectrometry.* J Biol Chem, 2013. **288**(44): p. 31458-67.

255. Sirbu, B.M., F.B. Couch, and D. Cortez, *Monitoring the spatiotemporal dynamics of proteins at replication forks and in assembled chromatin using isolation of proteins on nascent DNA.* Nat Protoc, 2012. **7**(3): p. 594-605.

256. Sirbu, B.M., et al., *Analysis of protein dynamics at active, stalled, and collapsed replication forks.* Genes Dev., 2011. **25**(12): p. 1320-1327.

257. Game, J.C., *The Saccharomyces repair genes at the end of the century.* Mutat Res, 2000. **451**(1-2): p. 277-93.

258. Alvaro, D., M. Lisby, and R. Rothstein, *Genome-Wide Analysis of Rad52 Foci Reveals Diverse Mechanisms Impacting Recombination.* PLoS Genet., 2007. **3**(12): p. e228.